



Norwegian University of
Science and Technology

Improvements of a Kaplan type small turbine

Forbedre og videreutvikle en Kaplan småturbin

Lars Fjærvold

Master of Science in Product Design and Manufacturing

Submission date: Januar 2012

Supervisor: Torbjørn Kristian Nielsen, EPT

Norwegian University of Science and Technology
Department of Energy and Process Engineering

EPT-M-2011- 103

MASTEROPPGAVE

for
Stud.techn.

Lars Fjærvold
Høsten 2011

Forbedre og videreutvikle en Kaplan småturbin
Improvements of a Kaplan type small turbine

Bakgrunn

Det er utviklet og produsert en småturbin for bruk i landsbyer i Afghanistan. Turbinen er av produksjonsmessige hensyn veldig forenklet. Turbinen skal innmonteres i Vannkraftlaboratoriet, og som prosjektoppgave for en annen student skal kartlegging av virkningsgrader og karakteristikk gjennomføres.

Kandidaten skal delta i gjennomføring av virkningsgradmålingene, men oppgaven skal i hovedsak være å søke å forbedre turbinen. I tillegg skal rusingskarakteristikk og kavitasjonsforhold undersøkes.

Mål

Optimalisere Kaplan turbinen samtidig med at det legges vekt på forenklet geometri.

Opgaven bearbeides ut fra følgende punkter:

1. Delta i montering og instrumentering av turbinen i Vannkraftlaboratoriet. Dette innebærer også å lære seg å kjøre testriggen i laboratoriet.
2. I samarbeid med prosjektkandidaten, kartlegge turbinens karakteristikk og virkningsgrader
3. Foreslå og verifisere forbedringstiltak for turbinen. Her inngår:
 - a. Inn- og avløpsforhold
 - b. Skovlgeometri
 - c. Rusing
 - d. Kavitasjonsforhold

Senest 14 dager etter utlevering av oppgaven skal kandidaten levere/sende instituttet en detaljert fremdrift- og eventuelt forsøksplan for oppgaven til evaluering og eventuelt diskusjon med faglig ansvarlig/veiledere. Detaljer ved eventuell utførelse av dataprogrammer skal avtales nærmere i samråd med faglig ansvarlig.

Besvarelsen redigeres mest mulig som en forskningsrapport med et sammendrag både på norsk og engelsk, konklusjon, litteraturliste, innholdsfortegnelse etc. Ved utarbeidelsen av teksten skal kandidaten legge vekt på å gjøre teksten oversiktlig og velskrevet. Med henblikk på lesning av besvarelsen er det viktig at de nødvendige henvisninger for korresponderende steder i tekst, tabeller og figurer anføres på begge steder. Ved bedømmelsen legges det stor vekt på at resultatene er grundig bearbeidet, at de oppstilles tabellarisk og/eller grafisk på en oversiktlig måte, og at de er diskutert utførlig.

Alle benyttede kilder, også muntlige opplysninger, skal oppgis på fullstendig måte. For tidsskrifter og bøker oppgis forfatter, tittel, årgang, sidetall og eventuelt figurnummer.

Det forutsettes at kandidaten tar initiativ til og holder nødvendig kontakt med faglærer og veileder(e). Kandidaten skal rette seg etter de reglementer og retningslinjer som gjelder ved alle (andre) fagmiljøer som kandidaten har kontakt med gjennom sin utførelse av oppgaven, samt etter eventuelle pålegg fra Institutt for energi- og prosesseteknikk.

I henhold til ”Utfyllende regler til studieforskriften for teknologistudiet/sivilingeniørstudiet” ved NTNU § 20, forbeholder instituttet seg retten til å benytte alle resultater og data til undervisnings- og forskningsformål, samt til fremtidige publikasjoner.

Ett -1 komplett eksemplar av originalbesvarelsen av oppgaven skal innleveres til samme adressat som den ble utlevert fra. Det skal medfølge et konsentrert sammendrag på maksimalt én maskinskrevet side med dobbel linjeavstand med forfatternavn og oppgavetittel for evt. referering i tidsskrifter).

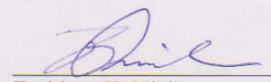
Til Instituttet innleveres to - 2 komplette kopier av besvarelsen. Ytterligere kopier til eventuelle medveiledere/oppdragsgivere skal avtales med, og eventuelt leveres direkte til de respektive. Til instituttet innleveres også en komplett kopi (inkl. konsentrerte sammendrag) på CD-ROM i Word-format eller tilsvarende.

NTNU, Institutt for energi- og prosesseteknikk

Dato:

20/1-2012


Olav Bolland
Instituttleder


Torbjørn K. Nielsen
Faglig ansvarlig/veileder

Medveileder: Ole Gunnar Dahlhaug
Anders Austegaard

Preface

During this thesis my knowledge about testing hydraulic machinery, error analysis and CFD has increased drastically. Also getting the opportunity of “hands on” experience helping Trygve Opland constructing the test rig in the laboratory have been inspirational and eye opening. There are a lot of things that can be taught in theory but there are so many things that require experience in laboratory work. I would like to thank Trygve for all help and guidance during the tests and construction of the turbine.

The efficiency tests and a lot of work have been done in collaboration with fellow student Remi Andre Stople. The end result of this master thesis would probably not have been as good without Remi. I would like to thank Remi for all the hours spent together working and socializing.

Next I would like to thank Bjørn Wither Solemslie for all the hours of help received on the Matlab programs developed and guidance in calibration and uncertainty calculation.

Torbjørn K. Nielsen has been my Professor during this thesis. During the weekly meetings in the beginning of the semester he was very good in guiding me and Remi in what to do next and what we should look for. Having the opportunity of always being able to come into his office and always get help is from my side very appreciated, thank you Torbjørn.

Bård Brandstø, Joar Grilstad and Halvor Haukvik also deserve thanks for helping throughout the project.

Last but not least I would like to thank my family for supporting me during the entire process.

Lars Fjærvold
Trondheim, January 20, 2012

Abstract

The goal with this master thesis was to establish Hill diagrams and improve a Kaplan turbine intended for use in Afghanistan.

The turbine efficiency has been tested in setting 1 and 2. Turbine efficiency in setting 3 and 4 could not be tested because the runner blades interfere with the housing making it impossible to rotate the turbine. The efficiency was tested with an effective pressure head ranging from 2 to 8 meters. Best efficiency point was not reached because of limitations in the test rig making it impossible to reach a lower effective head. The best efficiencies tested in the two different settings are presented in the table below together with the uncertainty in the actual test point. All tests are done according to the IEC standard for model testing of hydraulic turbines.

| | Efficiency | Rotational speed | Effective head |
|-----------|--------------|------------------|----------------|
| Setting 1 | 76.4 ± 1.57% | 552 rpm | 2.25 m |
| Setting 2 | 83.8 ± 1.59% | 602 rpm | 2.72 m |

The *computational fluid dynamics* (CFD) simulations done on the inlet bend indicates that the bend should be rounded and flow controllers should be extended over the entire bend. This should be considered to get a more even velocity distribution at the inlet of the guide vane.

An alternative placement of the lower bearing was designed but is discarded because of the disadvantages the modification leads to. High wear due to sand erosion on the seals causing high maintenance and costly stops makes the solution not optimal for use in water with high sand content.

The runner blade design is checked against the design procedure presented by Professor Hermod Brekke in *Pumper og Turbiner* and found to be satisfying. It is concluded that time should rather be spent on optimizing the inlet of the turbine.

Fluctuations in the measurements make it necessary to change the measuring equipment or search for error in the existing equipment before further tests can be carried out. In order to be able to test in setting 3 and 4 the runner needs to be placed while the blades are fixed in setting 4.

Sammendrag

Målet med denne masteroppgaven var å etablere Hill diagram for en Kaplan turbin designet for bruk i Afghanistan og se på muligheten for forbedringer.

Virkningsgraden til turbinen er blitt testet i innstilling en og to. Turbinen har fire innstillinger, innstilling tre og fire lot seg ikke teste da turbinen kilte seg fast i turbinhuset allerede ved innstilling tre. Virkningsgraden ble bestemt for effektive fallhøyder fra to til åtte meter. Best punktet til turbinen ble ikke fastsatt da testriggeren gjorde det umulig å oppnå lave nok fallhøyder. Den beste virkningsgraden testet i hver innstilling er presentert i tabellen under med usikkerheten i det aktuelle testpunktet. Alle testene gjennomført er gjennomført i henhold til IEC standarden for modelltesting av vannkraftturbiner.

| | Virkningsgrad | Omløpshastighet | Effektiv fallhøyde |
|---------------|---------------|-----------------|--------------------|
| Innstilling 1 | 76.4 ± 1.56% | 552 o/m | 2.25 m |
| Innstilling 2 | 83.8 ± 1.60% | 602 o/m | 2.72 m |

Computational fluid dynamics (CFD) simuleringene utført antyder at innløpet bør avrundes og at strømningsforbedrende spenner seg over hele bendet. Dette bør vurderes for å få en jevnere hastighetsfordeling inn på ledeskovlene.

Det er utarbeidet ett forslag til en ny plassering av det nederste lageret, men denne løsningen ble forkastet grunnet ulempene forandringen fører med seg. Mye sand i vannet hvor turbinen skal benyttes vil slite ned pakningene og ødelegge lageret. Dette vil føre til kostbare stopp og høye vedlikeholdskostnader. Dermed er ikke løsningen optimal i for vann med høyt sandinnhold.

Løpehjuldesignet er kontrollert mot professor Hermod Brekkes fremgangsmetode for å designe Kaplan løpehjul i Pumper og Turbiner. Designet er designet i samsvar med metoden beskrevet i Pumper og Turbiner, det er derfor konkludert med at tid heller bør bli brukt på å optimalisere innløpet på turbinen.

Svingninger i målingene gjør det nødvendig å skifte måleutstyret eller finne hva som skaper signingene i målingene før nye tester kan utføres. Løpehjulet må installeres mens skovlene er satt i innstilling fire for å kunne teste i innstilling tre og fire.

Contents

| | |
|---|-----|
| Preface..... | i |
| Abstract | iii |
| Sammendrag | v |
| Contents | vii |
| List of Figures..... | xi |
| List of Tables..... | xiv |
| List of symbols | xv |
| 1 Introduction..... | 1 |
| 2 Preface study..... | 3 |
| 2.1 Related work at the Water power laboratory..... | 6 |
| 2.2 Design of a Kaplan runner | 6 |
| 2.3 Main dimensions | 9 |
| 2.4 Potential flow | 12 |
| 3 Testing of Kaplan turbine | 15 |
| 3.1 Efficiency test | 15 |
| 3.2 Cavitation test | 16 |
| 3.3 Runaway speed | 18 |
| 3.4 Calibration | 18 |
| 3.5 Pressure gauge | 19 |
| 3.6 Torque gauge..... | 19 |
| 3.7 Trip meter | 21 |
| 3.8 Flow meter | 22 |
| 3.9 Frequency analysis | 23 |

| | | |
|-------|---|----|
| 3.10 | LabView program | 23 |
| 3.11 | Clearance water test | 23 |
| 3.12 | Risk Assessment | 23 |
| 4 | Uncertainties in measuring | 25 |
| 4.1 | Spurious error..... | 25 |
| 4.2 | Random error | 25 |
| 4.3 | Systematic error | 25 |
| 4.4 | Total uncertainty | 27 |
| 4.5 | Uncertainties in the Calibration | 27 |
| 4.5.1 | Uncertainties in the calibration of the flow meter | 27 |
| 4.5.2 | Uncertainties in the calibration of the pressure gauge..... | 29 |
| 4.5.3 | Uncertainties in the calibration of the torque gauge..... | 31 |
| 4.5.4 | Uncertainty in calibration of the thermometer | 32 |
| 4.6 | Uncertainties in the tests | 32 |
| 4.6.1 | General uncertainty in the tests..... | 32 |
| 4.6.2 | Uncertainty in the pressure measurements..... | 34 |
| 4.6.3 | Uncertainty in the torque measurements..... | 35 |
| 4.6.4 | Uncertainty in the volume flow measurements | 36 |
| 4.6.5 | Uncertainty in the rotational speed measurements | 36 |
| 4.6.6 | Uncertainty in the calculation of density of water..... | 37 |
| 4.6.7 | Total uncertainty in the hydraulic efficiency..... | 37 |
| 5 | Test rig setup..... | 39 |
| 5.1 | Detailed description of the rig..... | 39 |
| 6 | The Afghani Kaplan turbine..... | 41 |
| 6.1 | The Turbine design | 41 |

| | | |
|-------|---|----|
| 6.2 | Specifications..... | 42 |
| 6.3 | Main dimensions | 43 |
| 6.4 | Runner blade design..... | 43 |
| 7 | Changes and limitations on the rig and turbine..... | 45 |
| 7.1 | Pipe dimensions | 45 |
| 7.2 | Runner blade friction..... | 47 |
| 7.3 | Upper bearing..... | 48 |
| 7.3.1 | Bearing load calculation | 51 |
| 7.4 | Plexiglass cover..... | 52 |
| 8 | Optimisations of inlet bend using CFD. | 55 |
| 8.1 | CFD analysis of inlet bend | 55 |
| 8.2 | Velocity measurements in inlet bend..... | 58 |
| 8.3 | Outlet..... | 61 |
| 9 | Results | 63 |
| 9.1 | Efficiency tests..... | 63 |
| 9.1.1 | Setting 1..... | 66 |
| 9.1.2 | Setting 2..... | 68 |
| 9.2 | Cavitation tests..... | 70 |
| 9.3 | Clearance water..... | 70 |
| 9.4 | Mechanical power | 71 |
| 9.5 | Torque | 72 |
| 9.6 | Fluctuations in measurements | 72 |
| 9.7 | CFD of inlet bend | 73 |

| | | |
|------|----------------------------|----|
| 9.8 | Velocity measurements..... | 77 |
| 10 | Discussion of results..... | 79 |
| 10.1 | Efficiency tests..... | 79 |
| 10.2 | Clearance water..... | 79 |
| 10.3 | Inlet bend | 79 |
| 10.4 | Outlet..... | 81 |
| 11 | Conclusion | 83 |
| 12 | Further work..... | 85 |
| 12.1 | Rig setup..... | 85 |
| 13 | Bibliography..... | 87 |

List of Figures

| | |
|--|----|
| Figure 2-1 Cross section of a Kaplan turbine, Voithhydro..... | 3 |
| Figure 2-2 Efficiency curves for Kaplan turbines | 4 |
| Figure 2-3 S-turbine..... | 5 |
| Figure 2-4 Bulb turbine..... | 5 |
| Figure 2-5 Vector components of forces acting on a runner blade | 8 |
| Figure 2-6 Axial cut of a Kaplan turbine with guide vanes | 9 |
| Figure 2-7 Speed number plotted vs. axial speed | 10 |
| Figure 2-8 Relation between d/D and B_0/D plotted against n_s | 11 |
| Figure 2-9 Suction head and number of blades | 12 |
| Figure 3-1 Definition of heights..... | 17 |
| Figure 3-2 Efficiency curve with changing Thoma number | 17 |
| Figure 3-3 The dead weight calibration setup..... | 20 |
| Figure 3-4 Calibration curve for the torque gauge..... | 21 |
| Figure 3-5 Trip meter and reflex ribbon ready to use | 21 |
| Figure 3-6 The flow meter use in the test | 22 |
| Figure 4-1 Calibration curve with a 95% confidence interval | 29 |
| Figure 4-2 Calibration curve for the pressure gauge with a 95% confidence interval | 30 |
| Figure 4-3 Calibration curve for the torque gauge with a 95% confidence interval | 32 |
| Figure 4-4 Test for drift in measurements 300rpm, setting 1..... | 33 |
| Figure 4-5 Test for drift in measurements 300rpm, setting 1..... | 34 |
| Figure 5-1 Test rig setup..... | 40 |
| Figure 6-1 Complete turbine, (Inventor drawing) | 41 |
| Figure 7-1 Original pipe section | 45 |
| Figure 7-2 Configured pipe section | 46 |
| Figure 7-3 Runner blade with broken blade section, seen from below..... | 48 |
| Figure 7-4 Temperature plotted vs. rpm at 2.5 meter pressure head. Setting 2..... | 50 |
| Figure 7-5 Temperature plotted vs. pressure head. Setting 1, 800rpm..... | 50 |
| Figure 7-6 Temperature plotted vs. pressure head. Setting 2, 650rpm..... | 50 |
| Figure 7-7 Flow after the turbine outside BEP | 53 |
| Figure 8-1 Velocity and pressure distribution in pipe bend. | 56 |
| Figure 8-2 Original geometry | 57 |
| Figure 8-3 Geometry 1 | 57 |
| Figure 8-4 Geometry 2 | 57 |

| | |
|--|----|
| Figure 8-5 Geometry 3 | 58 |
| Figure 8-6 Pitot tube mounted on the turbine..... | 59 |
| Figure 8-7 Height difference in a knife Pitot measurement..... | 60 |
| Figure 8-8 Bearing when placed inside the guide vane centre piece..... | 62 |
| Figure 9-1 2nd order poly fit | 63 |
| Figure 9-2 3rd order poly fit | 64 |
| Figure 9-3 4th order poly fit | 64 |
| Figure 9-4 Smoothing spline..... | 65 |
| Figure 9-5 Hill diagram, efficiency plotted against effective head and rotational speed | 66 |
| Figure 9-6 Raw data measurements. Efficiency curves at constant RPM plotted vs. effective head. | 68 |
| Figure 9-7 Hill diagram, efficiency plotted against effective head and rotational speed | 69 |
| Figure 9-8 Raw data measurements. Efficiency curves at constant RPM plotted vs. effective head | 69 |
| Figure 9-9 Clearance water at constant rpm..... | 70 |
| Figure 9-10 Clearance water at constant inlet pressure head in setting 2 | 71 |
| Figure 9-11 Mechanical power at 500rpm | 72 |
| Figure 9-12 Torque at 500rpm | 72 |
| Figure 9-13 Original geometry with inlet velocity of 1.0814m/s | 74 |
| Figure 9-14 Geometry 1. Inlet velocity 1.25m/s..... | 75 |
| Figure 9-15 Geometry 2. Inlet velocity 2.387m/s..... | 75 |
| Figure 9-16 Outlet velocity profiles with original geometry and different inlet velocities..... | 76 |
| Figure 9-17 Outlet velocity profiles for geometry 3..... | 77 |
| Figure 13-1 Inflation along wall of the inlet | R |
| Figure 13-2 Front panel | T |
| Figure 13-3 Data acquisition and translation of volt signals | T |
| Figure 13-4 RPM subVI for readings of the rotational speed..... | U |
| Figure 13-5 Block diagram for the RPM sub VI..... | V |
| Figure 13-6 Calculation node and front panel values | V |
| Figure 13-7 Storage | W |
| Figure 13-8 Plotting of efficiency-head graph..... | W |

List of Tables

| | |
|--|----|
| Table 1 Component errors | 27 |
| Table 2 Uncertainties in the calibration of the flow meter | 28 |
| Table 3 Uncertainties in the calibration of the pressure gauge | 30 |
| Table 4 Uncertainties in the calibration of the torque gauge | 31 |
| Table 5 Errors in the tests..... | 34 |
| Table 6 Uncertainties in the torque measurements | 36 |
| Table 7 Uncertainties in the volume flow measurements | 36 |
| Table 8 Volume flow..... | 42 |
| Table 9 Main turbine characteristics | 43 |
| Table 10 Actual and scaled outlet velocity..... | 77 |
| Table 11 Scaled velocity vs. average velocity..... | 78 |
| Table 12 Velocity measurements at constant pressure head..... | 78 |
| Table 13 Weight calibration calculation..... | N |

List of symbols

| Symbol | Description | Unit |
|-----------|---|----------------------|
| L | Lift | [N] |
| C_L | Lift coefficient | [-] |
| ρ | Density | [kg/m ³] |
| v | Velocity | [m/s] |
| L | Length | [m] |
| D | Drag | [N] |
| C_D | Drag coefficient | [-] |
| F | Force | [N] |
| β_0 | Angle between angular velocity and inlet velocity | [°] |
| λ | Angle between lift and drag component | [°] |
| P | Turbine power | [W] |
| u | Turbine velocity | [m/s] |
| P' | Available power in water | [W] |
| g | Gravity constant | [m/s ²] |
| Q | Volume flow | [m ³ /s] |
| H | Head | [m] |
| η | Efficiency | [%] |
| Z | Number of runner blades | [-] |
| t | Distance between runner blades | [m] |

| | | |
|----------------------|------------------------------------|---------------------|
| $^0\Omega$ | Speed number | [-] |
| $\underline{\omega}$ | Reduced angular velocity | [m ⁻¹] |
| c_m | Axial velocity of water | [m/s] |
| D | Turbine diameter | [m] |
| η_h | Hydraulic efficiency | [%] |
| P_m | Mechanical Power | [W] |
| P_h | Hydraulic Power | [W] |
| η_m | Mechanical efficiency | [%] |
| T_m | Torque | [Nm] |
| E | Specific energy | [J] |
| p | Pressure | [Pa] |
| z | Height | [m] |
| σ | Thoma number | [-] |
| q_v | Volume flow | [m ³ /s] |
| m | Mass of water | [kg] |
| ε | Correction factor for air buoyancy | [-] |
| f | Relative error in measurements | [%] |
| s_y | Standard deviation | [Varies] |
| e_y | Absolut error in measurements | [Varies] |
| B | Arc length | [m] |
| r | Radius | [m] |
| β | Angle | [°] |

| | | |
|------------|------------------------|------------|
| c | Measured flow velocity | [m/s] |
| c' | Scaled flow velocity | [m/s] |
| Δh | Height difference | [m] |
| φ | Pitot coefficient | [-] |
| Re | Reynolds number | [-] |
| μ | Dynamic viscosity | [kg/(m·s)] |

1 Introduction

Remote Hydrolight is a company designing turbines that aims to be cost efficient and easy to produce. Remote Hydrolight represented by Anders Austegård wanted to establish Hill diagrams for four runner vane settings on a Kaplan turbine they had produced.

Austegård also requested cavitation and runaway speed tests. If time allowed it he also wanted suggestions on how the turbine could be improved. The improvements should not make the turbine more difficult to produce.

2 Preface study

The Kaplan turbine was invented and developed by Austrian Victor Kaplan around 1913, and is designed to operate at low heads and high flow rates. The turbine is an axial turbine, meaning that the direction of the water flow is parallel to the bulb and driveshaft through the runner blades. It is common to compare the Kaplan turbine with a propeller due to its distinct shape.

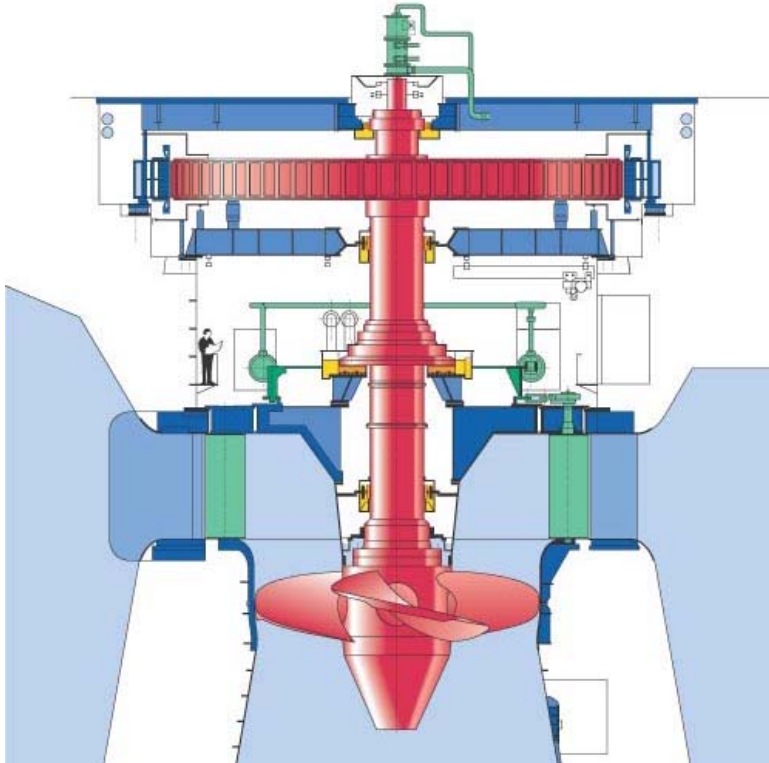


Figure 2-1 Cross section of a Kaplan turbine, Voithhydro

Vertical axis Kaplan turbines are in many ways similar to Francis turbines as well as propellers. Besides the shape of the runner blades, the Kaplan turbine uses the same water way system and method to generate electricity as Francis turbines. Like the Francis turbine the Kaplan have a spiral casing to distribute the water around the turbine. Guide vanes are used to regulate the volume flow through the turbine. The guide vanes are also used to induce a swirl in the water, so that the water hits the runner blades in the most efficient angle as possible. The runner blades can in many cases also be adjusted to maintain as

optimal flow conditions as possible. With the opportunity to regulate two parameters makes the Kaplan turbine efficient over a wide spectre of loads and heads. This means that the high efficiency range of a Kaplan turbine is greater than efficiency range of a Francis turbine where you only may adjust the guide vanes.

Kaplan turbines can also be produced with fixed runner blades and guide vanes. By mounting fixed blades or-/and guide vanes the efficiency range is reduced. See Figure 2-2 for the effect fixed guide vanes and rotor blades have on the efficiency range of a Kaplan turbine.

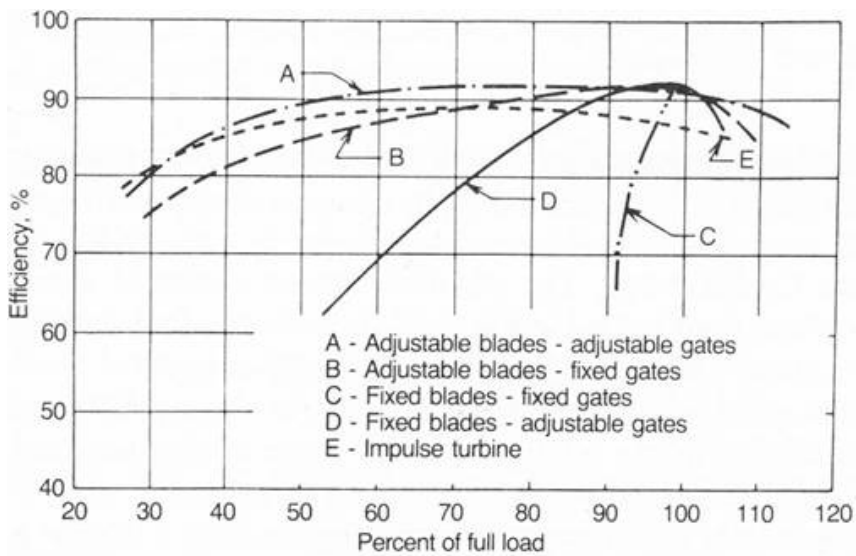


Figure 2-2 Efficiency curves for Kaplan turbines

Kaplan turbines have also the opportunity to be mounted with a horizontal axis. They are then often referred to as S-turbines and Bulb turbines. S-turbines are used in the same spectre of head and flow rates as vertical axis Kaplan's. Price and available space are factors that govern the choice between S-turbines and vertical axis Kaplan's. Vertical axis Kaplan's requires a smaller land area than S-turbines. S-turbines have smaller hydraulic losses compared to a vertical axis Kaplan's, due to the fact that the water does not have to change direction through the turbine.

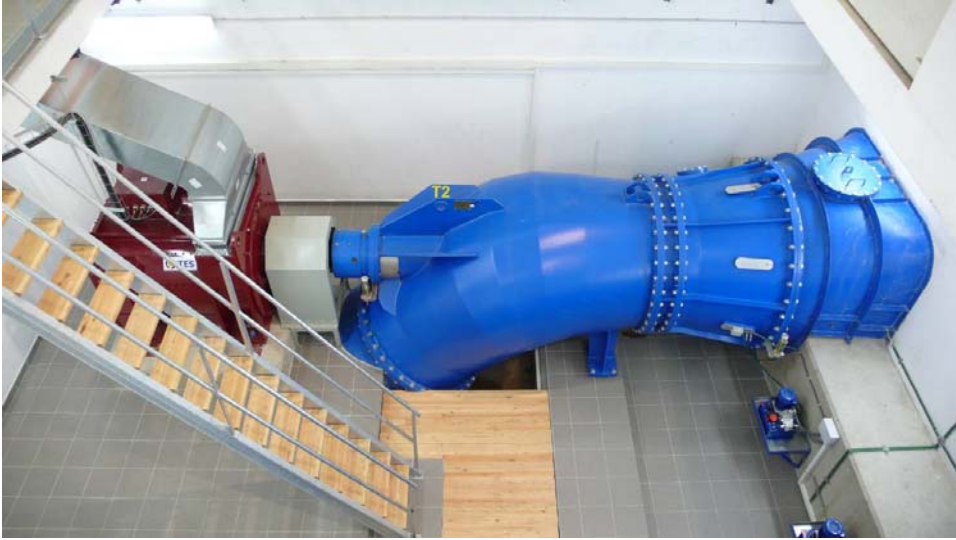


Figure 2-3 S-turbine

The bulb turbine is only used in high energy sites with low head and high volume flow. On the bulb turbine the generator and drive shaft is mounted inside the bulb in front of the runner. A full grown man is able to stand upright inside the bulb.

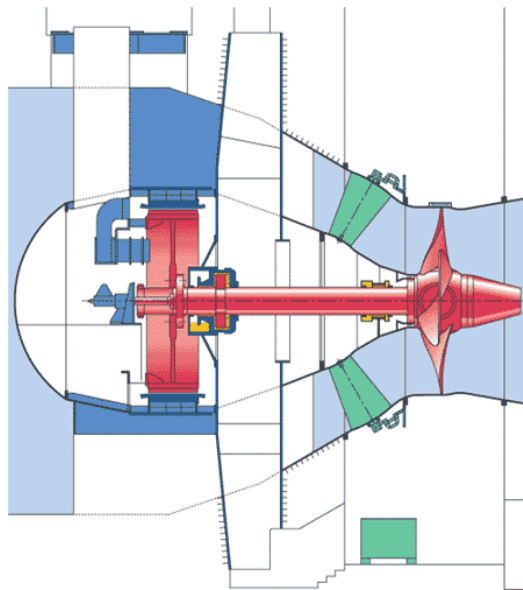


Figure 2-4 Bulb turbine

Like the vertical axis Kaplan, S-turbines and bulb turbines have guide vanes and runner blades with the possibility to be adjustable. They all have a draft tube to regain pressure after the runner. It is normal for all the solutions to be dived to prevent cavitation at the end of the runner blades.

2.1 Related work at the Water power laboratory

There are a number of reports written on similar cases as the one in this master thesis available at the Water power laboratory.

Bjørn Winther Solemslie made a master thesis on how to optimize a distributor on a Pelton turbine. The report contains a relatively good uncertainty analysis that is used as guidance in this report.

Pål Tore Storlie performed extensive uncertainty calculations on equipment used in the test performed in this thesis in his master thesis.

Eve Walseth have performed and written a good report on tests and optimization of a crossflow turbine. Walseths report is based on the same points as in this report and much of the work Walseth did can be correlated with tasks that will be performed in this thesis.

Anders Linde Holo have performed CFD calculations and written a short introduction on CFD modelling.

Øyvind Andresen did CFD analysis as well as establishing Hill charts for a Francis turbine.

2.2 Design of a Kaplan runner

The Kaplan runner consists of a variable number of blades, depending on head and volume flow, and a hub the blades are attached to. The runner blades are usually designed as curved hydrofoils using pressure differences to create torque which is transferred to electrical power. Designing the runner blades to perform optimal with the given flow conditions is extremely important to gain high efficiency.

Forces from the water acting on the runner blades can be broken down into two main forces, lift and drag force.

$$L = C_L \cdot \rho \cdot \frac{v_\infty^2}{2} \cdot l \cdot dr \quad [N] \quad (2.1)$$

Equation(2.1) and equation(2.2) gives us the lift and drag force. To be able to calculate the forces the lift and drag coefficients have to be known. Lift and drag coefficients can be found using certain programs, such as x-foil or it is possible to find lift and drag curves for certain NACA and Göttingen foils. To get as accurate coefficients as possible model tests are necessary. Especially when the blades are mounted in a cascade, which is the case for a Kaplan turbine, model tests are important to calculate lift and drag coefficients. It is on the other hand possible to use x-foil and correct the results from the program with test done on other cascade sections to get reasonable coefficients. A thick air foil have a good peak performance while a more slender air foil have a wider spectre with high performance, but peak performance for a slender air foil is not as good compared with a thicker air foil. Since a thick air foil have a high peak performance they are also have a larger risk for cavitation and the efficiency falls drastically outside best angle of attack.

$$D = C_D \cdot \rho \cdot \frac{v_\infty^2}{2} \cdot l \cdot dr \quad [N] \quad (2.2)$$

When lift and drag is found, we can find the force acting in the rotational direction.

$$F_u = F \cdot \cos\left(\frac{\pi}{2} - \beta_\infty + \lambda\right) = F \cdot \sin(\beta_\infty - \lambda) \quad [N] \quad (2.3)$$

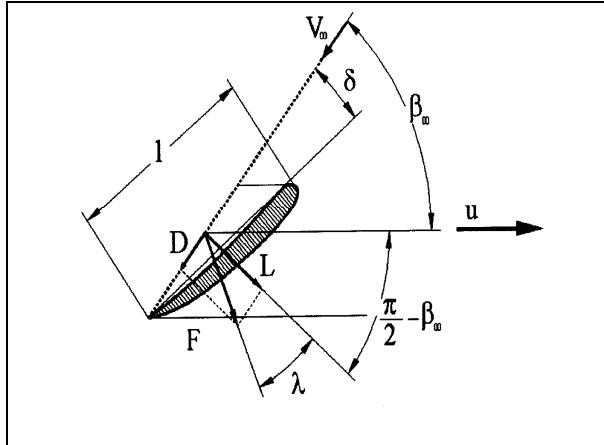


Figure 2-5 Vector components of forces acting on a runner blade

F is found by using equation(2.4). It is important to evaluate the force F in correlation with the thickness and strength of the runner blade. If F is large and the blade profile is thin, the blade can break or deform.

$$F = \frac{L}{\cos \lambda} = \frac{C_L \cdot \rho \cdot v_{\infty}^2}{2 \cdot \cos \lambda} \cdot l \cdot dr \quad [N] \quad (2.4)$$

After F_u is found the energy output from the turbine can be determined. By taking the sum of all forces acting on each small section on each blade, and multiply the sum with the rotational speed of the turbine, the energy output is determined.

$$P = F_u \cdot u = \frac{C_L \cdot \rho \cdot v_{\infty}^2}{2 \cdot \cos \lambda} \cdot \sin(\beta_{\infty} - \lambda) \cdot u \cdot dr \quad [W] \quad (2.5)$$

The energy the turbine produces cannot be higher than the available energy in the water passing the turbine. A simple way to calculate the available energy in the water is by using equation(2.6). Here η represent losses in the waterway, valves and other factors that reduce the effective head.

$$P' = \rho \cdot g \cdot \Delta Q \cdot H \cdot \eta = \rho \cdot g \cdot 2\pi r \cdot dr \cdot \frac{c_z}{z_1} \cdot H \cdot \eta \quad [W] \quad (2.6)$$

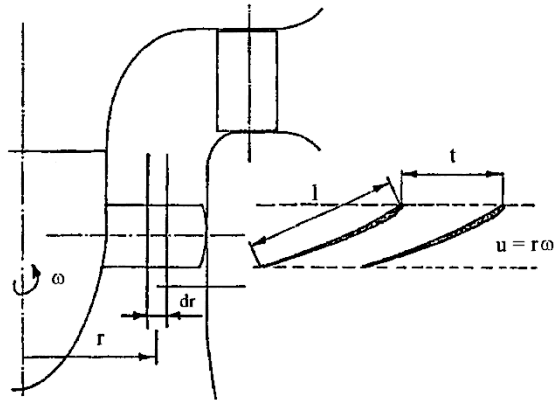


Figure 2-6 Axial cut of a Kaplan turbine with guide vanes

z_1 is the number of runner blades on the turbine, while t is the distance between each blade (1).

$$t = \frac{2\pi r}{z_1} \quad [m] \quad (2.7)$$

$$C_L \cdot \frac{l}{t} = \frac{2g \cdot \eta \cdot H_n \cdot c_z \cdot \cos \lambda}{v_\infty^2 \cdot u \cdot \sin(\beta_\infty - \lambda)} \quad [-] \quad (2.8)$$

2.3 Main dimensions

When designing a Kaplan turbine many parameters are chosen and based on experienced data. The speed number is an important parameter. The speed number for Kaplan turbines spans from 1.5 to 3 and can be used to determine if a Kaplan or Francis turbine should be used. If the speed number is lower than 1.5 a Francis turbine might be the best choice, but there are grey areas where other parameters have to be considered to be able to choose which turbine that is optimal for the site. The speed number is a function of angular velocity and the volume flow.

$$^0\Omega = \underline{\omega} \cdot \sqrt{\underline{Q}_n} \quad (2.9)$$

The axial flow is dependent on how fast the turbine is rotating, so c_m is found from Ω if experienced values if minor simplifications and linear relations are accepted. In Figure 2-7 the linear dependence and equation is shown.

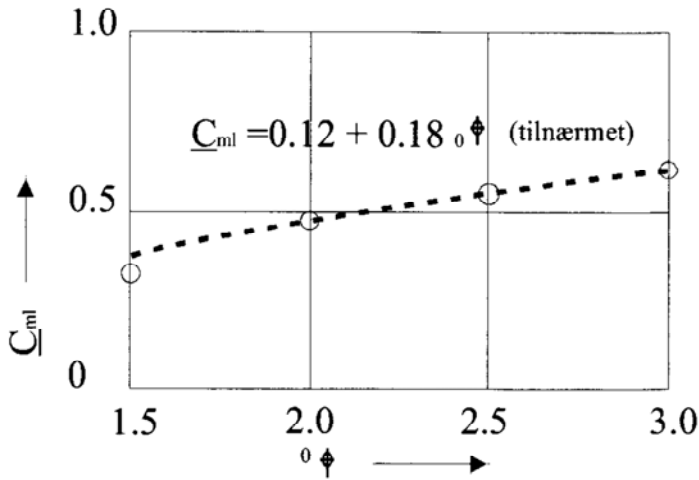


Figure 2-7 Speed number plotted vs. axial speed

From the speed number the largest runner diameter is found through

$$D_2 = \sqrt{\frac{4 \cdot \Omega^2}{\omega^2 \cdot \pi \cdot (0.12 + 0.18 \cdot \Omega)}} \quad [m] \quad (2.10)$$

Small Kaplan turbines can be made with a cylindrical housing to reduce the cost of manufacturing, but cylindrical housing lead to increased clearance loss between the runner blades and the housing. When a spherical housing is used the narrowest part on the draft tube is produced with a diameter 3-5% narrower than D_2 .

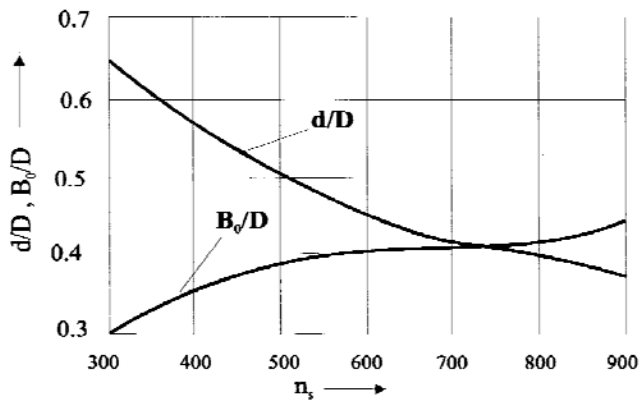


Figure 2-8 Relation between d/D and B_0/D plotted against n_s

The diameter of the hub d and the height of the intake B_0 also need to be calculated. Both of these two parameters can be read directly of Figure 2-8. B_0 and d are dependent on the specific revolution number n_s .

Number of runner blades and suction head is dependent on the pressure distribution around the runner blade. Number of blades and suction head is chosen so that the pressure around the blade for a wide range as possible not falls under the boiling pressure or under the critical cavitation number. The pressure distribution around blades changes when blades are placed in a cascade like in a runner. Suction head and number of blades can be found by using Figure 2-9 Suction head and number of blades and is a function of the specific revolution number (1).

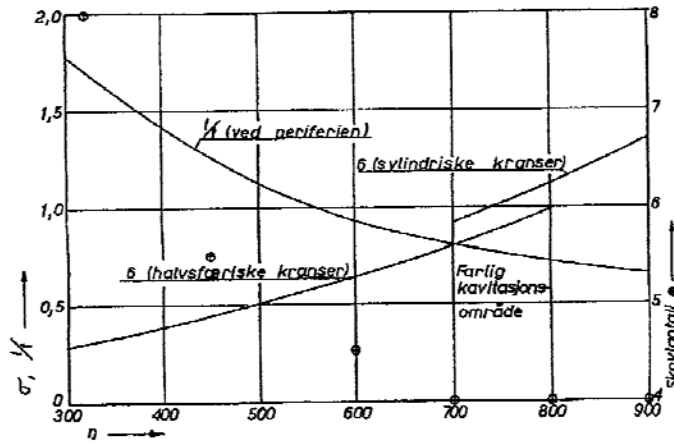


Figure 2-9 Suction head and number of blades

2.4 Potential flow

The two previous chapters describe how the main dimensions of a runner should be when a blade profile is already chosen. Standard foils could be used with known lift and drag but the optimal is to design a profile that is designed for the intended flow conditions. To be able to create such a profile fundamental equations like the continuity-, Navier-Stokes- and the Euler equation have to be solved with a geometry profile. This is an iterating process where the equations are used on the geometry, the geometry is changed for every time the equations are applied until desired velocity and pressure fields are obtained for the given geometry.

The continuity equation in fluid dynamics states that in a steady state process, the rate at which mass enters a system is equal to the rate at which mass leaves the system.

Continuity equation in general form:

$$\frac{D\rho}{Dt} + \rho \cdot \text{div}V = 0 \quad (2.11)$$

The Navier-Stokes equation describes the motion of a fluid substance. It gives the velocity of a fluid particle at a given point in a flow at a given time. When

Navier-Stokes is applied to a series of points in a flow one obtain a flow velocity field. After the velocity field is found the drag force may be found.

Navier-Stokes equation:

$$\rho \frac{DV}{Dt} = \rho \cdot g - \nabla p + \frac{\partial}{\partial x_j} \left[\mu \left(\frac{\partial v_i}{\partial x_j} + \frac{\partial v_j}{\partial x_i} \right) + \delta_{ij} \cdot \lambda \cdot \text{div} V \right] \quad (2.12)$$

If the flow is incompressible and viscosity and density is constant we get:

$$\rho \frac{DV}{Dt} = \rho \cdot g - \nabla p + \mu \cdot \nabla^2 V \quad (2.13)$$

When futher assuming that the viscous terms are negligible equation (2.13) is reduced to the Euler equation for inviscid flow.

Euler equation for inviscid flow:

$$\rho \frac{DV}{Dt} = \rho \cdot g - \nabla p \quad (2.14)$$

The Euler equation for steady, incompressible and frictionless flow along a streamline between two points 1 and 2 becomes the Bernoulli equation.

3 Testing of Kaplan turbine

The standard IEC 60193 contain rules and guidelines for how to perform model acceptance tests in laboratories. The Kaplan turbine that will be tested is not a model turbine but a full scale prototype. This implies that the testing will be performed as on a model turbine according to the IEC 60193 standard, but the scaling to prototype is not necessary.

3.1 Efficiency test

Total efficiency(3.3) is defined as the amount of mechanical power delivered by the turbine shaft relative to the total available hydraulic power. The total efficiency can be divided in hydraulic efficiency(3.1) and mechanical efficiency(3.2), where hydraulic efficiency is defined as mechanical power transmitted from the runner through bearings and couplings to the shaft relative to the available hydraulic power. The mechanical efficiency is defined as power delivered by the shaft relative to the mechanical power.

Hydraulic efficiency:

$$\eta_h = \frac{P_m}{P_h} \quad (3.1)$$

Mechanical efficiency:

$$\eta_m = \frac{P}{P_m} \quad (3.2)$$

Efficiency:

$$\eta = \eta_h \cdot \eta_m = \frac{P}{P_h} \quad (3.3)$$

To calculate the efficiency of the turbine torque (T_m), rotational speed (n), volume flow (Q) and pressure has to be measured. Also the gravity constant (g) and the density (ρ) of the water have to be calculated in order to find the efficiency. The mechanical power is calculated with equation(3.4).

$$P_m = 2\pi \cdot n \cdot T_m \quad [W] \quad (3.4)$$

The hydraulic power is calculated with equation(3.5) where index 1 indicates that the density and volume flow is measured at the high pressure and inlet side of the turbine. E is the specific energy calculated with equation(3.6).

$$P_h = E \cdot (\rho Q)_1 \quad [W] \quad (3.5)$$

$$E = \frac{P_{abs1} - P_{abs2}}{\bar{\rho}} + \frac{v_1^2 - v_2^2}{2} + (z_1 - z_2) \cdot g \quad [J] \quad (3.6)$$

Index 2 refers to the outlet and low pressure side of the turbine (2), (3).

3.2 Cavitation test

Cavitation is formation of water vapour bubbles in water with low pressure which implodes and condensates when the bobbles enter a region with higher pressure. The creation of water vapour bobbles happens when the pressure in the water drops below the vapour pressure. When the pressure in the water rises above the vapour pressure again the vapour bubbles condensates in fractions of a second. When this happens a small jet of water is created from the bubbles. If the bubbles condensates and collapse near a surface and the jet from the water hits the surface, small fractions of the surface may be destroyed leaving small “craters”. This type of cavitation is called erosion cavitation.

Thoma number:

$$\sigma = \frac{NPSE}{E} \quad (3.7)$$

In hydro power cavitation can be a big problem and lower the efficiency by several per cent. Low pressure zones are created in the outlet of turbines with draft tubes and that use pressure differences to produce energy.

The Net Positive Suction specific Energy is defined according to the IEC standard (3) as follows:

$$NPSE = \left[\frac{p_2}{\rho} + gZ_2 + \frac{C_2^2}{2} \right] - \frac{p_v}{\rho} - gZ_{ref} \quad \left[\frac{J}{kg} \right] \quad (3.8)$$

Where C_2 is defined as the mean velocity at point 2 found by Q/A_2 . P_v is the vapour pressure at Z_{ref} .

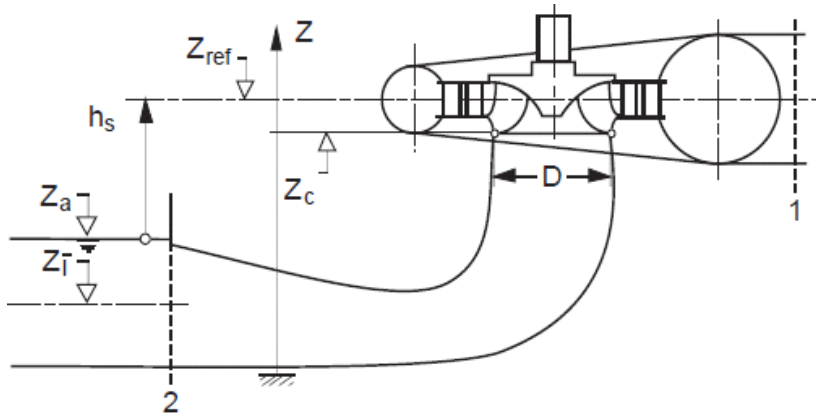


Figure 3-1 Definition of heights

By studying equation (3.8) and (3.6) it becomes clear that the Thoma number is simply related to the height difference h_s also referred to as the diving of the turbine.

When testing for cavitation the IEC standard suggests that the specific energy coefficient, see equation(3.9), is kept constant while the Thoma number is slowly reduced while the efficiency is logged.

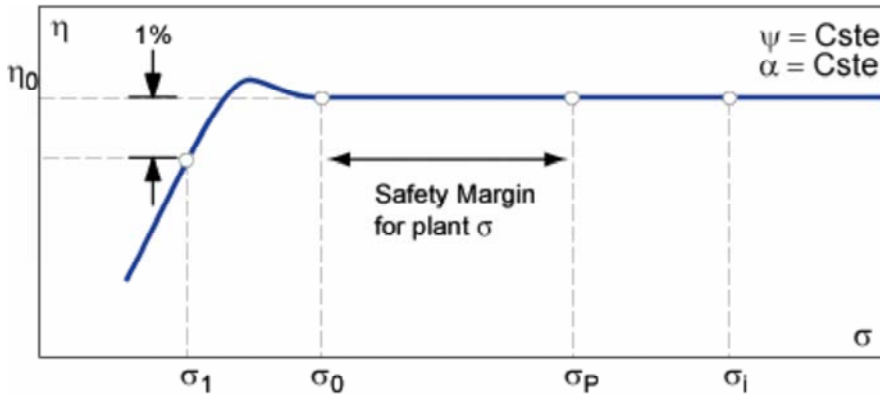


Figure 3-2 Efficiency curve with changing Thoma number

When lowering the Thoma number the efficiency will keep constant until it reaches σ_0 is reached. Here the efficiency will increase because of the

lubrication effect the cavitation bubbles have on the runner blades before the efficiency falls drastically.

$$\psi_c = \frac{2NPSE}{\omega^2 R^2} \quad (3.9)$$

3.3 Runaway speed

Runaway speed is defined as when $\eta_h=0$ and $P_{ED}=P_{ND}=0$ (3). The runaway speed is the highest achievable rotational speed the turbine can reach. When the efficiency is equal to zero all the available energy in the water is used to overcome centrifugal and friction forces in bearings and other components. Due to the friction torque in bearings the real runaway speed cannot be tested. To find the maximum runaway speed the tests should be done under the worst setting combinations for the turbine. If the tests are not tested under plant conditions cavitation have to be evaluated.

Runaway speed is found by increasing the RPM until hydraulic efficiency becomes zero.

Because of heat generation in the upper bearing runaway test could not be carried out in this thesis. Discussion of the heat generation in the upper bearing is found in chapter 7.3.

3.4 Calibration

Calibration of measuring equipment is done to minimize error in measurements. Calibration of measuring equipment is done according to the IEC (3). When calibrating equipment the measuring range of the equipment has to be known and the operating range of the turbine has to be known.

The equipment is calibrated by measuring a number of values outside and inside the range the actual testing will be carried out in against a known quantity. The values measured are given as a Volt signal that has to be correlated with the actual unit measured. By measuring values for the entire range linear regression is used to find a calibration line that the Volt signal is calibrated against to minimize the error. By increasing the number of values measured during calibration in the upper and lower range the uncertainties in the equipment is reduced.

The equipment calibrated in this case is pressure gauges, a flow meter and a torque gauge.

3.5 Pressure gauge

The pressure gauge was calibrated with an electronic pressure calibrator, Druck DPI601. This electronic calibrator uses air as fluid between the device that should be calibrated and itself. By using air the height difference between the calibrator and the device to be calibrated can be ignored and is not important because the surrounding pressure can be seen as constant as atmospheric pressure, so there will be now uncertainty in the measured value because of height difference. The DRUCK DPI2345 comes with a pre calibrated. The calibration certificate is found in Appendix I.

The electronic calibrator has a small pump to increase the required pressure and a valve that reduces pressure. The pressure can easy be adjusted with four digits in bar.

3.6 Torque gauge

The torque gauge was calibrated with the dead weight method. The dead weight calibration is carried out by adding weights with a known weight. The weights used are calibrated by the Norwegian Justervesen. The calibration certificate of the weights is found in Appendix J. An arm is mounted on the shaft and a weight bed is attached to the arm. They calibrated weights are placed one at a time in the bed and the volt signal from the torque gauge is recorded for every new weight added. It is important to calibrate the torque gauge for its intended measuring range and with a large number of calibration points to get as low uncertainty in the calibration as possible.



Figure 3-3 The dead weight calibration setup

When calibrating the torque gauge the measurements tended to deviate from each other even when the same dead weights were used. This was discovered when the measured value kept almost constant when weights were added or removed from the weight bed. It was quickly discovered that this was caused by friction between the runner blades and the housing and fixed by running the turbine until there was clearance between the blades and the housing. To secure that there were no friction affecting the measurements, values were measured first by adding weights in the entire calibration range and then values were measured when removing weights.

When the weights were added to the weight bed the measured volt value always was lower than the same volt value measured for the same weight when weights were removed from the weight bed. In Figure 3-4 the calibration curve and the actual values measured can be seen. This phenomenon is called hysteresis and is present in ferromagnetic materials. Ferromagnetic materials have “memory” due to magnetic properties in the material (4). Hysteresis is a common phenomenon in torque measurements.

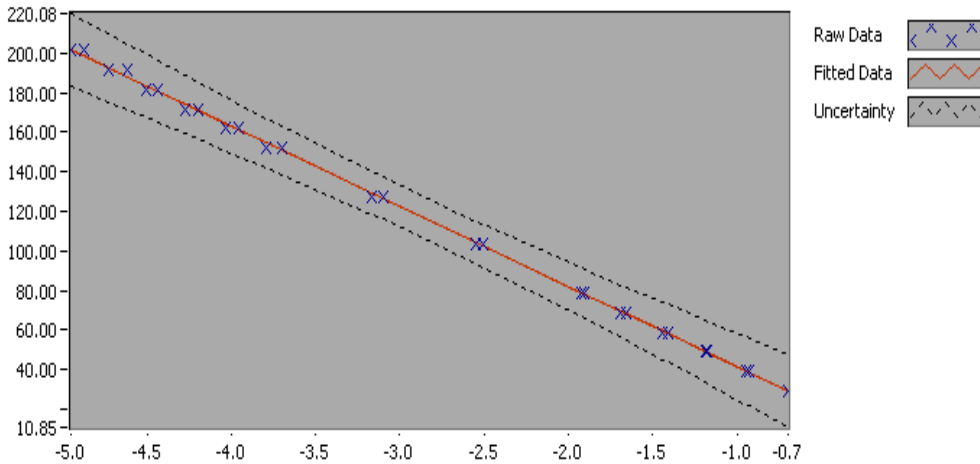


Figure 3-4 Calibration curve for the torque gauge

The calibration was performed two times both times resulting in the same values and hysteresis in the measurements was proven. The calibration report of the torque gauge is found in Appendix Q

3.7 Trip meter

There is now know method to calibrate the trip meter, it is only depending on time and is recording a pulse every time a reflex ribbon passes the sensor. The time between every pulse is measured and the rotational speed is calculated.

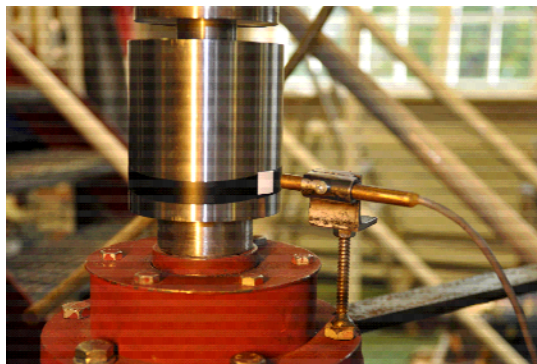


Figure 3-5 Trip meter and reflex ribbon ready to use

The trip meter is mounted on the turbine shaft as displayed in Figure 3-5 Trip meter and reflex ribbon ready to use.

3.8 Flow meter

A Krohne AQUAFLUX F6 was used to measure the volume flow in the Kaplan rig. It is an electromagnetic flow meter.

The flow meter was calibrated using the weighing method. The weighing method is a primary method with a high level of accuracy. The calibration procedure is given in the ISO standard (5). The standard is to lead water into a weighing tank with known initial weight, the time is taken over the interval when water is lead into the tank, the volume flow is found with the weight difference divided on the time interval water is lead into the tank.

$$q_v = \frac{m_2 - m_1}{\rho \cdot t} \cdot (1 - \varepsilon) \quad (3.10)$$

$$\varepsilon = \rho_a \left(\frac{1}{\rho} - \frac{1}{\rho_p} \right) \quad (3.11)$$

The last term in equation (3.10) is the correction factor for correction different in buoyancy exerted from the atmosphere on the measured water and the weights used during calibration of the weighing tank. ρ_a , ρ_p and ρ is respectively the density of the atmosphere, standard weights and water.



Figure 3-6 The flow meter use in the test

A LabView program created by Remi Andre Stople was used to log the volume flow. The program logged 1000 values from the flow meter every second. The regression line was found using built in functions in excel while uncertainties

linked to the measurements were calculated in Matlab. The flow meter is placed in a long straight section of the pipeline.

3.9 Frequency analysis

The frequency of any fluctuating signal can be analysed and assessed by a discrete Fourier Transform. Anders Tørklep has in his project thesis developed a program to analyse measured data. Remi A. Stople has used this program to evaluate the measured data in this project. The results of this analysis is presented in chapter 9.6.

3.10 LabView program

LabView was used to log data during tests and calibration. How the LabView programs used work are described in Appendix G

3.11 Clearance water test

A turbine may have leakages in seals and other components. Water not utilised by the turbine is regarded as loss in efficiency and is therefore important to document.

The clearance water measurements was done by filling a bucket with the clearance water for 60 seconds and then the weight difference between before and after the filling was found giving the volume flow. Measurements were done for constant pressure head and rotations per minute.

3.12 Risk Assessment

In order to perform tests at NTNU a risk assessment of the test rig has to be carried out. The risk assessment reveals potential risk to human and other instalments in the laboratory related to the test rig. The risk assessment is found in Appendix K

4 Uncertainties in measuring

All measurements have uncertainties attached to them. Uncertainties can be related to three types of error in measurements, error caused by spurious, random or systematic error.

4.1 Spurious error

Error that causes unreliability can be human errors or default errors in instruments. These types of error can make the measurements worthless. An example of a spurious error is air trapped in a lead from a water line to a manometer. If the error is of significant value, the measurement has to be repeated or discarded.

4.2 Random error

Small numerous independent happenings can influence a series of measurements, this is called random errors. They cause the values in the measurements carried out to deviate from each other and vary around a mean value when the input is constant. The values normally deviate from the mean value within the rules of probability for normal distribution, when the number of measurements carried out increases. The area of uncertainties of random errors is based on statically methods and can be calculated using the same methods as for systematic errors.

4.3 Systematic error

You cannot reduce systematic errors by increasing the number of measurements, unless you change the equipment and the conditions for the measurements, because systematic errors have the same magnitude for every measurement at the same operation point. Systematic errors are errors that still are present in the equipment and the measuring system after the calibration is done. Systematic errors should be eliminated before the measuring starts. This should be done by calibrating the equipment against another system, measuring dimensions and by installing equipment correctly. But even if all this is done extremely precise there will always be errors remaining in the system, these errors are called systematic errors.

The total systematic error can be found by combining the systematic error from each measuring device with the root-sum-square method. When calculating the uncertainty connected to the measurement a confidence interval of 95% should be used according to the standard. The root-sum-square method is expressed in equation(4.1).

$$f_s = \sqrt{\sum f_Y} \quad (4.1)$$

Here f_s is the combined uncertainty of each device in the system where the uncertainty in each component is f_Y . The uncertainty can either be known from the manufacturer of each device or it can be calculated. To calculate the uncertainty n number of measurements is taken at a constant operation point and the standard deviation is found with equation(4.2) (6) and (7).

$$s_Y = \sqrt{\frac{\sum_{r=1}^n (Y_r - \bar{Y}_r)^2}{n-1}} \quad (4.2)$$

\bar{Y}_r = mean value of measurements

Y_r = value of r th measurement

n = number of measurements

After the standard deviation is calculated the uncertainty in the standard deviation can be calculated. Since the error have a normal distribution but there are not an infinite number of measurements student-t distribution can be assumed. Student-t values can be found in table L-2 in IEC 60193 (3).

$$e_Y = \pm \frac{t \cdot s_Y}{\sqrt{n}} \quad (4.3)$$

The uncertainty in standard deviation is reduced as the number of measurements increases. Finally the uncertainty with a confidence level of 95% can be calculated. e_Y is the absolute uncertainty while f_Y is the relative uncertainty.

$$f_Y = \frac{e_Y}{Y} \quad (4.4)$$

4.4 Total uncertainty

f_T is found by combining random and systematic error. If they have the same probability distribution the total uncertainty is found in the same way as we calculate the total systematic error. The total uncertainty then has a distribution with probability that the true value of a measurement lies within a probability area of 95%.

$$f_t = \pm\sqrt{f_r^2 + f_s^2} \quad (4.5)$$

4.5 Uncertainties in the Calibration

During calibration there are different sources that can lead to uncertainties. The IEC 60193 standard has defined the different errors in chapter 3.9 and they are repeated in Table 1 in this thesis. The total uncertainty is found as explained in chapter 4.4 with combining the different uncertainties and the root-sum-square method (RSS method).

| Error | Description |
|-----------|--|
| $\pm f_a$ | Systematic error of the primary calibration method |
| $\pm f_b$ | Random error of the primary calibration method |
| $\pm f_c$ | Systematic error of the secondary equipment |
| $\pm f_d$ | Random error of the secondary equipment |
| $\pm f_e$ | Physical phenomena and external influences |
| $\pm f_f$ | Error in physical properties |

Table 1 Component errors

4.5.1 Uncertainties in the calibration of the flow meter

The errors that contribute to the uncertainties in the calibration of the flow meter are listed in Table 2. The calculation of the uncertainties is found in Appendix A.1

| Uncertainty | Description | Value |
|--------------------|---|-------------------|
| $f_{Q,a}$ | Systematic error in the weighing tank system | $\pm 0.072104\%$ |
| $f_{Q,b}$ | Random error in the weighing tank system | $\pm 0.0565366\%$ |
| $f_{Q,regression}$ | Systematic and random error in the instrument | $\pm 0.03404\%$ |

Table 2 Uncertainties in the calibration of the flow meter

By using the RSS-method the relative uncertainty for the calibration is calculated as follows for the highest efficiency point:

$$f_{Q,cal} = \pm \sqrt{f_{Q,a}^2 + f_{Q,b}^2 + f_{Q,regression}^2} = \pm 0.097745\% \quad (4.6)$$

The calibration curve with a confidence interval of 95% for the volume flow meter is shown in Figure 4-1. The Matlab programs used are found in Appendix C.

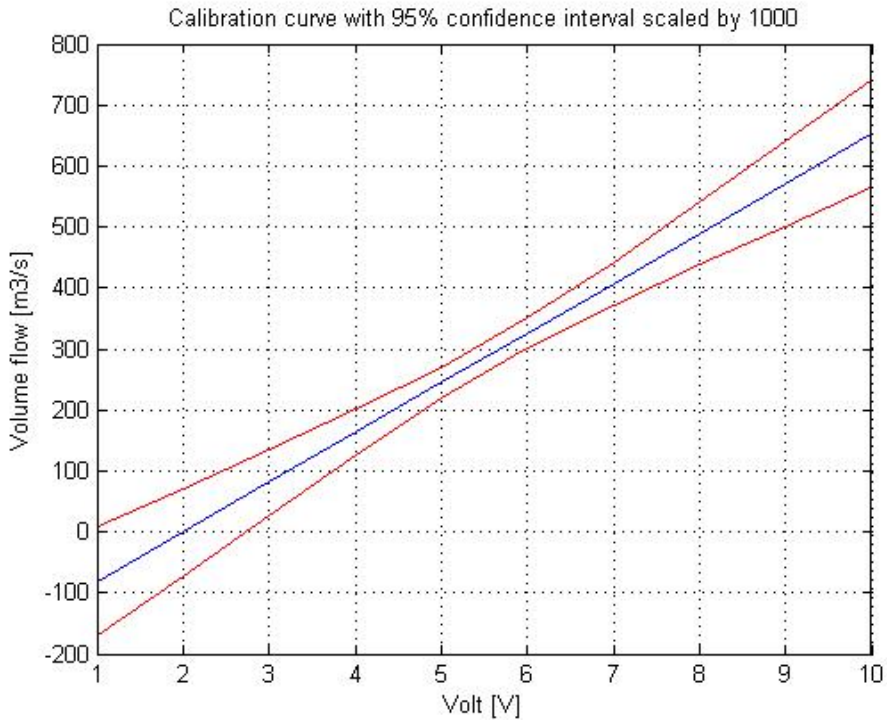


Figure 4-1 Calibration curve with a 95% confidence interval

4.5.2 Uncertainties in the calibration of the pressure gauge

The pressure gauge was calibrated against the electronic pressure calibrator with known systematic uncertainty f_a of 0.000% given in the calibration report. But the calibration of the calibrator was performed in 1996 and an uncertainty of $\pm 0.01\%$ is therefore used in this report. This uncertainty is included in the regression uncertainty found in the calibration report. The calibration certificate for the Druck DPI601 is found in Appendix I.

$f_{p,c}$ which is the random error in the instrument caused by scatter in the measured signal. When calibrating the instrument the signal is logged over time and the mean value of the signal for a constant pressure is used. The uncertainty due to scatter in the signal is included in the $f_{p,regression}$. Also the $f_{p,c}$ is included in the $f_{p,regression}$.

The calibration curve for the pressure gauge is shown in Figure 4-2. The calibration report can be found in Appendix L.

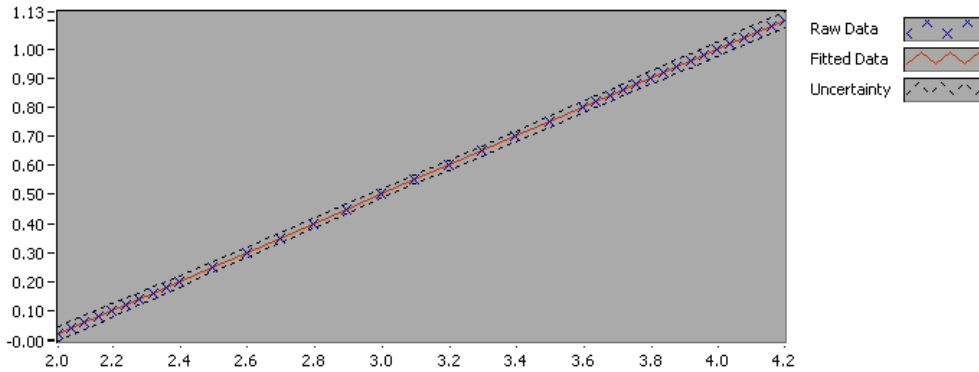


Figure 4-2 Calibration curve for the pressure gauge with a 95% confidence interval

f_e which is the error caused by physical phenomena and external influences can for the pressure gauge be temperature changes within the instrument. Since the pressure gauge had been located in the waterpower laboratory many days before the calibration was conducted the temperature within the instrument was assumed to be in equilibrium with the surrounding temperatures. f_e was therefore assumed neglect able.

$f_{p,f}$, the error in physical properties is for the calibration of the pressure gauge assumed to be neglected. This is because the pressure gauge was calibrated against air and the height difference between the pressure gauge and the electronically instrument do not contribute to pressure differences.

| Uncertainty | Description | Value |
|--------------------|--|------------------|
| $f_{p,a}$ | Systematic error in the electronic pressure calibrator | $\pm 0.010\%$ |
| $f_{p,regression}$ | Systematic and random error in the instrument | $\pm 0.066751\%$ |
| $f_{p,f}$ | Systematic error in the positioning of the pressure gauge. | $\pm 0.000\%$ |

Table 3 Uncertainties in the calibration of the pressure gauge

With the use of the RSS-method the relative uncertainty of the calibration of the pressure gauge was found to be:

$$f_{p,cal} = \pm\sqrt{f_{p,regression}^2} = \pm 0.066751\% \quad (4.7)$$

4.5.3 Uncertainties in the calibration of the torque gauge

Errors contributing to the maximum relative uncertainty for the calibration of the torque gauge are $f_{\tau,arm}$, $f_{\tau,weights}$, f_c and f_d . f_c and f_d is combined with the RSS-method to be $f_{\tau,regression}$. All calculations of uncertainties in the calibration of the torque gauge are found in Appendix A. The calibration report is found in Appendix M.

| Uncertainty | Description | Value |
|-----------------------|--|-------------------|
| $f_{\tau,w}$ | Systematic error in weights and the weight bed | $\pm 0.0114325\%$ |
| $f_{\tau,arm}$ | Systematic error in the length of the arm | $\pm 0.2\%$ |
| $f_{\tau,regression}$ | Systematic and random error in the instrument | $\pm 1.235138\%$ |

Table 4 Uncertainties in the calibration of the torque gauge

By combining the given errors with the RSS-method the relative uncertainty for the calibration in best efficiency point for the torque gauge was found to be

$$f_{\tau,cal} = \pm\sqrt{f_{\tau,w}^2 + f_{\tau,arm}^2 + f_{\tau,regression}^2} = \pm 1.25128\% \quad (4.8)$$

In Figure 4-3 the calibration curve for the torque gauge is presented. As seen in the figure the calibration is affected by hysteresis. Hysteresis is a phenomenon which is normal for torque gauges. The measured value has a “memory” from the previous measurement. This means that if for instance the torque gauge measures a higher value for one given value if the previous measurement had a higher value than if the previous measured value was lower.

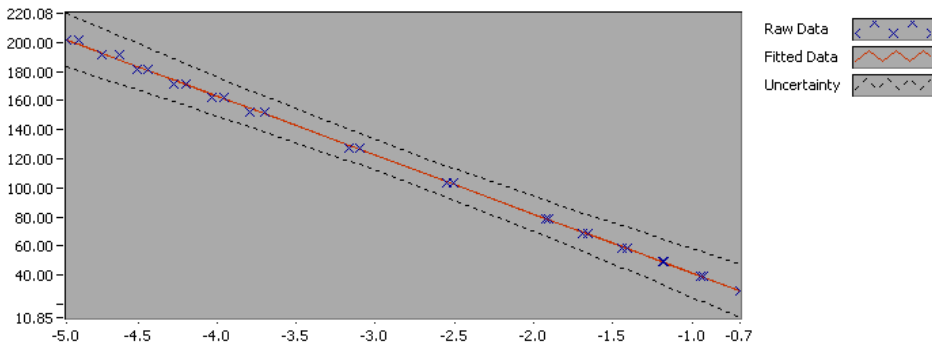


Figure 4-3 Calibration curve for the torque gauge with a 95% confidence interval

In Figure 4-3 you can see the hysteresis because the raw data seems to be given in pairs. The actual case is that the raw data with the lowest volt value (*here low value is less negative than a high value*) is measured with adding more weights, hence from a lower value, and the raw data with the highest volt value is measured from a higher value.

4.5.4 Uncertainty in calibration of the thermometer

The thermometer is calibrated by the manufacturer. The uncertainty of the thermometer is $\pm 0.001^{\circ}\text{C}$ and with test temperatures around 20°C this results in an uncertainty of $\pm 0.005\%$

4.6 Uncertainties in the tests

Even if the calibration is done according to the standards errors will occur in the test measurements which will lead to uncertainty. After the tests were performed the total uncertainty was calculated. The total uncertainty is a combination of uncertainty in the calibration and in the tests.

4.6.1 General uncertainty in the tests

$f_{p,h}$ is error caused by drift in the output signal over time from the measuring equipment. To check for drift the first test series was retested after all the other series were tested. As seen in Figure 4-4 the last test series has a slightly higher efficiency than the first series especially for low pressure head. If Figure 4-5 is studied in correlation with Figure 4-4 it becomes clear that the increase in efficiency in the last series is caused by an increase in volume flow. The increase in volume flow is most certain caused by inaccuracy in the positioning

of the runner blades when setting the position after it had been tested in setting two causing the blades to have a steeper angle of attack in the last run compared to the first run.

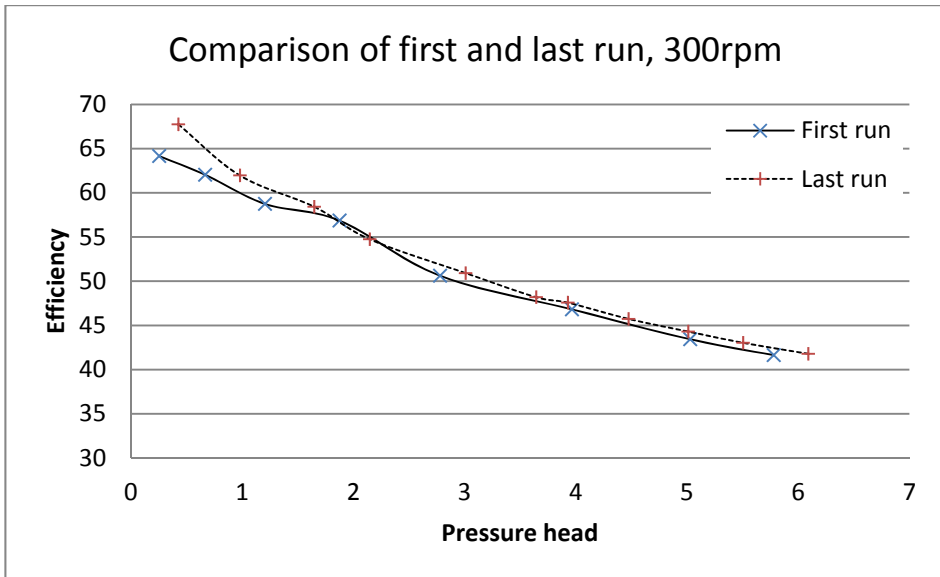


Figure 4-4 Test for drift in measurements 300rpm, setting 1

By analysing the two graphs it is concluded that the measurements are unaffected by drift so that the uncertainty related to drift is neglected.

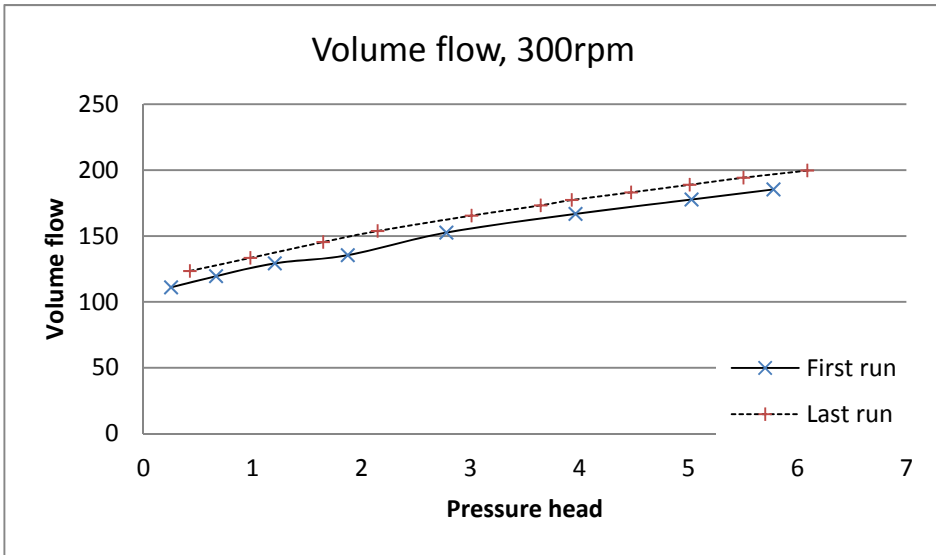


Figure 4-5 Test for drift in measurements 300rpm, setting 1

| Error | Description |
|---------------|--|
| $\pm f_{cal}$ | Systematic error in the calibration |
| $\pm f_h$ | Additional systematic error in the instrument |
| $\pm f_j$ | Error in physical properties |
| $\pm f_{ks}$ | Systematic error due to physical phenomena and external influences |
| $\pm f_{kr}$ | Random error due to physical phenomena and external influences |
| $\pm f_l$ | Random error in repeatability of secondary equipment |

Table 5 Errors in the tests

f_h is presented above Table 5 and can be present in all the measuring devices. But for the tests conducted in this report drift is not present and the uncertainty is therefore neglected in the following calculations.

4.6.2 Uncertainty in the pressure measurements

The uncertainties in the pressure measurements must be divided into two different uncertainties $f_{p,1}$ and $f_{p,2}$ which are the uncertainties linked to the inlet and the outlet pressures. Detailed calculations are found in Appendix A.

f_{cal} is the uncertainty from the calibration of the pressure gauge. The uncertainty is not a constant value but varies with the operation state. The

pressure transducer was calibrated against air but during tests the operating fluid is water. This creates an uncertainty in the measured inlet pressure value.

The systematic error due to an offset of 4.65cm in the pressure transducer placement relative to the centre of the pipe is denoted as $f_{p1,offset}$. The systematic uncertainty is calculated to be with an offset of 4.65cm while the error in the ruler used was ± 0.2 cm which give an $f_{p1,offset}$ of $\pm 0.7853\%$ for the pressure measured at the given operation conditions of 500rpm and 0.25468meter pressure head.

$f_{p1,l}$ is calculated with a student-t confidence interval on the measured data from the tests. A Matlab program was created to do the calculations and is found in Appendix C. The random uncertainty for test series 500rpm in setting 2 was calculated to be $\pm 10.6552\%$. This value is extremely high and is caused by severe fluctuations in the pressure readings. This will be discussed in chapter 9.6.

The total relative uncertainty in the pressure measurements was calculated with the RRS-method to be

$$\begin{aligned} f_{p1} &= \pm \sqrt{f_{p,cal}^2 + f_{p1,l}^2 + f_{p1,z}^2} = \pm 10.6843\% \\ f_{p2} &= \pm \sqrt{f_{p,H}^2 + f_{p,flotation}^2 + 2f_{v2}^2} = \pm 3.0633\% \end{aligned} \quad (4.9)$$

It is clear that the relative uncertainty in the outlet pressure measurements is much higher than the relative uncertainty in the inlet pressure measurements. This is because of the equipment used to calculate the pressure. While the inlet pressure is calculated with costly equipment the outlet pressure is measured with cheap “homemade” equipment with a high level of uncertainty.

4.6.3 Uncertainty in the torque measurements

As for the pressure measurements f_{ks} and f_{kr} are ignored, $f_{t,j}$ is also ignored. The errors that influence the torque measurements are listed in table 6.

| Uncertainty | Description | Value |
|----------------|-------------------------------------|-----------------|
| $f_{\tau,cal}$ | Systematic error in the calibration | $\pm 1.25128\%$ |
| $f_{\tau,l}$ | Random error in the measurements | $\pm 0.0312\%$ |

Table 6 Uncertainties in the torque measurements

By combining the two uncertainties with the RRS-method a total uncertainty in the torque measurements is found:

$$f_{\tau} = \pm \sqrt{f_{\tau,cal}^2 + f_{\tau,l}^2} = \pm 1.2516\% \quad (4.10)$$

It is clear that the uncertainty linked to the calibration of the torque gauge is dominant in the test uncertainty.

4.6.4 Uncertainty in the volume flow measurements

The errors causing uncertainties in the volume flow measurements are the same as for the errors in the torque measurements and they are calculated with the same equations and the same Matlab program as in the pressure measurements.

| Uncertainty | Description | Value |
|-------------|-------------------------------------|------------------|
| $f_{Q,cal}$ | Systematic error in the calibration | $\pm 0.097745\%$ |
| $f_{Q,l}$ | Random error in the measurements | $\pm 0.0394\%$ |

Table 7 Uncertainties in the volume flow measurements

When combined the $f_{Q,l}$ and $f_{Q,cal}$ give a total uncertainty in the volume flow of:

$$f_Q = \pm \sqrt{f_{Q,cal}^2 + f_{Q,l}^2} = \pm 0.105387\% \quad (4.11)$$

4.6.5 Uncertainty in the rotational speed measurements

There is now method available to calibrate an optical speed counter. The IEC standard (3) gives a systematic uncertainty of $\pm 0.05\%$ used in this thesis. The

random uncertainty in the rpm measurements was calculated to be $\pm 0.0363\%$. This gives a total uncertainty in the rotational measurements of

$$f_{rot} = \pm \sqrt{f_{IEC}^2 + f_{rot,l}^2} = \pm 0.061787\% \quad (4.12)$$

4.6.6 Uncertainty in the calculation of density of water

The density of water is calculated as a function of pressure and temperature and the uncertainty in the calculation of the density is $\pm 0.01\%$ (8). This uncertainty is ignored because it is too small to have influence on the total hydraulic uncertainty.

4.6.7 Total uncertainty in the hydraulic efficiency

The total uncertainty of hydraulic efficiency can be calculated with the RSS-method combining all the different uncertainties and is given in equation(4.13). The equation is derived from equation(3.1).

$$f_{\eta_h} = \pm \frac{(e_{\eta_h})}{\eta_h} = \pm \sqrt{(f_Q)^2 + (f_E)^2 + (f_P)^2} \quad (4.13)$$

To find the different uncertainties in equation(4.13) the equations following is used and explained. f_Q is found in chapter 4.6.4. Uncertainties in the density and the gravitation constant are assumed to have a so small value that they can be neglected. Uncertainty in g is 0.01milliGal stated in the calibration report of measured gravity in the laboratory.

$$f_E = \pm \frac{e_E}{E} = \pm \frac{\sqrt{\left(\frac{e_{p1}}{\bar{\rho}} + \frac{e_{p2}}{\bar{\rho}}\right)^2 + (g \cdot e_{z_1})^2 + (g \cdot e_{z_2})^2 + \left(\frac{e_{v_1^2}}{2}\right)^2 + \left(\frac{e_{v_2^2}}{2}\right)^2}}{\frac{p_1 - p_2}{\bar{\rho}} + g(z_1 - z_2) + \frac{v_1^2 - v_2^2}{2}} \quad (4.14)$$

The uncertainty in energy in equation(4.14) is given as absolute uncertainties while in this thesis relative uncertainties are used. In equation(4.15), (4.16) and (4.17) the relation between absolute and relative uncertainty is given.

$$e_p = (p) \cdot f_p \quad (4.15)$$

$$\frac{e_{v^2}}{2} = v^2 \cdot f_v \quad (4.16)$$

$$f_v = \pm \sqrt{f_Q^2 + 2 \left(\frac{e_r}{r} \right)^2} \quad (4.17)$$

Next the uncertainty in pressure is found by using equation(4.18). When this is done the total uncertainty can be calculated using equation(4.13).

$$f_p = \pm \sqrt{(f_r)^2 + (f_\omega)^2} \quad (4.18)$$

$$f_\omega = f_{rot} \quad (4.19)$$

The total relative uncertainty in the hydraulic efficiency is calculated with data from setting 2 at 500rpm. The reason for choosing values from 500rpm and setting 2 is because this is the setting closest to the best design setting which is according to Anders Austgård setting 3 and 490rpm. For a detailed calculation of the total relative uncertainty see Appendix A.

The total relative uncertainty in the hydraulic efficiency is calculated to be

$$f_{\eta h} = \pm 2.2145\%$$

5 Test rig setup

The waterpower laboratory provides two different alternative loops to test the Kaplan turbine. Alternative one is an open loop where water is pumped from the lower reservoir and up to the upper reservoir, which is a free water channel where the water is in open air at atmospheric pressure. From the upper reservoir the water runs through the turbine and down into the lower reservoir. Alternative two is also an open loop but differ from alternative one because water is pumped from the lower reservoir into a pressure tank. From the pressure tank the water is run through the turbine and back down to the lower reservoir.

Alternative one has a maximum gross head of 16 meters while alternative two can deliver a gross head up to 100 meters. The head in alternative one is regulated through an energy dissipater while alternative two regulates the head by changing the rotational speed of the pump and by open and closing the air intake on the pressure tank.

Remote Hydrolight represented by Anders Austgård have requested that the turbine is tested with a volume flow ranging from 90 litres per second to 590 litres per second and a pressure head ranging from 1 to 10 meters. In order to meet the requirement alternative two has to be chosen. This is because alternative one has a too low gross head to be able to deliver the desired volume flow and effective head. Alternative one have 16 meters gross head while the effective head would be significantly lower because of losses in bends and area change in the pipeline. Alternative two also have the advantage of easier volume flow regulation compared to alternative one.

5.1 Detailed description of the rig

A pipe with diameter of 600mm leads out of the pressure tank, the pipe is quickly reduced down to a pipe diameter of 200mm. The flow meter is connected to the 200mm pipe. After the flow meter the pipe continuous with a diameter of 200mm before the diameter is expanded to 400mm. The 400mm pipe is connected with the turbine which also has a diameter of 400mm. At the end of the 400mm pipe four taps is mounted which is connected to the pressure gauge. They are mounted to measure the pressure in front of the turbine in order to be able to calculate the efficiency of the turbine.

The rig is controlled and run with one laptop which controls the pump and a pc that log data and a box that controls the rotational speed of the generator. This “control station” is located next to the turbine. The pumps are originally controlled from the control room located on the second floor in the water power laboratory. The Kaplan turbine and the control station are located on the first floor. Remote desktop enables control of the pumps via the laptop in the control station.

During calibration of the volume flow meter the 200mm pipe is connected directly to the 600mm pipe that leads to the weight tank. This implies that the water circuit do not run though the turbine.

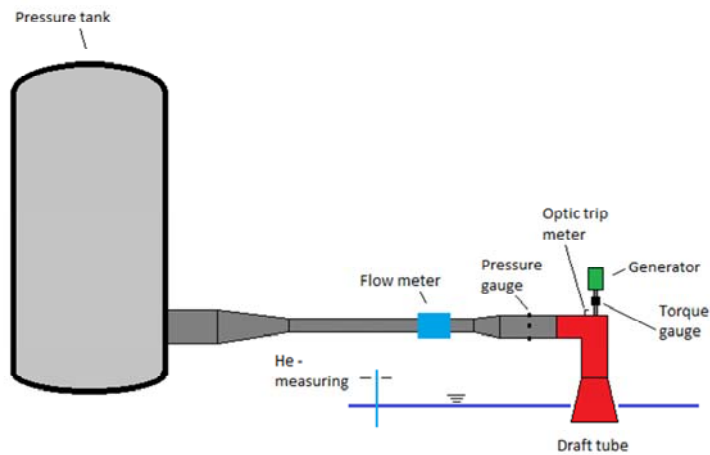


Figure 5-1 Test rig setup

The under water level is determined with the use of a floating cylinder which follows the under water level. The floater is placed some distance from the outlet to not be disturbed by air in the water coming out of the draft tube.

The trip meter is mounted on the top of the turbine while the reflex ribbon is placed on the shaft.

The torque gauge is placed in the middle of the turbine and the generator on the shaft.

6 The Afghani Kaplan turbine

The Kaplan turbine studied in this master thesis is designed by Anders Austegård. The turbine is meant to provide small villages in Afghanistan with electricity. It is designed with the thought that it should be easy to manufacture with simple means and tools. This implies that some choices made in the design not are optimal for the efficiency and the load range of the turbine. There are for example no spiral casing or adjustable guide vanes in the design.

6.1 The Turbine design

In front of the runner blades curved plates are welded in a fixed position to create spin in the water flow acting as guide vanes. This makes this Kaplan turbine a single regulated Kaplan turbine.

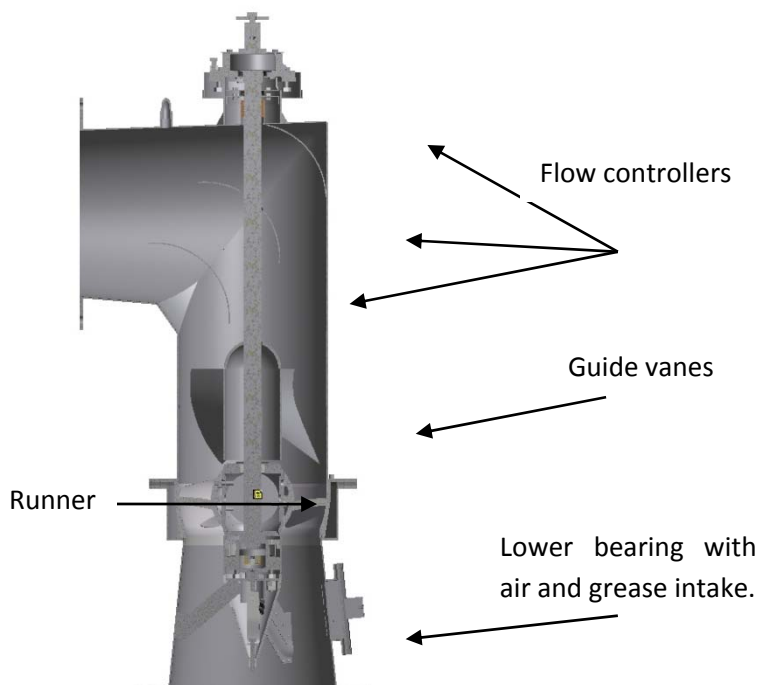


Figure 6-1 Complete turbine, (Inventor drawing)

The inlet pipe has a 90 degree bend in front of the guide vanes, this is unfortunate and can cause turbulent and a chaotic flow right in front of the

turbine. In order to reduce this three bent plates are placed in the 90 degree bend acting as flow controllers in a cascade.

The runner consists of four blades mounted on a cube. Four blades are chosen simply because a frame with 90 degrees angles is easier to make than a frame with five or six sides. If the runner is placed off centre the runner blades will interfere with the outer casing in sections of the revolution, this may break the turbine or cause severe efficiency losses. It is also important that the runner is placed dead centre to reduce leakage between the runner blades and the outer casing. The runner is produced with a diameter a fraction wider than the inner diameter of the outer casing. At first start up the blades should quickly be grounded down to fit the outer casing perfectly which minimizes the leakage.

Underneath the runner the lower bearing is placed. The bearing housing is shaped as a cylinder and a cone. The lower bearing is held in place by three support fins. The pressure after the runner can be lower than the ambient pressure; this means that water can be sucked into the lower bearing. To avoid this air is sucked in through a small tube in one of the fins from outside the draft tube. Grease is injected into the bearing through the same fin as air is sucked through. If water enters the lower bearing it can lead to corrosion and the bearing break down because of sand particles in the water.

6.2 Specifications

According to Anders Austegård the turbine is designed for an effective head ranging from 1.5 meters to 6 meters and a volume flow from 0.09 to 0.41m³/s. He has also given an estimated flow table and estimated the cavitation number to be 0.7.

| Head [m] | Minimum volume flow [m ³ /s] | Optimal volume flow [m ³ /s] | Maximum volume flow [m ³ /s] |
|----------|---|---|---|
| 1.5 | 0.09 | 0.18 | 0.21 |
| 2 | 0.11 | 0.21 | 0.24 |
| 3 | 0.13 | 0.26 | 0.29 |
| 4 | 0.15 | 0.30 | 0.34 |
| 6 | 0.18 | 0.36 | 0.41 |
| 8 | 0.21 | 0.42 | 0.47 |
| 10 | 0.23 | 0.47 | 0.53 |

Table 8 Volume flow

The minimum volume flow is estimated volume flow when the runner blades are fixed in setting 1, maximum volume flow is in setting 4 while optimal volume flow is obtained in setting 3.

6.3 Main dimensions

The main design characteristics of the turbine are presented in Table 9. The values presented in table 9 are design values, not measured values.

| Turbine characteristics | |
|--------------------------------|------------------------|
| BEP effective pressure head | 2 m |
| BEP volume flow | 0.21 m ³ /s |
| BEP rpm | 490 rpm |
| Runner diameter | 0.345 m |
| BEP setting | 3 |

Table 9 Main turbine characteristics

6.4 Runner blade design

Anders Austegård has designed the runner blades used in the turbine. In Appendix N the some of the calculation procedures are presented. The formulas presented are used in an Excel sheet and results from the calculations in the work sheet are exported into Scilab. Scilab is a freeware program similar to Matlab. In Scilab the flow around the blade is calculated using potential flow theory presented in chapter 2.4. When the desired flow field is reached after an iterating process coordinates of the blade profile are exported into Inventor. Mechanical drawings can now be made and the runner blades can be produced.

The formulas used in excel are checked against formulas and equations given in Pumper and Turbiner (1) and found satisfying.

Designing a runner blade is extremely time consuming and demands a lot of work. The Scilab program Austegård have created could have been used create a new profile or a Matlab program could have been created.

The time demanded to get familiar with Austegårds work or create a Matlab program have been considered to be to high compared with the actual gain in performance of the runner. Austegård has been confronted with this and agreed that time rather should be used on optimizing the inlet bend.

7 Changes and limitations on the rig and turbine

Before and during tests a series of challenges were encountered making it difficult to calibrate and run the efficiency test on the Kaplan turbine. Many of the challenges encountered were of such character that they had to be improved and fixed before the calibration and the test could continue while others could be improved during operation. Some problems were time consuming and stopped operation of the rig for several days while improvements were made.

7.1 Pipe dimensions

The pressure tank has three pipes connected to it. All pipes have a diameter of 600mm. The only available volume flow meter was a flow meter with a diameter of 200mm. This meant that the pipe diameter had to be reduced from 600mm to 200mm. This was originally done by welding a pipe with a diameter of 200mm to a flat plate; see Figure 7-1 Original pipe section. The plate was connected to the pipe with a diameter of 600mm. The solution created a large area reduction over a small distance which created a stagnation point and forced a heavy acceleration in the water over the area reduction.

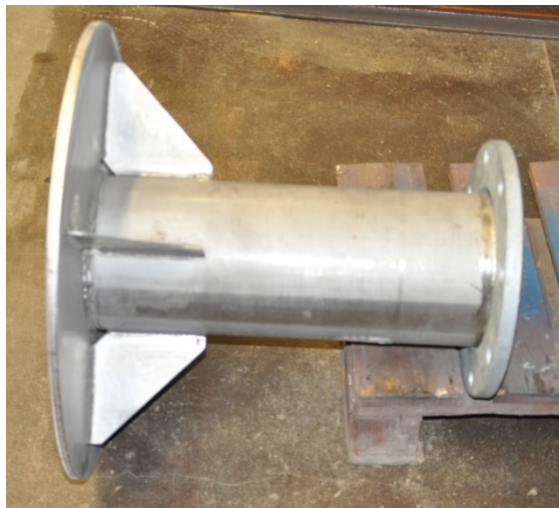


Figure 7-1 Original pipe section

When the calibration started it quickly became obvious that the large diameter reduction created heavy cavitation. This was problematic because the flow

meter is sensitive to air bubbles and noise. Cavitation creates both of these problems.

To be able to continue the calibration tests the area reduction had to be done smoother to avoid cavitation. There were no available pipe cones available with the right diameters in the waterpower laboratory. A new cone therefor had to be made reducing the diameter from 600mm down to 300mm. A cone reducing the diameter from 300mm to 200mm was available.

Plate steel with a thickness of 3mm was used to create the cone. Equation(7.1) with r_1 , r_2 , B_1 and B_2 was used to calculate the dimensions of the cone. B is the arc length that had to be cut to give the given radius, r.

$$\begin{aligned} B_1 &= r_1 \frac{\pi}{180^\circ} \beta \\ B_2 &= r_2 \frac{\pi}{180^\circ} \beta \end{aligned} \tag{7.1}$$

The finished cone mounted in the rig setup is shown in Figure 7-2. After the installation of the new cone the pressure head to be able to reach desired volume flow was drastically reduced and cavitation was eliminated in this pipe section.



Figure 7-2 Configured pipe section

Even though the cavitation was eliminated from the first pipe section with an area change cavitation still occurred during tests in another pipe section. The

inlet on the turbine has a pipe diameter of 400mm. Since the pipe diameter from the first area reduction is 200mm it demands a new area change to be able to connect the two diameters together. This area expansion is done immediately after a 90 degree bend a few meters in front of the turbine. The cavitation became so severe in setting two that the inlet pressure could not be increased as desired. The cavitation bubbles created in the expansion got so severe that they entered the turbine, making the tests invalid. Some of the measuring series performed in setting two is therefore stopped before a pressure head of 6 meters is reached.

7.2 Runner blade friction

The runner blades and the turbine housing should be produced such that the runner blades outer diameter is a fraction smaller than the housing diameter. This is done to reduce leakage hence reduce loss in hydraulic efficiency. Before the tests and the calibration the turbine therefore had to be run to tear the blades down so that there were no friction between the blades and the housing.

In setting one this caused little problem, after a couple of hours the blades were torn down and had no friction with the housing. The problem occurred when blades should be adjusted to setting two. The housing is not produced to follow the curvature of the runner blades in setting 3 or higher causing the blades to jam in the housing making it almost impossible to rotate the turbine. To not destroy the torque gauge and the generator the calibration arm was mounted on the shaft and the turbine was manually torn down. This was done by pushing the arm around until there was almost no friction left. When the friction was assumed to be low enough so that the momentum on the torque gauge would not be so high that it would be destroyed, water was let through the turbine making the turbine tear the blades down while rotating.

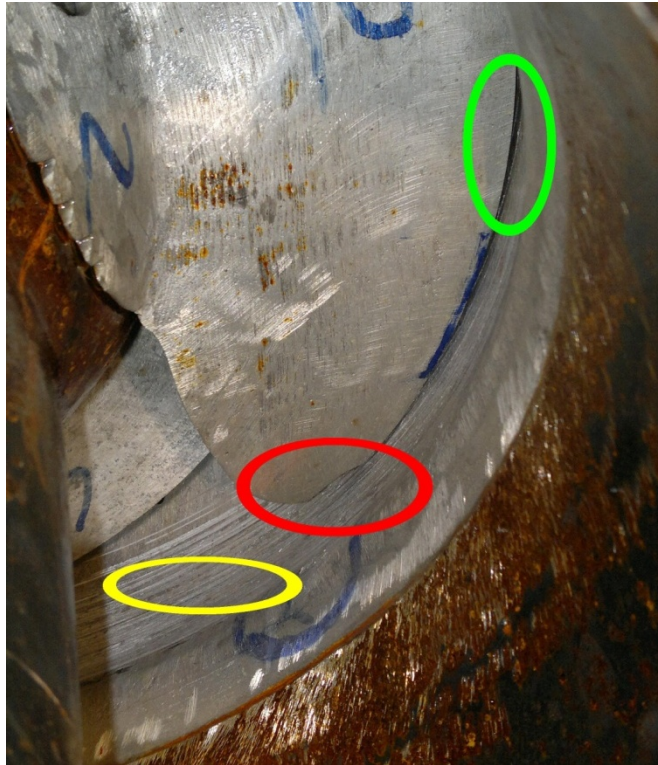


Figure 7-3 Runner blade with broken blade section, seen from below

As seen in Figure 7-3 the rear end of the runner blade is touching the housing marked with a red circle. By looking closely it is possible to see that a piece of the blade is broken off inside the red circle. While the rear end is jammed into the housing the front part has a large gap between the blade and the housing marked with a green circle. In the area of the yellow circle erosion from the blade on the housing can be seen.

An attempt to adjust the blades to setting three was made but was not managed. A piece of one of the blades broke off in the attempt to adjust the blades into setting three. This made it impossible to perform test in setting three and four.

7.3 Upper bearing

While running the tests it was discovered by an incident that the upper bearing became warm. The bearing is a spherical roller bearing that takes all forces acting in the axial direction in the shaft. The bearing also takes small forces

acting in the radial direction. C0 of the bearing is supposed to have value of 200kN according to Anders Austegård. C0 is a constant that give the life time a bearing depending on force, revolutions per second and the viscosity of the grease used in the bearing. A high C0 indicates that a bearing can withstand high forces and high numbers of revelations per minute for a longer period of time than a bearing with a lower C0.

Harry Opdal at the SKF group was contacted and gave an introduction in how to calculate life time on bearings using a calculation tool on the SKF home page on internet. With an axial force of 10kN, 1000rpm and a viscosity of 25mm²/s the life time of a bearing with the same specifications as the bearing used in the turbine is calculated to be 497300 hours or 56 years. This means that the bearing should be able to withstand the forces acting in the axial direction without any problems. A screenshot of the calculation page is found in Appendix E. An extreme axial force of 20kN was also calculated and gave an expected life time of 5.6 years. This is a force way outside the design range of the turbine.

When the life times are evaluated the quality of the bearing has to be taken into consideration. The calculations are med with an SKF bearing which is a high quality product. The bearing in the turbine is most likely produced in China and do not have the same quality and wear resistance as the SKF bearing.

The shaft used in the turbine is not completely straight and have a maximal cast of 0.25mm. Radial movements in the shaft results in cyclical high radial force acting on the bearing. Since the bearing is designed to withstand forces in the axial direction this may cause the increase in temperature.

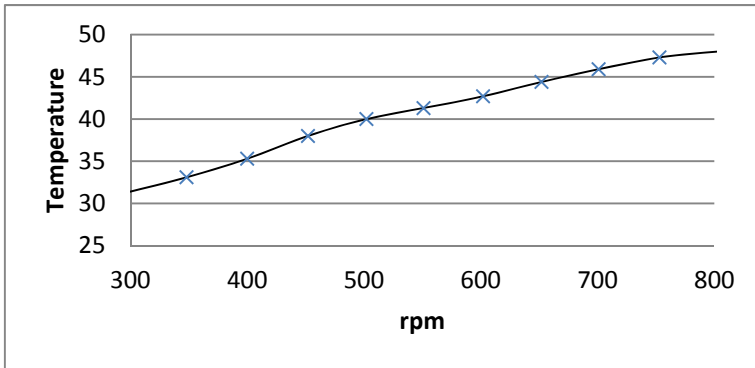


Figure 7-4 Temperature plotted vs. rpm at 2.5 meter pressure head. Setting 2

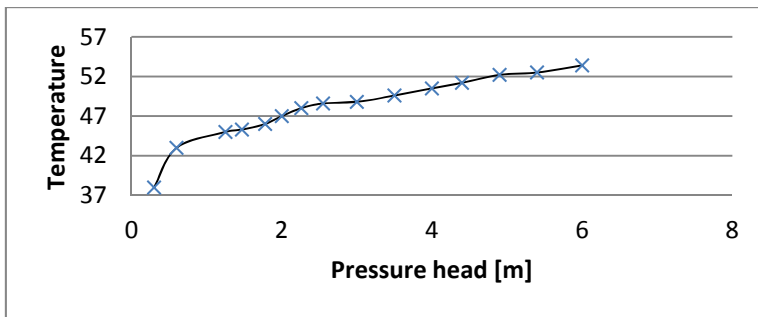


Figure 7-5 Temperature plotted vs. pressure head. Setting 1, 800rpm

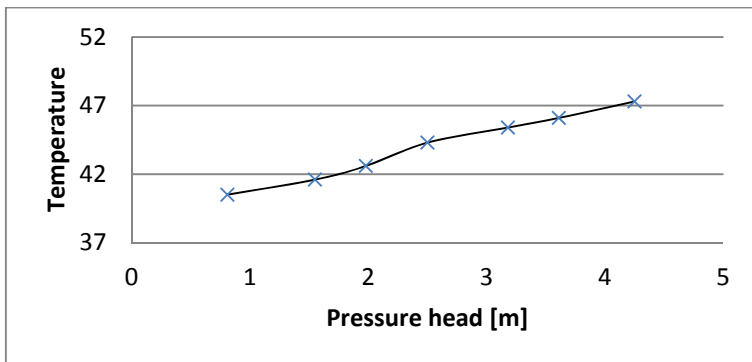


Figure 7-6 Temperature plotted vs. pressure head. Setting 2, 650rpm

As seen in the three figures above the temperature increase with revolutions and pressure head. In the figures where temperature is plotted vs. pressure head the revolutions per second is kept constant and when temperature is plotted vs. rpm the pressure head is kept constant. The operating conditions

were kept constant in each measuring point until the temperature was almost constant.

These measurements were done to find if there was an upper limit for the temperature increase and where it may be. It is clear that the temperature would increase if the pressure or number of revolutions were increased.

Since the temperature also increase with pressure head the bearing most likely heats up due to friction in the bearing itself.

The situation was discussed with professor Ole Gunnar Dalhaug, what should be done regarding the temperature to be able to continue the tests. To dismount the entire turbine, change the bearing and straighten the shaft was considered by was found to be way to time consuming. The conclusion was to constantly measure the temperature on the bearing house and stop measurements if the temperature approached temperatures that could cause the bearing to malfunction or jam. The critical value of the temperature was assumed to be around 60°C based on previous experiences of technician Trygve Opland and engineer Bård Brandstø. These temperature sett clear boundaries for the tests conducted.

7.3.1 Bearing load calculation

The values above is as mentioned calculated using the SKF life time calculator with guidance from Harry Opdal found on the SKF home page. The governing equations in the program are here presented. Values of variables and factors can be found in PDF file (9).

When loads are acting in radial and axial direction on the bearing at the same time the hypothetical load acting in the centre of the bearing which gives the lifetime of the bearing when only axial forces are acting is called the dynamic equivalent load.

The dynamic equivalent axial load of a spherical thrust roller bearing is given in equation(7.2).

$$P = F_a + 1,2F_r \quad (7.2)$$

Static equivalent axial load is a hypothetical load which would cause permanent deformation on the bearing at the point on the bearing under most stress when both axial and radial force is applied. For a spherical roller bearing the static equivalent axial load is calculated with equation(7.3) provided that $F_r/F_a \leq 0.55$.

$$P_{0a} = F_a + 2.7F_r \quad [N] \quad (7.3)$$

P_{0a} is the static equivalent axial load, F_a and F_r are actual axial load and actual radial load respectively.

The operating life time of a spherical roller thrust bearing can be calculated using equation(7.4).

$$L_{nm} = a_1 a_{skf} \left(\frac{C}{P} \right)^{10/3} \quad (7.4)$$

7.4 Plexiglass cover

The turbine had originally two steel covers that can be opened to access the runner so that the runner blades can be adjusted without having to dismount the complete turbine. One cover is placed above the runner and one under the runner. The cover under the runner was replaced with a Plexiglas cover. This was done in order to be able to use a high speed camera to record and take pictures in the draft tube to check for cavitation on the runner blades. Mechanical drawings of the Plexiglas cover are found in Appendix O.

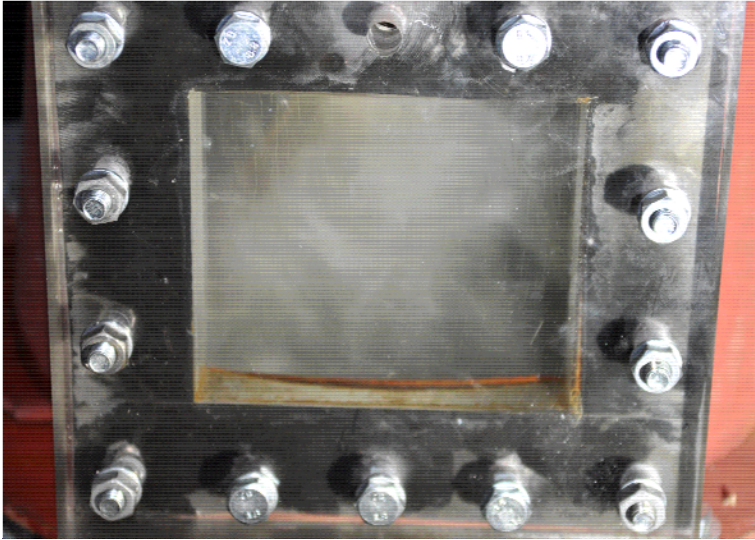


Figure 7-7 Flow after the turbine outside BEP

Figure 7-7 shows how the flow looks like outside best point. As seen the flow almost appears as a mist flowing through the turbine. Air bubbles from the air intake in the lower bearing and cavitation contribute to create the “mist”. The mist made it impossible to document cavitation on the runner blades because it was impossible to see the blades. When the water had no spin the flow was clearer hence less bubbles but it was still impossible to document cavitation with a high speed camera.

8 Optimisations of inlet bend using CFD.

CFD is short for Computational Fluid Dynamics and is a simulating tool that solves fluid flow or heat exchange characteristics. CFD is widely used in the industry because of its capability to give accurate solutions at a low cost compared with model tests in laboratories (10). Even though results with CFD may be obtained quickly and cost effective CFD will not always give the real solution. It is therefore recommended to perform tests to validate the CFD results.

CFD simulations of water flowing through pipes are basically solved using two governing equations. The two equations are the Navier-Stokes equation and the conservation of mass equation.

When performing CFD test there is a wide range of settings, factors and parameters to use and monitor to get good results. A detailed description of these parameters, factors and settings is found in Appendix F.

8.1 CFD analysis of inlet bend

Sharp corners are never ideal in pipe flow. Sharp corners can cause backflow, cavitation and separation right after the corner forming a low pressure region. Flow in pipe bends will tend to have high velocity and low pressure at the inner corner of the bend while the outer corner then will have high pressure and low velocity. If a turbine is placed right after such a bend this could be unfortunate for the efficiency of the turbine since the velocity and pressure distribution across the pipe area will be unevenly distributed.

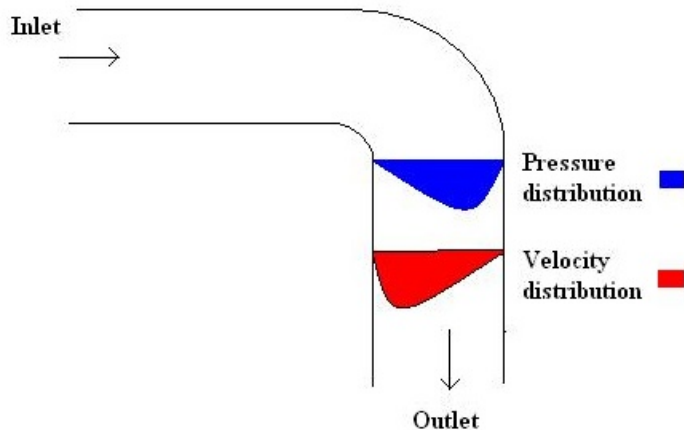


Figure 8-1 Velocity and pressure distribution in pipe bend.

In Figure 8-1 the velocity and pressure distribution is shown right after the bend. The difference in velocity and pressure distribution will increase with the velocity in the flow.

The turbine tested in this thesis is placed after a sharp corner bend as described above. A CFD analysis was therefore conducted to check if the bend could be optimized. A wide range of different bend solutions were tested in the CFD analysis and compared against the geometry of the actual inlet bend of the Afghani turbine.

The geometry of the actual inlet bend is complex and parts of the bend are difficult to measure. Measures and the geometry used to create the model in FLUENT are therefore based on measurements taken on the physical turbine and measures found in the Inventor drawings created by Anders Austegård. The reason for not base all measures on the Inventor drawings is that there are significant differences in the drawings and the actually produced turbine.

The intended volume flow range for the Kaplan turbine is $0.09\text{m}^3/\text{s}$ to $0.53\text{m}^3/\text{s}$ which gives an inlet velocity in average of $0.71619\text{m}/\text{s}$ and $4.2176\text{m}/\text{s}$. Optimal design inlet velocity is $1.6711\text{m}/\text{s}$. CFD simulations of the different geometries was done at inlet velocities ranging from $1.0814\text{m}/\text{s}$ to $2.387\text{m}/\text{s}$.

Four different geometries are tested, the original geometry plus three new geometries. The four geometries are presented in the figures below.



Figure 8-2 Original geometry



Figure 8-3 Geometry 1



Figure 8-4 Geometry 2



Figure 8-5 Geometry 3

In Geometry 1 the bend is rounded one flow controller is placed in the middle of the bend spending from the inlet to the outlet of the bend, the section after the bend is extended with 50cm compared to the original geometry.

Geometry 2 has the same dimensions as geometry 1 and the only difference is that geometry 2 has two flow controllers in the bend.

Geometry 3 has the same bend as geometry 2 but has the same length after the bend as the original geometry.

8.2 Velocity measurements in inlet bend

Velocity test where performed to be able to check if the CFD results where realistic. The velocity test was done with a Pitot tube and different volume flows where measured.

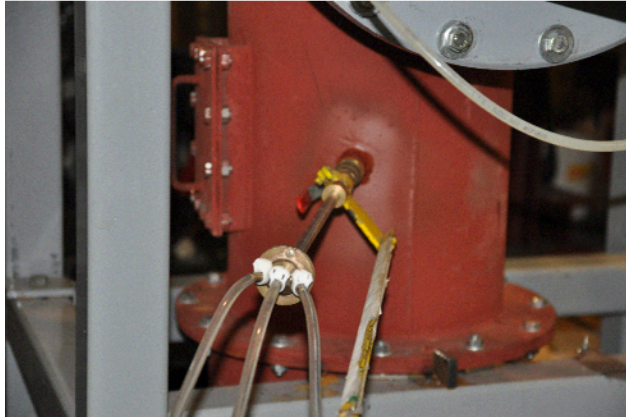


Figure 8-6 Pitot tube mounted on the turbine

The velocity from the measurements is calculated with equation(8.1). The equation is derived from Hydraulisk Måleteknikk (2).

$$c = \sqrt{\frac{\Delta h \cdot 2 \cdot g}{\varphi}} \quad [m/s] \quad (8.1)$$

Δh is here the height difference between the hydraulic pressure and the stagnation pressure while φ is the Pitot coefficient given by Kjølle (2) to range from 0.98 to 1.00. The measurements are only valid if the Reynolds number is above 100.

$$Re = \frac{\rho \cdot c \cdot d}{\mu} \quad (8.2)$$

When measuring the velocity a Pitot tube with three pressure holes was used. The centre hole measures the stagnation pressure and the two holes on the side of the tube, in this case the side of the “knife” measures the hydraulic pressure. The height of the two water columns leading from the hydraulic pressure measurements have to be levelled in order to have a valid measurement. In Figure 8-7 the two columns measuring dynamic pressure is levelled and the measurement is valid. The velocity in the flow can then be calculated using equation(8.1). In real measurements it is difficult to get the two hydraulic columns to be exactly levelled due to fluctuations in the flow and

time lag in the measurements, meaning that when the Pitot is twisted in order to level the water columns it takes time from when the tube is twisted to when the water level is stable.

In the tests performed in this thesis an allowed height difference in the two dynamic measurements is set to 5mm. A 5mm height difference is found acceptable since the goal with the measurements is to confirm CFD results which have a high level of uncertainty. The velocity measurements also have uncertainties linked to them, they are not considered in this thesis since the uncertainties in the measurements are small compared to the CFD analysis.

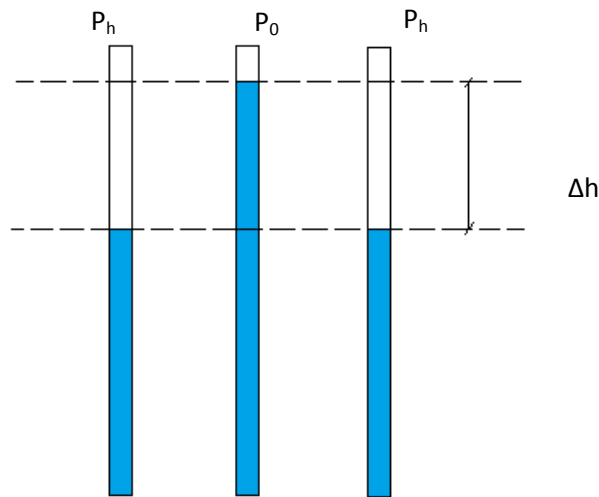


Figure 8-7 Height difference in a knife Pitot measurement

The velocity distribution in the outlet may vary with different pressure heads. To be able to compare the measured velocity profile with the CFD results where the inlet and the outlet pressure is governed by the volume flow the actual velocity measurements have to be scaled against a dimensionless factor.

$$c' = c \cdot \frac{\sqrt{2gH^*}}{\sqrt{2gH}} \quad [m/s] \quad (8.3)$$

In equation(8.3) H^* and H is the height difference the measured static pressure in the inlet and outlet. H^* is the reference value kept constant and has to be set at an appropriate value. The value can be set when for instance for a desired

volume flow. If the pressure is kept constant during the test this is not necessary.

8.3 Outlet

The outlet of the turbine consists of a draft tube, three fins and a hub under the turbine. The draft tube and the hub help improve the performance of the turbine. The fins on the other hand do not necessary give a positive contribution to the performance of the turbine. Frequency analysis conducted by Remi Andre Stople also show that fluctuations in the measurements can be caused by the blades passing the three support fins.

The water coming out of the runner have in most cases swirl because the turbine is not operating at best efficiency point. The fins will disturb the water swirl and may cause pressure fluctuations when the runner blades pass the fins.

To avoid disturbance of the swirl after the turbine the bearing placed under the turbine can be moved into the already existing guide vane housing directly above the runner.

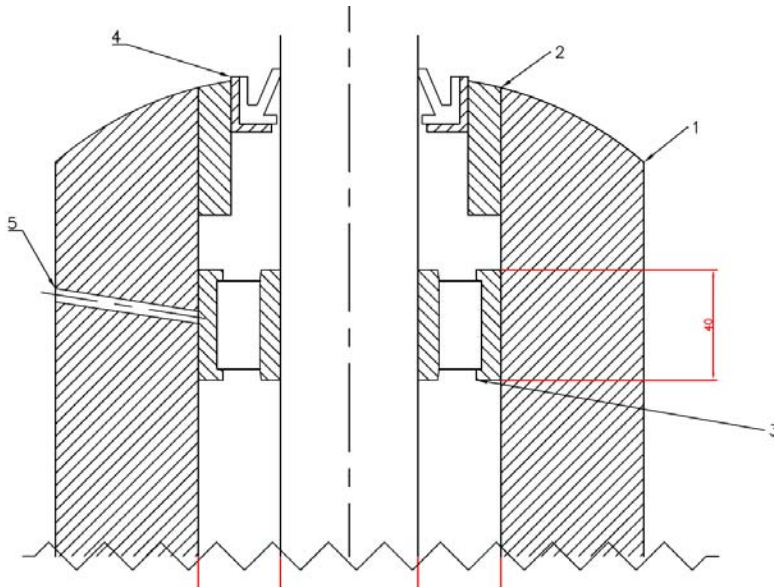


Figure 8-8 Bearing when placed inside the guide vane centre piece

A cylindrical roller bearing is chosen with an NU design. NU design let there be minor movements in the axial direction. This type of bearing does not take any load in the axial direction. In Figure 8-8 the bearing is indicated with index 3.

The bearing should be placed as close to the runner as possible to prevent cast in the shaft and runner.

To prevent leakage from the water way into the bearing a viper seal can be chosen, index 4. AHPseals (11) offers a wide range of seals for rotating equipment. The Rotaflon series is a high performance series of seals for rotating shafts. The RB-series is chosen for this particular case. The RB-series is chosen because it can tolerate the pressure, temperature and rpm of the turbine shaft produces and operating conditions. The life time of the seal is not given because it is highly dependent on the working conditions. An identical seal is necessary under the bearing. This seal is not included in the drawing.

Index 5 is the grease intake from outside the turbine. A small tube has to be inserted into the guide vanes connecting the outside with the bearing.

The mechanical drawing of the bearing is found in Appendix P.

9 Results

9.1 Efficiency tests

To create the hill diagram curve fitting was performed in Matlab to create smooth lines. Four different curve fitting functions were tried in order to find the function that created the best curve for the Hill diagram. The functions used were a 2nd, 3rd and 4th degree polynomial curve fitting functions as well as a smoothing spline function. An uncertainty of $\pm 2\%$ in each point was selected to evaluate if the fitted curve is within an acceptable range of the actual measurements.

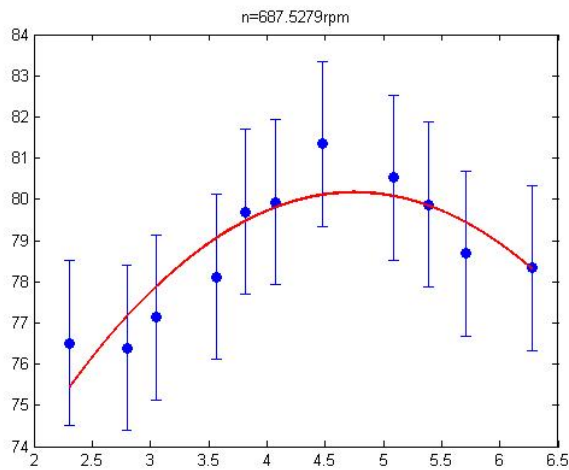


Figure 9-1 2nd order poly fit

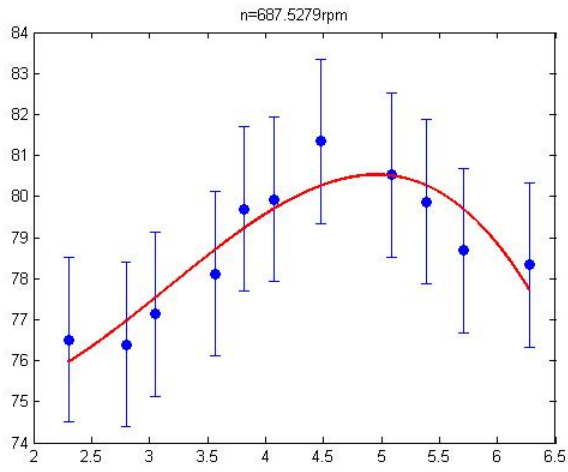


Figure 9-2 3rd order poly fit

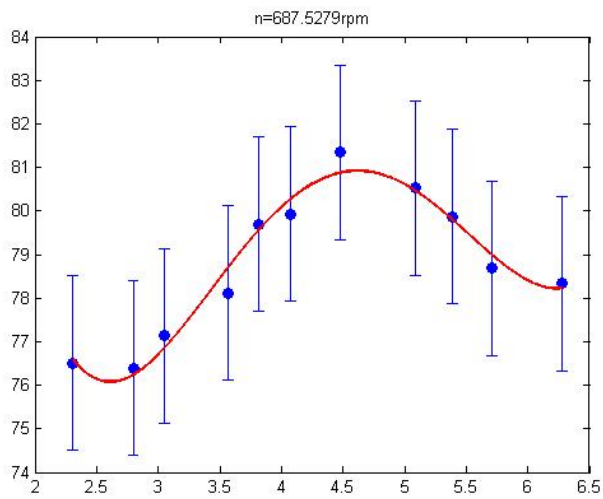


Figure 9-3 4th order poly fit

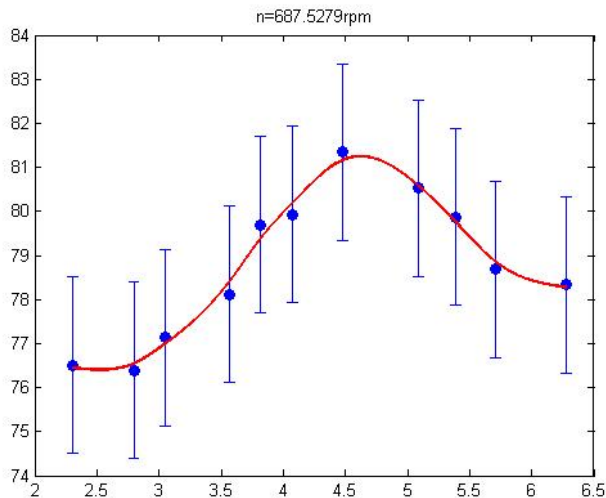


Figure 9-4 Smoothing spline

Above the four curve fitting functions are presented used on a measured setting 2 series with a rotational speed of 687rpm and varying effective head. The blue dots are the measured data while the red line is the fitted curve. The vertical lines are error bars with a value of $\pm 2\%$ relative to the measured data. The curve fitting for all the measured series are found in Appendix H.

Smoothing of curves is done in order to obtain a Hill diagram which is easy to read and to find values between the measured values. The fitting function creates a function which allows the user of the Matlab program developed to find the efficiency at any given operational point.

The smoothing spline function is the function which results in the lowest deviation between the fitted data curve and the measured data while the 2nd order poly fit function gives the highest deviation. Even though the 2nd order poly fit function results in the highest deviation only one point on the fitted curve lies outside the $\pm 2\%$ uncertainty value. The 2nd order function is the function which gives the most realistic curve when evaluating all the lines for all the functions. The 3rd and 4th order functions creates unrealistic gains in efficiency at low heads. This is caused by high uncertainty in the measurements while the smoothing spline creates uneven curves.

The efficiency test were strongly affected and limited by the test rig setup and the turbine. For a detailed description of the limitations and challenges encountered while testing see chapter 7.1, 7.2 and 7.3.

9.1.1 Setting 1

The Hill diagrams presented in Figure 9-5 and Figure 9-7 are presented as H_e vs. rotational speed diagram. The reason for not presenting the Hill diagram as a Q_{ED} vs. n_{ED} diagram is that the turbine is not a model or a prototype so that the flow, head and rotational speed does not have to be scaled when the turbine is taken into production to find the efficiency and power output. The turbines performance is governed by the head and the rotational speed. The rotational speed governs the volume flow. A 2nd order poly fit function is used to create the curves used to create the Hill diagrams.

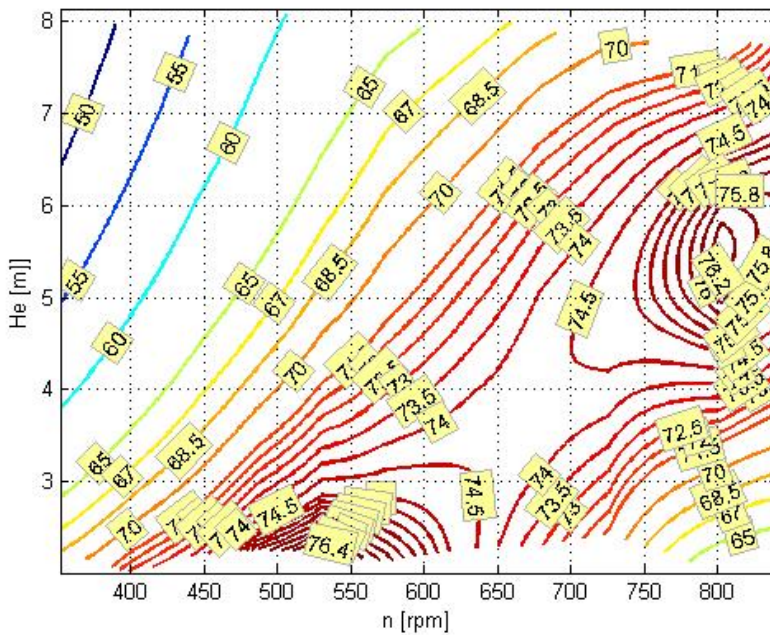


Figure 9-5 Hill diagram, efficiency plotted against effective head and rotational speed

The Hill diagram in Figure 9-5 indicates that there is a best efficiency point with efficiency of 76.4% at around 575 rpm and 2.25 meter effective head in setting 1. But when studying Figure 9-6 it becomes clear that the best efficiency point

most likely lies outside the tested range. BEP is most likely found with an effective head less than 2 meters and with an rpm around 500.

The reason why the Hill diagram produces a BEP at 575rpm and 2.3m effective head is because of the 2nd order polyfit function used to generate the diagram does not match the measured data completely. The Hill diagram is therefore only showing trends in the efficiency.

Figure 9-5 has a saddle point around 675rpm and 3 meter effective head. This is most likely caused by uncertainties in the measurements and the fact that more tests should be carried out around 675 rpm. The contour function used to create the Hill diagrams interpolates values between the fitted curve values. More measurement series would mean that the uncertainty in the interpolation would be reduced.

The highest efficiency point is not tested due to limitations in the rig. See chapter 7.1.

The highest efficiency measured was 76.4% at an effective head of 2.25 meters and 552 rpm but the graphs in Figure 9-6 shows that lines have not reached the top efficiency around 550 rpm.

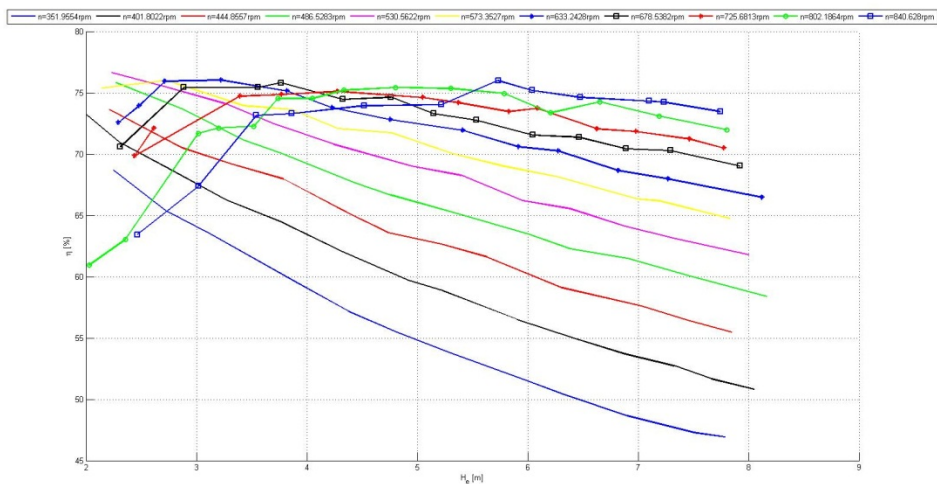


Figure 9-6 Raw data measurements. Efficiency curves at constant RPM plotted vs. effective head.

9.1.2 Setting 2

Due to the same limitations in the rig as in setting 1 the BEP is not found in setting 2.

The Hill diagram in Figure 9-7 make it appear like there are three different best efficiency points. Since not all rotational speeds are measured with different heads the interpolation between each measured series can make the Hill diagram appear edgy and not continuous. If too series with rpm kept constant at 525 and 675 were measured the peaks around 450 and 600 would probably disappear and the diagram would look more similar to the one in setting 1.

The Hill diagram shows BEP at 725rpm at an effective head of 5 meters. The highest efficiency measured is 83.8% at an rpm of 602 and effective head of 2.72 meters. As seen in Figure 9-8 the best efficiency point in setting 2 is probably not reached.

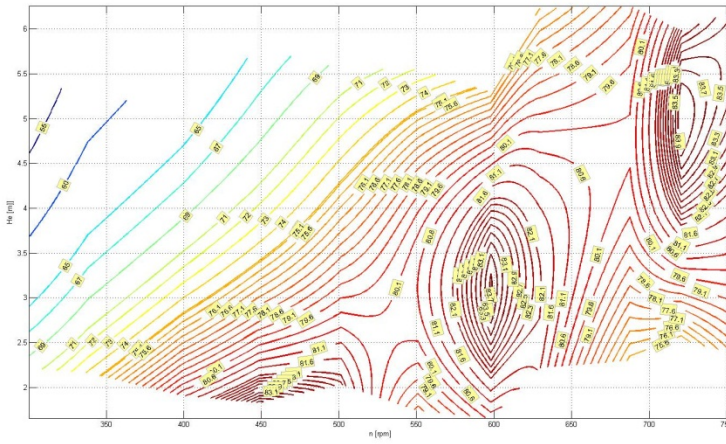


Figure 9-7 Hill diagram, efficiency plotted against effective head and rotational speed

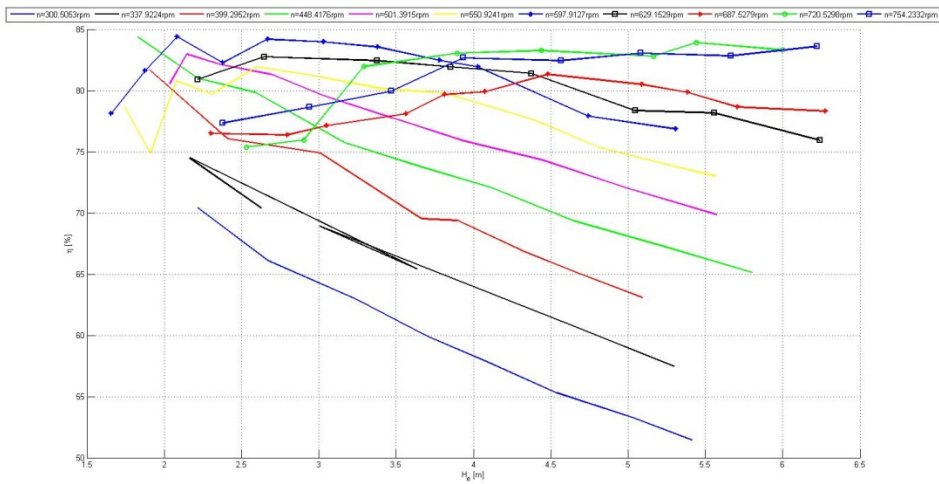


Figure 9-8 Raw data measurements. Efficiency curves at constant RPM plotted vs. effective head

9.2 Cavitation tests

Manual cavitation test was performed using high speed camera and strobe lights to light up the runner blades. Unfortunately the test did not give any results since the flow was too chaotic and the light conditions inside the turbine was not nearly good enough to be able to detect formation of air bubbles. See chapter 7.4 for a picture of the flow under the turbine.

9.3 Clearance water

Figure 9-9 and Figure 9-10 show how much clearance water leaking from the upper bearing seal at different pressure heads and rpms. While leakage increase when pressure head is raised the leakage stabilize when pressure head is kept constant and the rpm is raised hence volume flow increase.

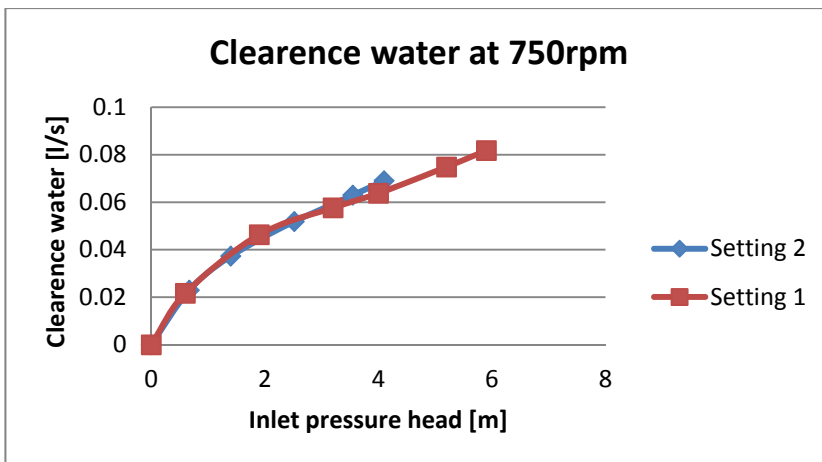


Figure 9-9 Clearance water at constant rpm

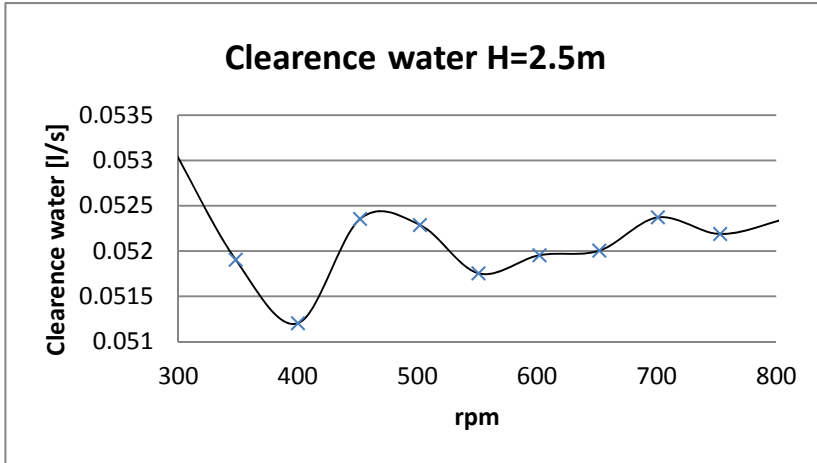


Figure 9-10 Clearance water at constant inlet pressure head in setting 2

The fluctuation in clearance water is only varying with $\pm 2\%$ around a mean value of 0.052l/s. It is clear that the leakage is dependent on the pressure and not the volume flow and rpm.

With a volume flow of 227l/s at 750 rpm and 6m pressure head in setting 1 the clearance water only give a 0.035% maximum loss in volume flow. In setting 2 the maximum volume flow loss is 0.0225%.

9.4 Mechanical power

The mechanical power output at a rotational speed of 500 is presented in Figure 9-11. 500rpm is chosen because this is the closest measured value to the design rpm of 490.

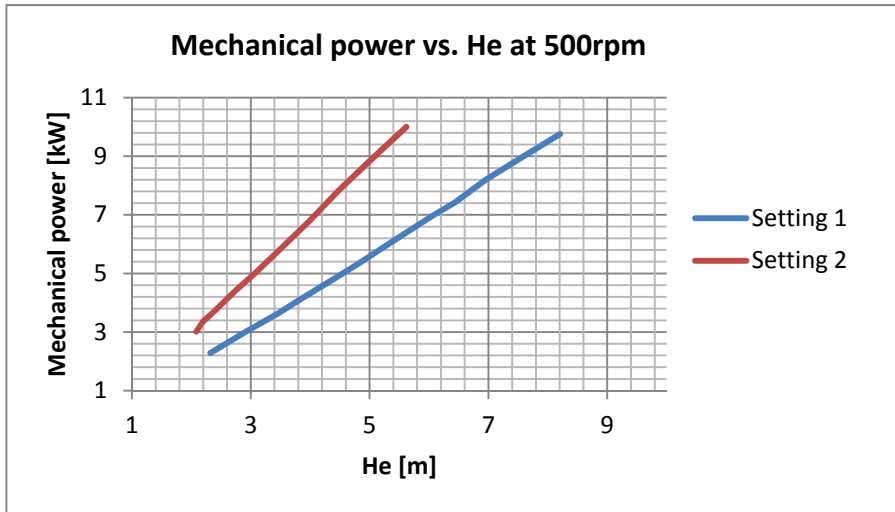


Figure 9-11 Mechanical power at 500rpm

9.5 Torque

The torque generated at 500rpm is presented in Figure 9-12. As seen from the figure the measurements are performed close up to the maximum value of the torque gauge of 200Nm.

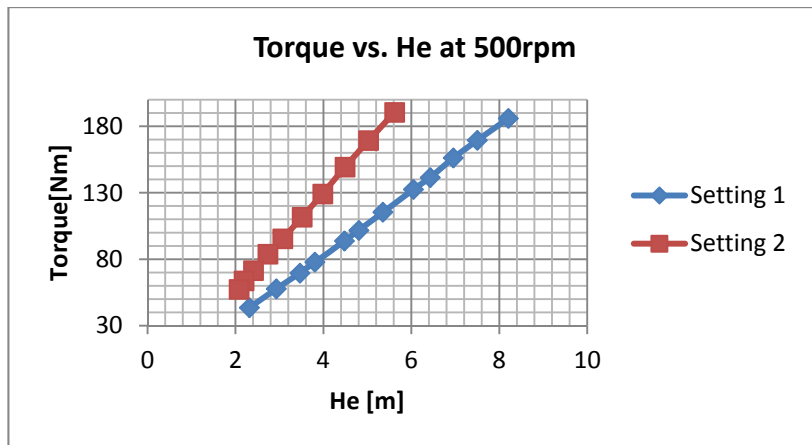


Figure 9-12 Torque at 500rpm

9.6 Fluctuations in measurements

Project student Remi Stople have calculated and found fluctuations in torque, pressure and volume flow in the test results. The fluctuations became clear at

an early stage in the testing of turbine because values were plotted in the user interphase in LabView. Stople performed a frequency analysis of the fluctuations using a Matlab program developed by student Anders Tørklep.

A measurement series Stople studied showed fluctuation in torque with a mean value of 43Nm of ± 7.5 Nm. Stople found that the dominating factors when analysing the frequencies most likely are blade frequency, electric noise, rotational frequency and blade passing frequency from the lower bearing.

The frequency analysis shows that there is a peak in the frequency every time a blade passes a guide vane. This frequency varies with the rotational speed. Electric noise occurs with a frequency around 50Hz. This electric noise does most likely origin from the asynchronous generator. Rotational frequencies do most likely origin from the cast in the shaft with an increase in friction once every time the shaft turns (12).

A frequency occurs every time a blade passes the fins that support the lower bearing.

Stople also did a frequency analysis of the pressure and volume flow fluctuations. The analysis did not give clear results in why the pressure and volume flow fluctuate at operation conditions that should give stable measurements. No dominating frequencies where found and there were no direct correlation between the frequencies in pressure and volume flow. Since the measuring equipment used to measure pressure and volume flow are independent and the analysis show no correlation Stople concludes that the error most likely lies in the logging card, the analogue-digital conversion or that the two equipment are malfunctioning.

9.7 CFD of inlet bend

In the simulations performed the residuals in all simulations converged with a value lower than $10E-4$. The highest y plus value obtained when simulating was 3.016. Y plus values and residuals are described in Appendix F. The highest y plus value occurred in the original geometry when simulating with an inlet velocity of 2.386m/s on the lower flow controller in the bend.

A series of different geometries have been used in the CFD analysis of the inlet bend. None of the geometries stand out performing better than the other geometries at all conditions tested.

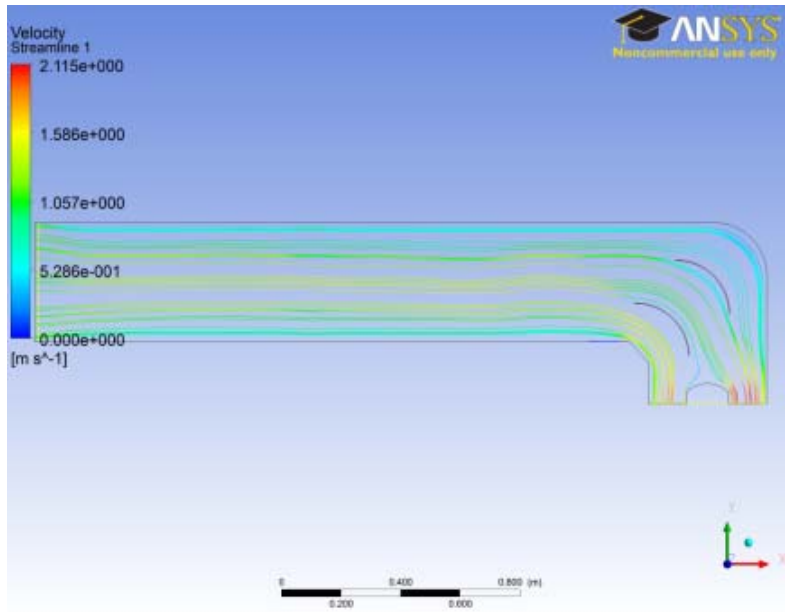


Figure 9-13 Original geometry with inlet velocity of 1.0814m/s

With an inlet velocity of 1.0814m/s the original geometry is the geometry giving the most uniform outlet velocity. The difference in outlet velocity between inner and outer corner is 0.3m/s. The outlet velocity profile can be seen in Figure 9-16 to the left.

When the inlet velocity is increased to 1.25m/s geometry 1 give the best result. At 1.25m/s the geometry gives the most uniform velocity distribution at the outlet Geometry 1 can be seen with velocity stream lines in Figure 9-14 with an inlet velocity of 1.25m/s.

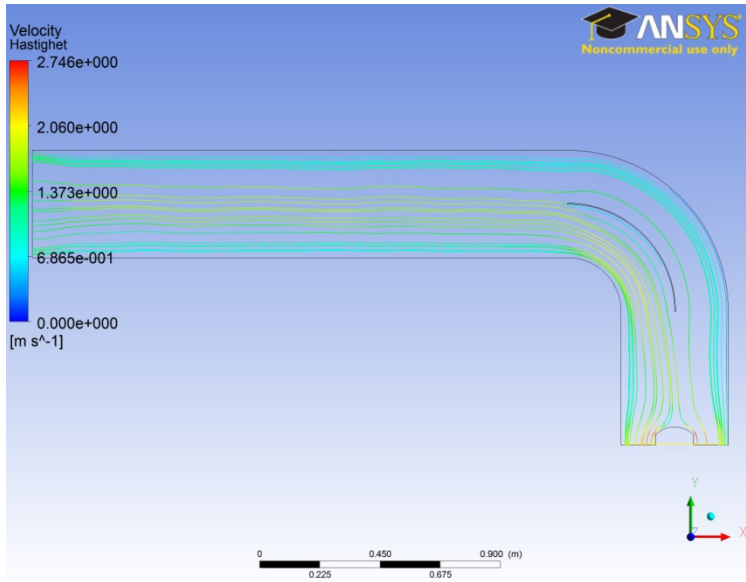


Figure 9-14 Geometry 1. Inlet velocity 1.25m/s

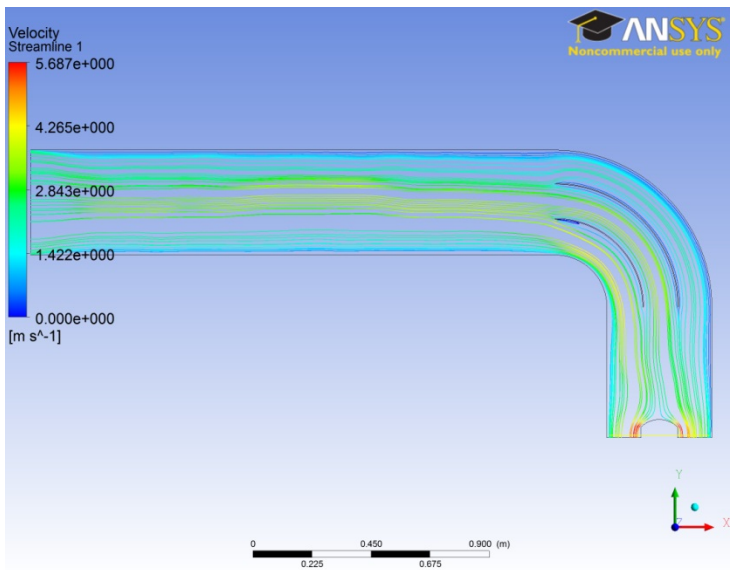
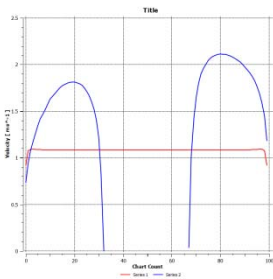


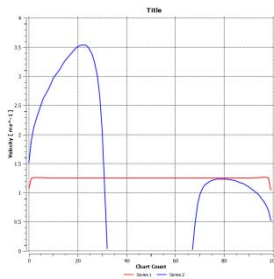
Figure 9-15 Geometry 2. Inlet velocity 2.387m/s

When the velocity is further increase to 2.378m/s geometry 2 with two flow controllers performs best. Geometry 2 gives a completely uniform outlet velocity when the inlet velocity is 2.378m/s.

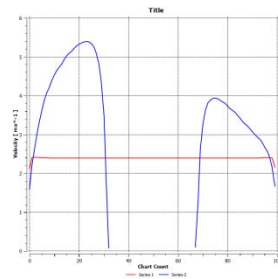
All geometries tested have a unique inlet velocity which gives a uniform outlet velocity. When the inlet velocity is increased or decreased outside this unique flow rate the tendency of all the tested geometries is that the outlet velocity at the inner corner increases hence the outer corner velocity decreases.



$V_{inlet} = 1.0814\text{m/s}$



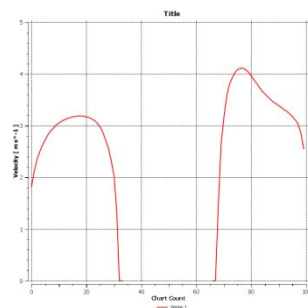
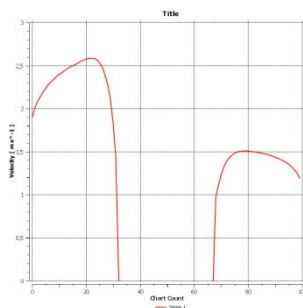
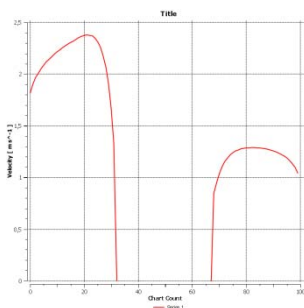
$V_{inlet} = 1.25\text{m/s}$



$V_{inlet} = 2.387\text{m/s}$

Figure 9-16 Outlet velocity profiles with original geometry and different inlet velocities.

The original geometry have a maximum velocity difference on the outlet between the inner and outer outlet of 2.25m/s while geometry 3 has a maximum velocity difference of 1.5m/s at an inlet velocity of 1.6m/s. This makes geometry 3 the geometry giving the most stable flow conditions at the outlet for a wide range of inlet velocities.



$$V_{\text{inlet}} = 1.0814$$

$$V_{\text{inlet}} = 1.2$$

$$V_{\text{inlet}} = 2$$

Figur 9-17 Outlet velocity profiles for geometry 3

The original geometry has a shift in outlet velocity distribution at an inlet velocity around 1.0825m/s while the shift comes at an inlet velocity around 1.4m/s in geometry 3.

It is important to point out that the shift in outlet velocity is in opposite direction in the original geometry and geometry 3. While the inner corner velocity increases with increasing inlet velocity with the original geometry the opposite happens in geometry 3. In geometry 3 the outer corner velocity is increased with increased inlet velocity. Geometry 1 and 2 does not get a shift in outlet velocity. The inner corner velocity is higher for all simulated inlet velocities except for the inlet velocity resulting in a uniform outlet velocity.

9.8 Velocity measurements

Velocity measurements were taken in two different measuring series with two different Pitot tubes. One series with varying pressure head and one series with constant pressure head.

The first measurement series was not taken at a constant pressure height so the values measured velocities had to be scaled. The reference height, H^* , was chosen when the inlet velocity was 1.0814m/s. As described in the previous chapter there is a shift in the velocity profile around 1.0825m/s (inlet velocity) found in the CFD results, the velocity of 1.0814 is the closest value measured hence chosen as reference head.

| Inlet Velocity [m/s] | Average Outlet Velocity [m/s] | Measured Outlet Velocity [m/s] | Scaled Outlet Velocity [m/s] |
|----------------------|-------------------------------|--------------------------------|------------------------------|
| 0.9885 | 1.1264 | 0.9631 | 1.09206 |
| 1.0814 | 1.2327 | 1.1136 | - |
| 1.2623 | 1.4385 | 1.2405 | 1.80446 |

Table 10 Actual and scaled outlet velocity

When the scaled velocities are divided on the average velocities a value of 1 give that the outlet velocity is uniform across the outlet area. A value above

one result in an outlet velocity profile as in the right hand side graph in Figure 9-16. A value under one result in an outlet velocity profile as seen in the left hand side graph in the same figure. The average values are found by dividing the volume flow on the outlet area and is therefore only a theoretical value and does not change with the pressure and does therefore not have to be scaled against a reference value.

| Inlet Velocity [m/s] | Scaled velocity/average velocity [-] |
|-----------------------------|---|
| 0.9885 | 0.9695 |
| 1.2623 | 1.2544 |

Table 11 Scaled velocity vs. average velocity

In the second measurement series the pressure head were kept constant to check if the pressure had the impact on the results as suggested in the previous section.

| Measurement | Inlet velocity [m/s] | Avg. Outlet velocity [m/s] | Measured outlet velocity [m/s] | Deviation from avg. in % |
|--------------------|-----------------------------|-----------------------------------|---------------------------------------|---------------------------------|
| 1 | 1.122049 | 1.27868 | 2.423435 | 89.52631 |
| 2 | 1.241416 | 1.414709 | 2.635236 | 86.27407 |
| 3 | 1.018597 | 1.160787 | 2.163922 | 86.41852 |
| 4 | 0.946977 | 1.079169 | 2.011873 | 86.42798 |

Table 12 Velocity measurements at constant pressure head

The velocity difference between the average outlet velocity and the measured is almost constant for all measurements with maximum variation of only 3.25%.

10 Discussion of results

10.1 Efficiency tests

The Hill diagrams created are based on a 2nd order poly fit function. When performing the curve fitting the uncertainty was kept constant at a value of $\pm 2\%$. This is done in order to check if the curve created by the poly fit function lies within the uncertainty in the measurements. When performing curve fitting the individual uncertainty in each point should be used and not a constant uncertainty.

The 2nd order poly fit function was used to create the Hill diagrams. The curve the 2nd order poly fit function creates has the highest deviation between measured data and the curve value. The function is still chosen because it creates the most realistic curves when comparing the curves with curves in Figure 2-2.

10.2 Clearance water

The amount of water coming from the upper bearing is in the test found to be so small that the loss in efficiency is negligible.

When discussing the results with Anders Austegård it became clear that the leakage increased with the amount of sand in the water. The sand erodes the seal allowing more water to flow through the clearance water outlet. This is of course not ideal because this makes the risk of water and sand coming into the upper bearing increases. On the other hand, the water flowing through the clearance water outlet helps to cool down the upper bearing. So far the clearance water has not been a problem during tests in Afghanistan.

10.3 Inlet bend

Velocity measurements

The results from the CFD analysis of the original geometry are closer to the second measuring series than the first series. The first velocity measuring series was done under varying pressure while the second series was done under constant pressure like in the CFD analysis.

Even though the trend in the outlet velocities in the first series matches the trend in the CFD with a switch in outlet velocity at around 1.085m/s the second measuring series have velocities closer to the velocities obtained from the CFD analysis. In the CFD analysis the outlet values are close to or above 2m/s while all measured values in the second series lies above 2m/s. The first series only correlate with the CFD after scaling the values. The scaling method used can be questioned and may not be the best way to evaluate the velocities against each other.

Since the velocities in the second series are overall higher than in the first series. The first series is found to be invalid. The reason for this is because the equipment used is old and the Pitot tube clogs up fast. When performing the test the Pitot tube was changed between the two series because one of the holes on the first Pitot had clogged itself during a two week period. The possibility of the two others being almost clogged is therefore reasonably high.

What the results from the CFD analysis and the second measuring series shows is that the bend makes the velocity distribution uneven which is not optimal for the performance of the turbine.

The absolute optimal solution would have been to place a spiral casing where the bend is today. This would definitively make the velocity and pressure distribution before the runner even and frequencies from the guide vanes would disappear. A spiral casing would also give the opportunity of adjustable guide vanes. Adjustable guide vanes does in most cases make the turbine efficiency higher for a wider flow range because it is easier to obtain optimal angle of attack for the runner. Adjustable guide vanes would not higher the BEP.

The challenge with a spiral casing is that they are difficult to produce because of their complex geometry. Spiral casing is not considered as an option for this turbine because of this.

CFD analysis

When a spiral casing is out of the question the three other geometries simulated has to be considered. Geometry 1 and 2 are extended with 50cm from inlet to outlet. This can cause a problem because the minimum effective

head that can be reached is increased compared to the original geometry. When it is clear that the blades are designed for low effective heads this is not fortunate. Geometry 3 has the same length between inlet and outlet as the original geometry so if the bend is changed to geometry 3 the runner will operate with the same effective heads as with the original geometry if losses in the bend are neglected.

The velocity measurements show that the inner corner velocity is higher than the outer corner velocity at all inlet velocities. The original geometry and geometry 3 does not give higher velocities at the inner corner for all inlet velocities. The reason for this can be that the distance from bend to the outlet is too short so the effect the cascade and the bend create does not have the time to develop in the CFD simulations. This can be a reasonable assumption since when the section after the bend is lengthened with 50cm the inner corner velocity shows more realistic behaviour.

A 2d simulation does not pick up all the effects that occur in the real turbine bend. Swirls in the cross section is for example not picked up in a two dimensional simulation. In the real turbine there is a shaft in the middle of the bend that will affect the flow. The shaft is not present in the two dimensional simulations. To be able to get CFD result closer to the real measured values a 3d CFD analysis must most likely be performed.

If the bend is rounded this means that the upper bearing needs modifications. A structure must be placed on top of the bend in order to support the bearing. Such a structure is not created in this thesis.

10.4 Outlet

When moving the lower bearing above the runner the bearing is placed in a high pressure zone. The high pressure makes the solution of sucking air into the bearing house impossible. If air with higher pressure should be used to keep water leaking into the bearing air has to be pumped in with a compressor. This is not an ideal solution since the turbine is meant to be cost efficient and should be easy to maintain.

In the suggestion made for a design of a bearing house above the turbine high performance seals are used to keep water from leaking into the turbine. This type of seals has a high life time and high tear resistance. The problem is that

the water in Afghanistan can have a very high concentration of sand. The sand would most likely tear the seals down causing leaks within 100 hours of operation. This implies that the turbine had to be taken apart and seals and bearings had to be replaced very often causing production stop. New parts are costly and production stop would add to the cost of replacing the parts.

11 Conclusion

The Kaplan turbine tested has a reasonably high efficiency taken the design into account. The best efficiency point is not tested and configurations have to be made in the rig and the runner position has to be raised in order to reach best efficiency point. The uncertainty in the measurements does not lie within the IEC standard limit. The high uncertainty in the measurements does origin from the pressure measurements.

The CFD analysis of the original bend does not show any separation or backflow in the bend. The simulations cannot be found valid since the outlet velocities do not match measured velocities.

The results from the CFD analysis performed on the new geometries can be used as guidance for further work. The conclusion that can be drawn from these simulations is that two flow controllers is better than one for the desired flow rate and that the rounded bend give more uniform outlet velocity distribution than the original bend. A rounded bend should therefore be simulated in a three dimensional CFD analysis with two flow controllers spanning through the entire bend.

The lower bearing should be kept as it is today when the turbine is used in water with high sand content. If the water has a low sand content it should be considered to move the bearing above the runner, this would cancel the frequency from the blades passing the support fins.

12 Further work

In order to complete the efficiency tests the runner needs to be adjusted and placed a fraction higher in the housing in order to perform tests in setting three and four. The piping system in front of the turbine needs to be reconfigured in order to obtain a lower inlet pressure than the rig allows today.

The runner shaft should be replaced or the existing shaft should be straightened in order to get rid of cast.

A new spherical bearing should be installed in the upper bearing. The bearing installed today should be able to withstand the forces acting in the axial direction. The bearing could be damaged so a new one with the same dimensions is recommended to avoid breakdown during tests.

To be able to test for cavitation a new section may be designed under the turbine housing where the bearing is today. A straight section made of plexi glass is recommended to give sufficient light conditions for a high speed camera test. A straight section would also open the possibility for outlet pressure measurements directly after the runner eliminating the high uncertainty the method used today gives.

When bearing and shaft problems have been solved runaway tests can be carried out.

The new geometry derived from the CFD analysis should be further investigated. A three dimensional CFD analysis is recommended in order to check for three dimensional effects. More simulations can also be performed for different inlet conditions. The outlet pressure can be controlled to check if separation occurs at the bend in the existing geometry with outlet velocities found in the velocity measurements.

12.1 Rig setup

To be able to carry out more test and measure the best efficiency point a solution can be to attach the blue tank in front of the turbine to the existing piping. It is important that the existing system not is completely removed in order to be able to test higher heads. The connection to the blue tank will only allow low heads to be tested.

13 Bibliography

1. **Brekke, Hermod.** *Pumper og Turbiner*. Trondheim : Vannkraftlaboratoriet, NTNU, 2003.
2. **Kjølle, Arne.** *Hydraulisk Måleteknikk*. Trondheim : Arne Kjølle, 2003. -.
3. **INTERNATIONAL STANDARD.** *IEC 60193 Hydraulic turbines, storage pumps and pump-turbines. Model acceptance tests*. -: Norsk nasjonalkomite for International Electrotechnical Commission, IEC, 1999.
4. **Sethna, Jim.** Cornell University Laboratory of Atomic and Solid State Physics. [Online] 30 June 1994. [Cited: 11 12 2011.] <http://www.lassp.cornell.edu/sethna/hysteresis/WhatIsHysteresis.html>.
5. *ISO 4185*.
6. **Solemslie, Bjørn Winther.** *Optimalisering av ringledning for pelton turbin*. Trondheim : NTNU, 2010. -.
7. **Ronald E Walpole, Raymond Myers, Sharon Myers, Keying Ye.** *Probability & Statistics for Engineers & Scientists*. London : Pearson , 2007. 0-13-0204767-5.
8. **Storli, Pål Tore.** *Modelltest av francis turbin* . NTNU, Trondheim : s.n., 2006.
9. **SKF.** www.karb-tech.hu. www.karb-tech.hu. [Online] - - 2003. [Cited: 28 10 2011.] http://www.karb-tech.hu/letoltesek/skf%20axialis%20beallo%20gorgoscsapagy%20katalogus%205104_.pdf.
10. **H K Versteeg, W Malalaseekera.** *An introduction to Computational Fluid Dynamics, The Finite Volume Method, second edition*. s.l. : Pearson Prentice Hall, 2006. 978-1-930934-21-4.
11. **APHSEALS.** American High Performance Seals. *American High Performance Seals*. [Online] APH Seals, 10 1 2012. [Cited: 10 1 2012.] http://www.ahpseals.com/products/rotaflon_rb.php.
12. **Stople, Remi Andre.** *Testing efficiency and characteristics of a Kaplan-type small turbine*. Trondheim : Remi Andre Stople, 2011.

13. **Andersen, Arne Georg.** *Certificate of calibration.* Kjeller : Justervesenet, 2006. CAL 016-06/730-3.
14. **CFD-online.** www.cfd-online.com. [Online] 28 February 2011. [Cited: 27 December 2011.] http://www.cfd-online.com/Wiki/SST_k-omega_model.
15. **Holo, Anders Linde.** *CFD Analysis of Distributor Flow.* Trondheim : Anders L. Holo, 2011.
16. **Wheeler AJ, Gnaji AR.** *Discrete Sampling and Analysis of Time-Varying Signals. Introduction to an Engineering Experimentation.* 2010.

Appendix A

A.1 Flow meter

Systematic error in the weighing tank system:

- $f_{Q,\Delta w}$ is the systematic uncertainty in the weight cells has been found by Pål Tore Storli to be $\pm 0.05043\%$ in (8)
- $f_{Q,t}$ is the systematic uncertainty of time measurements. The uncertainty related to time is assumed to be so small that it can be ignored.
- $f_{Q,divider}$ is the systematic uncertainty of the divider. The uncertainty was found to be $\pm 0.050555\%$ by Pål Tore Storli in (8) for a flow rate of 200 l/s. The value for 200 l/s is assumed to be a good estimate for all flow rates in this calibration.
- $f_{Q,\rho}$ is the systematic uncertainty in the density in the water and may be assumed according to IEC 60193 (3) to be $\pm 0.01\%$

When combining the uncertainties listed above with the RSS-method it results in a total systematic error in the primary calibration method of

$$f_{Q,a} = \pm \sqrt{f_{Q,\Delta w}^2 + f_{Q,divider}^2 + f_{Q,\rho}^2} = \pm 0.072104\%$$

Random error in the weighing tank system:

- $f_{Q,\Delta w}$ is the random uncertainty of the weight cells and the calibration of them and is found by Pål Tore Storli to be $\pm 0.00072\%$ in (8).
- $f_{Q,divider}$ is the random uncertainty of the divider is found by Pål Tore Storli to be $\pm 0.056532\%$ in (8) for a volume flow of 200 l/s. The random uncertainty is assumed to be a good estimate for all volume flows in this test.

When combining the uncertainties listed above with the RSS-method it results in a total random error in the primary calibration method of

$$f_{Q,b} = \pm \sqrt{f_{Q,\Delta w}^2 + f_{Q,divider}^2} = \pm 0.0565366\%$$

$f_{Q,c}$, the systematic error in the instrument, here being the volume flow meter. When calibrating the goal is to minimize the uncertainty in the signal given by the instrument by calibrating it against a given physical value, here the weighing tank. Since the flow meter not is calibrated against all possible volume flows this creates an uncertainty linked to values in volume flow not included in the calibration. This relative uncertainty is referred to as $f_{Q,regression}$. Also the random error $f_{Q,d}$ is included in the $f_{Q,regression}$.

It is important to mention that the volume flow meter is calibrated outside its guaranty range. This is done since the test require that the volume flow exceeds the guarantied volume range of the flow meter. There were no other flow meter available at the waterpower laboratory and the results have been discussed with Professor Torbjørn Nielsen and found acceptable.

$f_{Q,e}$, physical phenomena and external influences are assumed to be negligible since the calibration was done under the same conditions.

$f_{Q,f}$, the error in physical properties is also assumed to be negligible.

A.2 Torque gauge

- $f_{\tau,arm}$, with measured length of the arm of 0.5 meter and a uncertainty on the ruler of 0.001 meter the systematic uncertainty is found to be $\pm 0.2\%$
- $f_{\tau,w}$, the systematic uncertainty in the weights and the weight bed is calculated to have a maximum uncertainty of $\pm 0.0114325\%$. Documentation of uncertainties in the weights is done by Justervesenet (13).
- $f_{\tau,w}$, the regression uncertainty is calculated in the calibration program created by Bjørn Winther Solemslie and is found to be $\pm 1.235138\%$. [See Calibration report.](#)

A.3 Uncertainties in the pressure measurements

f_{kr} are ignored as is in chapter 4.5.2.

P1:

P2:

In the outlet pressure measurements the quantities causing uncertainties are as follows:

- Uncertainty in the radius of the outlet, r_2 . This uncertainty is assumed to be small but cannot be neglected.
- The uncertainty in the velocity of the water calculated to be equal for v_1 and v_2 . $f_v = \pm 0.10852\%$.
- The measured length from the bottom edge of the draft tube to the water surface. $f_H = 0.001\text{m}/0.5\text{m} = \pm 0.2\%$
- The uncertainty in the water level found by the flotation device created to read the water level in the lower reservoir. Due to friction in the device and the use of a normal ruler, the uncertainty is assumed to be $f_{\text{flot}} = \pm 2\%$. It would have been difficult to calculate a correct value for this uncertainty and an assumed value is therefore accepted.

By using the RSS-method the total relative outlet pressure uncertainty is found to be

$$f_{p2} = \pm \sqrt{0.2^2 + 2 \cdot 0.10852^2 + 2^2} = \pm 2.0158\% \quad (8.4)$$

A.4 Total relative hydraulic uncertainty

- f_E is dependent on the following quantities:

$$\begin{array}{lll}
 1) \frac{e_{p1}}{\rho} \text{ and } \frac{e_{p2}}{\rho} & 2) g \cdot e_{z1} \text{ and } g \cdot e_{z2} & 3) \frac{e_{v1}^2}{2} + \frac{e_{v2}^2}{2} \\
 4) \frac{p_1 - p_2}{\rho} & 5) g \cdot (z_1 - z_2) & 6) \frac{v_1^2 - v_2^2}{2}
 \end{array}$$

1. $e_{p1}/\rho = p_1 \cdot f_{p1} \cdot g = 0.25468 \cdot 9.82146516 \cdot 0.106843 = 0.267249681 \text{m}^2/\text{s}^2$
1. $e_{p2}/\rho = p_2 \cdot f_{p2} \cdot g = 0.411998 \cdot 0.020158 \cdot 9.82146516 = 0.0815678 \text{m}^2/\text{s}^2$
2. e_{z2} is zero because z_2 is set as reference level e_{z2} calculated to be $0.019643 \text{m}^2/\text{s}^2$ when the error in the measurements are 2mm.
3. $e_{v1}/2$ and $e_{v2}/2$ are calculated to be $0.221578 \text{m}^2/\text{s}^2$ and $0.06199 \text{m}^2/\text{s}^2$ when e_r is assumed to have a value of $\pm 0.1\text{mm}$.
4. $p_1/\rho = 2.044633 \text{m}^2/\text{s}^2$, $p_2/\rho = 4.04642 \text{m}^2/\text{s}^2$
5. Is calculated to be $21.0965 \text{m}^2/\text{s}^2$, $z_1 - z_2 = 2.148$.

6. $\frac{v_1^2}{2}$ and $\frac{v_2^2}{2}$ is calculated to be $1.1134\text{m}^2/\text{s}^2$ and $0.31148\text{ m}^2/\text{s}^2$ when Q is $0.18752[\text{m}^3/\text{s}]$.

This result in a total relative uncertainty in energy of:

$$f_E = \pm \frac{\sqrt{0.267249681^2 + 0.0815678^2 + 0.019643^2 + 0.221578^2 + 0.06199^2}}{2.044633 - 4.04642 + 21.0965 + 1.1134 - 0.31148} = \pm 1.8228\%$$

- f_p is calculated with the RSS-method and is found to be $\pm 1.253124\%$
- f_Q is calculated in chapter 4.6.4 to be $\pm 0.105387\%$
- By using the RSS-method the total relative uncertainty in the hydraulic efficiency is calculated to be:

$$f_{\eta h} = \pm \sqrt{1.8228^2 + 1.253124^2 + 0.105387^2} = \pm 2.2145\% \quad (8.5)$$

Appendix B

Appendix C

C.1 Matlab file Random Uncertainty

```
%% Leser inn raadatafilene for loggeverdier under målinger-
---

clear all
clc
temp=rawdata_import();
lengde=length(temp);
t=1.960;

%% Finner summen av alle voltverdiene ved alle målepunktene
og hvor mange
% punkter det i hver måleserie
m=0;
for i = 1:lengde
    nan_locations = find(isnan(temp{2,i}));
    temp{2,i}(nan_locations) = 0;
    n_rows(i) = size(temp{2,i},1);
    x_values(i) = temp(2,i);
    x = x_values{1,i};
    for j = 1:n_rows(i)
        m = m+1;
        AMIOMq(m,1)=x(j,1);           %All Matrix In One
Matrix
        AMIOMP(m,1)=x(j,2);
        AMIOMm(m,1)=x(j,3);
    end
end

% Finner så standardavvik til trykk-, moment- og
volumstrømsmålingene, for
% så å rene ut usikkerheten til hver enkelt størrelse.

n=sum(n_rows);
avrq = mean2(AMIOMq);
avrp = mean2(AMIOMP);
avrm = mean2(AMIOMm);
Sxq = std2(AMIOMq);
Sxp = std2(AMIOMP);
Sxm = std2(AMIOMm);
randomunc_q = (t*Sxq)/sqrt(n);
randomunc_p = (t*Sxp)/sqrt(n);
randomunc_m = (t*Sxm)/sqrt(n);

uncq=randomunc_q*100/avrq
```

```
uncp=randomunc_p*100/avrp
uncm=randomunc_m*100/avrm
```

C.2 Matlab file Uncertainty analysis

```
clc
```

```
%Leser inn filen-----  
-----
```

```
S=xlsread('R19.xlsx');  
format long  
%Finner antall elementer i filen og gjennomsnittet av  
verdiene i filen----
```

```
Num=size(S);  
Num_col=Num(1,2);  
Num_row=Num(1,1);  
Avg=mean2(S);  
n=numel(S);  
y(1,1)=0;
```

```
%Finner standardavviket i hver fil-----  
-----
```

```
for i=1:Num_row  
    for j=1:Num_col  
        x(i,j)=(S(i,j)-Avg)^2;  
        %y(i+1,j+1)=y(i,j)+x(i,j)  
    end  
end  
y=sum(x);  
z=sum(y);  
s_y19=sqrt((z)/(n-1))
```

```
a=0.2;  
t=1;
```

```
while a<0.5  
    if n>62  
        t=1.960;  
        a=1;  
    else  
        a=0;  
    end  
end  
e_y19=((t*s_y19)/sqrt(n))
```

```
f_y19=(e_y19/Avg)*100
xlswrite('ABC',e_y19,1,'B20')
```

C.3 Matlab file Efficiency calculation

```
clc
clear all
close all

% Kjører importprogram for å hente inn alle data som ble
logget under test

temp=rawdata_import;

% Finner størrelsen på rawdata filen for å kunne bestemme
hvor mange filer
% som ble lest inn. Oppretter konstanter som benyttes
senere

g = 9.82;
ops = length(temp);

% Finner virkningsgraden til hvert enkelt målte punkt-----
-----

for i = 1:ops
    select = temp{2,i};
    num=size(select,1);
    for j = 1:num
        M(j,i) = select(j,3);
        w(j,i) = (pi()*select(j,10))/30;
        rho(j,i) = select(j,7);
        he(j,i) = select(j,4)-0.0465;
        Q(j,i) = select(j,1)/1000;
        nhelp(j,i)=select(j,10);
        efficiency(j,i) =
((M(j,i)*w(j,i))/(rho(j,i)*g*he(j,i)*Q(j,i)))*100;
    end
end

% Finner gjennomsnittlig turtall for hver enkelte
måleserie-----

for k = 1:ops
    select = temp{2,k};
```

```

num=size(select,1);
for l = 1:num
    if nhelp(l,k) == 0
        alskj = 1;
    else
        n2(l)=nhelp(l,k);
    end
end
n(k)=mean(n2);
end

%% Kjører en løkke for å finne en finere linje og for å få
punkter mellom de
% målte verdiene
for i = 1:ops
    select = temp{2,i};
    num=size(efficiency,1);
    for j = 1:num
        if efficiency(j,i) == 0
            A(j,i) = NaN;
            B(j,i) = NaN;
            Lars(j,i) = NaN;
            Lars2(j,i) = 0;
            D(j,i) = 0;
            E(j,i) = 0;
        else
            A(j,i) = Q(j,i);
            B(j,i) = efficiency(j,i);
            Lars(j,i) = he(j,i);
            Lars2(j,i) = he(j,i);
            D(j,i) = Q(j,i);
            E(j,i) = efficiency(j,i);
        end
    end

end

[p,h] = polyfit(Lars2(:,i),E(:,i),4);

z=min(Lars(:,i)) : ((max(Lars(:,i))-
min(Lars(:,i)))/24999) :
max(Lars(:,i));
% z=min(A(find(~isnan(A(:,i))),i)) :
(max(A(find(~isnan(A(:,i))),i)
%)-min(A(find(~isnan(A(:,i))),i)))/24999 :
max(A(find(~isnan(A(:,i))),i));

hill.etha(:,i) = polyval(p,z);
polys{i}=p;
hill.he(:,i)=z;

```

```

        hill.n(1:25000,i)=n(1,i);

    i

end

%% Sorterer Hill-data

[hill.he,i]=sort(hill.he);
for u=1:25000
    for v=1:11
        n_temp(u,v)=hill.n(i(u,v),v);
        etha_temp(u,v)=hill.etha(i(u,v),v);
    end
end
hill.n=n_temp;
hill.etha=etha_temp;

%% Plotter hilldiagram

figure
grid on

[C,h]=contour(hill.n(1:100:end,:),hill.Q(1:100:end,:),hill.
etha(1:100:end,:),
[50:5:65 67:2:71 72:1:75 75.1:0.5:82
82.1:0.2:84], 'linewidth',1.5);
grid on
xlabel('n [rpm]')
ylabel('Q [m3/s]', 'rotation',90)
set(gca, 'fontSize',12)
clabel(C, 'fontsize',12)
figure
surf(hill.n(1:100:end,:),hill.Q(1:100:end,:),hill.etha(1:100:
end,:))
xlabel('n [rpm]')
ylabel('Q [m3/s]', 'rotation',90)
zlabel('\eta [%]')
figure
hold on
farge={'b' 'k' 'r' 'g' 'm' 'y' '*-b' 's-k' '*-r' 'o-g' 's-
b'};

for i=1:ops
    plot(A(:,i),B(:,i),farge{i}, 'linewidth',1.5);
    leg(i)={strcat('n=',num2str(n(i)), 'rpm')};

```



```
end
```

```
xlabel('Q [m3/s]')  
ylabel('{\eta} [%]')  
grid on  
legend(leg, 'orientation', 'horizontal', 'location', 'northouts  
ide')
```

C.4 Regression uncertainty

```
%% Leser inn data fra Veietanken og de loggede  
voltageverdiene-----  
clear all  
clc  
temp=rawdata_import();  
yi=xlsread('veietankverdier2.xls');  
lengde=length(temp);  
t=1.960;  
yavg=mean2(yi);  
%% Finner summen av alle voltageverdiene ved alle målepunktene  
og hvor mange  
% punkter det i hver måleserie  
  
for i = 1:lengde  
    nan_locations = find(isnan(temp{2,i}));  
    temp{2,i}(nan_locations) = 0;  
    m_rows(i) = size(temp{2,i},1);  
    n_cols(i) = size(temp{2,i},2);  
    tot_x(i) = sum(sum(temp{2,i}));  
    temp2(i)=mean2(temp{2,i});  
    x_values(i) = temp(2,i);  
end  
totalx=sum(tot_x);  
xavg=mean2(temp2);  
  
%% Regner ut Sxx Syy og Sxy og b. Kjører tre for-løkker for  
å hente ut hver  
% eneste enkeltverdi fra matrisene  
  
for i = 1:lengde  
    x_temp = x_values(i);  
    for j = 1:m_rows(i)  
        for k = 1:n_cols(i)  
            y = yi(i);  
            y_temp2(j,k) = (y-yavg)^2;
```

```

        x = x_temp{1,1};
        x_temp2(j,k) = (x(j,k)-xavg)^2;
        xy_temp2(j,k) = (x(j,k)-xavg)*(y-yavg);
    end
end
y_temp3(i)=sum(sum(y_temp2));
x_temp3(i)=sum(sum(x_temp2));
xytemp3(i)=sum(sum(xy_temp2));
maxtemp(i)=max(max(x));
mintemp(i)=min(min(x));
i
end

Sxx = sum(x_temp3)
Syy = sum(y_temp3)
Sxy = sum(xytemp3)

b=Sxy/Sxx

% Setter inn kalibreringsligningen som er funnet ved å
benytte excel:

% Regner ut varians og standardavvik og finner
confidensintervallet
% plotter så usikkerheten.

s2 = (Syy-b*Sxy)/(totalx-2)

s=sqrt(s2)

A=max(maxtemp);
B=min(mintemp);

for x0=1:8
    Y(x0) = (0.012415793*x0-0.024820801)*1000
    % Y(x0) = 81.49352283*x0-162.87533823;
    con_interval(x0)=t*s*sqrt((1/totalx)+((x0)-
xavg)^2)/Sxx);
    yeah(x0) = Y(x0)+con_interval(x0)*10000;
    yeah2(x0) = Y(x0)-con_interval(x0)*10000;
end

plot(Y)
xlabel('Volt [V]')
ylabel('Volume flow [l/s]')

```

```
title('Calibration curve with 95% confidence interval  
scaled by 1000')  
grid on  
hold on  
plot(yeah, 'color', 'red')  
hold on  
plot(yeah2, 'color', 'red')  
hold on
```

Appendix D

Table 13 Weight calibration calculation

| Weight number | Actual weight [kg] | Uncertainty [kg] | Uncertainty [%] | Uns^2 |
|------------------------------|--------------------|------------------|-----------------|--------------------|
| 24 | 1,997513 | 0,000062 | 0,00310386 | 9,63394E-06 |
| 40 | 4,99809 | 0,00015 | 0,003001146 | 9,00688E-06 |
| 44 | 4,99924 | 0,00015 | 0,003000456 | 9,00274E-06 |
| 45 | 4,99816 | 0,00015 | 0,003001104 | 9,00663E-06 |
| 51 | 1,999092 | 0,000065 | 0,003251476 | 1,05721E-05 |
| 52 | 1,998907 | 0,000089 | 0,004452433 | 1,98242E-05 |
| 53 | 1,999424 | 0,00006 | 0,003000864 | 9,00519E-06 |
| 54 | 1,999742 | 0,00006 | 0,003000387 | 9,00232E-06 |
| 55 | 1,999887 | 0,00006 | 0,00300017 | 9,00102E-06 |
| 56 | 1,999224 | 0,000059 | 0,002951145 | 8,70926E-06 |
| 57 | 1,999551 | 0,000062 | 0,003100696 | 9,61432E-06 |
| 58 | 1,999752 | 0,000059 | 0,002950366 | 8,70466E-06 |
| 59 | 1,998864 | 0,000062 | 0,003101762 | 9,62093E-06 |
| Total uncertainty [%] | | | | 0,011432591 |

Appendix E

SKF Bearing life - Mozilla Firefox

www.skf.com/skf/productcatalogue/calculationsFilter;jsessionid=6NmAOSfLv

Product data Print ? Calculations Close

Bearing life

Every care has been taken to ensure the accuracy of this calculation but no liability can be accepted for any loss or damage whether direct, indirect or consequential arising out of the use of the calculation.
See section "SKF rating life"

Bearing [22310 E](#)

Select η_c
0.5

| | |
|------------------------|------|
| d [mm] | 50 |
| D [mm] | 110 |
| C [kN] | 220 |
| P_u [kN] | 24 |
| P [kN] | 10 |
| n [r/min] | 1000 |
| v [mm ² /s] | 25 |

Calculate

| | | | | | |
|------------------|------|------------------|-----------|-------------------|-----------|
| κ | 1.91 | L ₁₀ | 29800 | L _{10h} | 497300 |
| v_1 | 13.1 | | | | |
| a _{SKF} | 50 | L _{10m} | > 1000000 | L _{10mh} | > 1000000 |

Old a₂₃ method for comparison

| | | | | | |
|-----------------|------|------------------|-------|-------------------|--------|
| a ₂₃ | 1.53 | L _{10a} | 45800 | L _{10ah} | 762900 |
|-----------------|------|------------------|-------|-------------------|--------|

For grease lubricated bearings, please check the grease life. See section "Grease lubrication"

For calculation of two bearings on a shaft, see the program "SKF Bearing Select"

For calculation of the contamination factor η_c , see the program "SKF Bearing Select"

Screenshot of bearing life time calculation. Date entered www.skf.com 15.10.2011.

Appendix F

The results generated by a CFD analysis is depending on the settings listed below. More parameters can influence the final result, but they have only a small impact and are considered to neglect able in this analysis.

Mesh

A mesh is generated by small nodes placed inside the geometry to be tested. The number of nodes will decide how fine the mesh is. A fine mesh is necessary to pick up boundary layer effects and other flow effects such as separation. Boundary layer effects caused by wall share are a major factor in flow analysis. To be able to pick up these effects a fine mesh near wall surfaces in necessary. An extremely fine mesh, above 20.000.000 nodes, is in most cases not possible do analyse on an ordinary computer it is common to use inflation along the walls. Inflation refines the mesh near the walls and makes the mesh grow with a factor towards the normal mesh size. This reduces the number of nodes needed in order to obtain a good mesh.

Boundary layers are present in all fluid flows and can be divided into three separate layers:

1. Viscous sub layer: Viscous shear is the dominant factor.
2. Buffer layer: Velocity and turbulence are dominant factors.
3. Overlap layer: Both viscous and turbulent shears are important.

There are several turbulence models to choose from when solving the fluid flow. The model used in the simulations will be described later.

When simulating it is normal to check for grid independence. This means that when changing the mesh the result does not change.

Boundary conditions

When the geometry and the mesh have been created initial boundary conditions have to be set to start the simulations. The boundary conditions give the initial condition in the first set of nodes. Simulation is an iterating process solved numerically where the state in one set of nodes is dependent on the state in the previous set of nodes which changes until the simulation has converged, if steady state has been chosen.

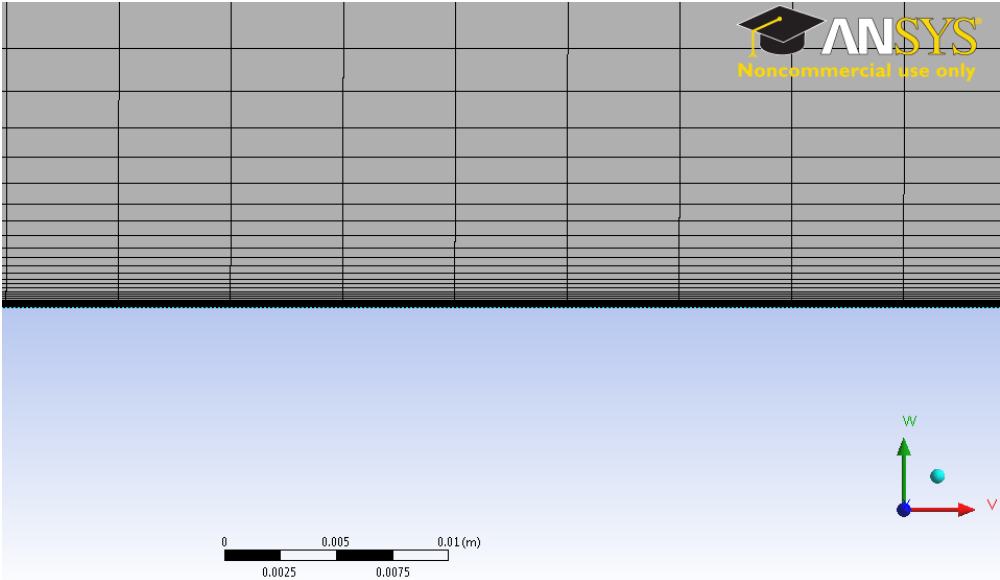


Figure 13-1 Inflation along wall of the inlet

The inlet condition in the simulations done in this thesis was inlet velocity. Inlet velocity was chosen on recommendations of Ph.D. Mette Eltvik and Martin Holst. The outlet condition was set to outflow, meaning that all flow in has to flow out of the specified boundary without any predetermined pressure or velocity. The simulation is free and the flow is not forced into a predetermined direction. The outlet condition was chosen after consulting Professor Torbjørn Nielsen.

Turbulence model

The turbulence model used in the simulation is the SST k-omega turbulence model. The model is good in the viscous sub layer and is also good in the free stream. The model also behaves well in adverse pressure gradients and in separating flow (14). The simulations are performed in order to find out if the sharp bend causes backflow and separation.

Residuals

Residuals are the difference between the iterated value and the exact solution. Since FLUENT does not know the real value the residuals gives the value between two iterations. The residuals should converge with a value lower than

10E-4. The simulation can converge with a value lower than 10E-4 without the solution to be correct. This is a mesh problem and a grid independence test is needed. See Mesh chapter above.

Y plus

The y^+ value is calculated as in equation(8.6):

$$y^+ = \frac{u_* \cdot y}{\nu} \quad (8.6)$$

Where u_* is the friction velocity at the nearest wall, y is the distance from the nearest wall to the first node and ν is the kinematic viscosity of the fluid (15). The y plus value should not exceed a value of 5 when using the SST k-omega turbulence model in order to pick up the effects in the viscous sub layer. The y plus value should have a value close to one for the turbulence model to perform optimal.

Appendix G

Three different LabView programs were used during test and calibration. The program used to calibrate pressure and torque is developed by Håkon Hjort Francke and further developed by Bjørn Winther Solemslie. The calibration program for the volume flow and the logging program used to log and collect data in the test is developed by Remi Andre Stople.

Calibration program for torque and pressure

The program logs the exact value from the given equipment and calculated the systematic error in the measurement. The program also calculate the calibration curve used in the actual measurements. The values are printed as a written report after the calibration is complete.

Calibration program for volume flow

Remi Andre Stople created a simple program to calibrate the flow meter. The program logs data and calculate the mean volume flow. Raw data and the mean value is written too two different output files. Random error in the calibration is calculated and is displayed in the front panel of the program.

LabView program used in experiments

The LabView program used in the experiment to acquire data logs x number of readings per second. The program simultaneously calculated efficiency and other important parameters for the tests (12).

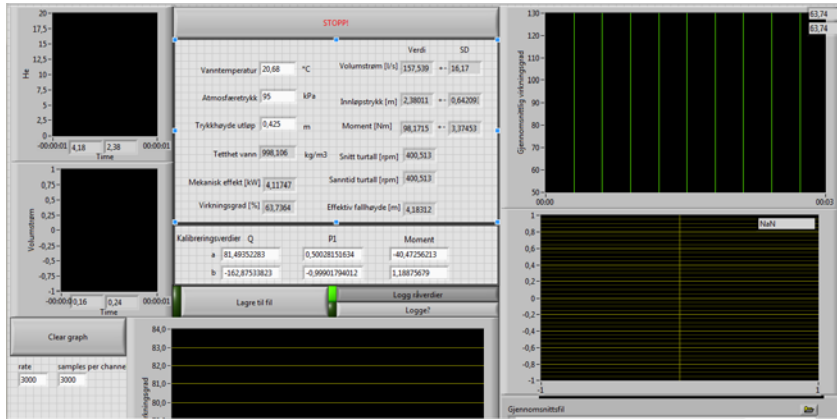


Figure 13-2 Front panel

In the user interphase of the program water temperature, atmospheric pressure, height difference between draft tube and the water surface are input that has to be set before tests begin. Outlet pressure and water density are calculated from the input parameters. Calibration values are also needed in order to translate the volt signal from the measuring equipment into physical values. Sample rate and samples per channel can be adjusted by the user in order to get as many readings as the user desires and find necessary.

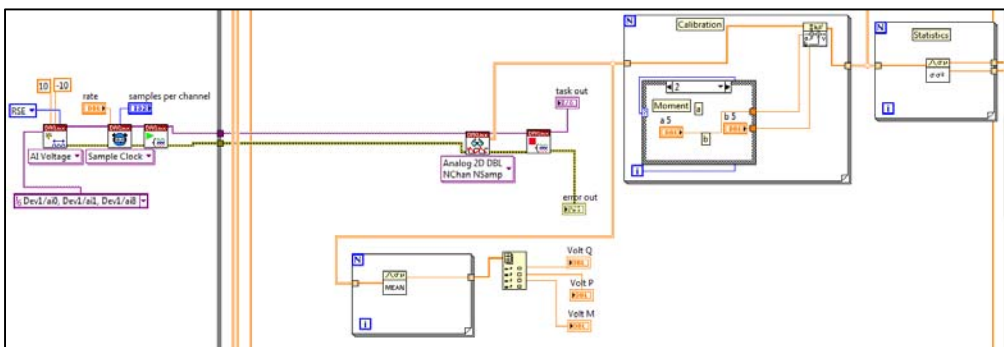


Figure 13-3 Data acquisition and translation of volt signals

A DaqMX package in LabView is used to read the Volt signal from each measuring device. The values from the DaqMX package are sent to a “for loop” where the signals are translated into physical values. Output values from the loop are sent to raw data storage and to a new “for loop” which calculated the mean value and the standard deviation in the measurements (12).

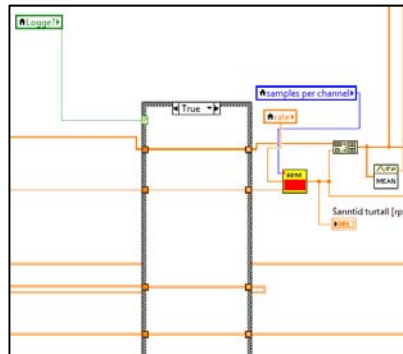


Figure 13-4 RPM subVI for readings of the rotational speed

Rotational speed is read by a program made by Joar Grilstad and implemented in the main program with help from Bjørn Winther Solemslie. The program continuously reads the rotational speed and delivers the last read rpm value to the main program. This is done to avoid the delay the sub VI creates in the main program. Delay occurs since the optical trip meter only produces a signal every time the reflex band passes the optical reader and is therefore dependent on the rotational speed. The main program on the other hand creates values at a pre-determined fixed rate (12). In Figure 13-5 the block diagram of sub VI is shown.

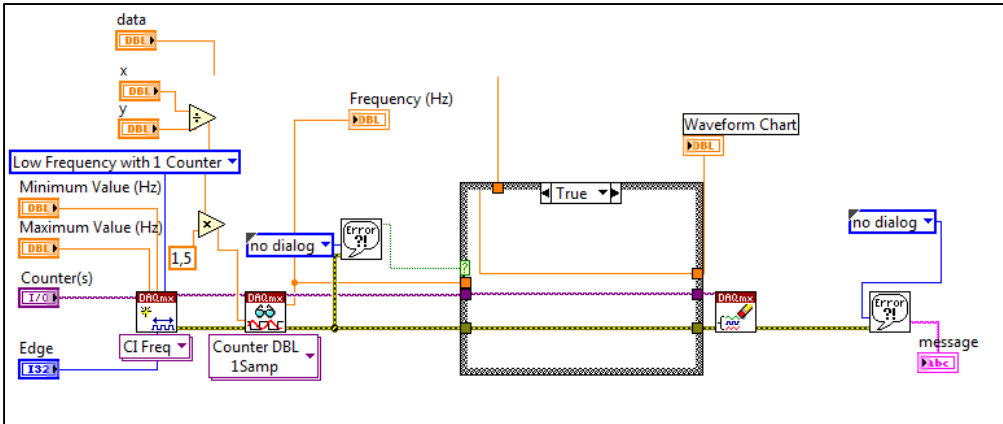


Figure 13-5 Block diagram for the RPM sub VI

After the calibration “for loop” the values are sent to a calculation node. All the calculations in the program are done in the calculation node. The calculated values are bundled together in a long array. Mean values from the measured calibrated parameters are added to the same array. The array is then send to mean value storage.

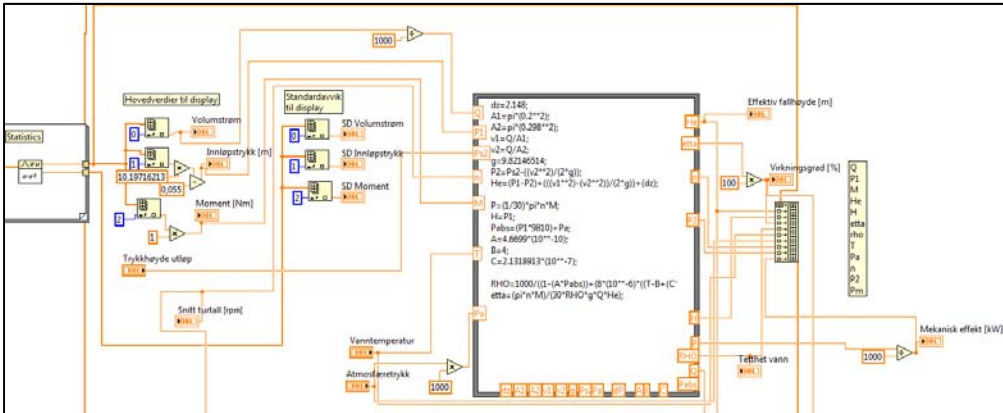


Figure 13-6 Calculation node and front panel values

In Figure 13-7 raw data storage, mean value storage and rpm storage are shown respectively from left to right. The rpm and mean value storage checks if there exist an rpm or mean value file every time the program is saved. If a file exists a new line is added to the file containing the last saved values else they create an rpm file and a mean value file. Raw data storage creates a new file every time the program is saved.

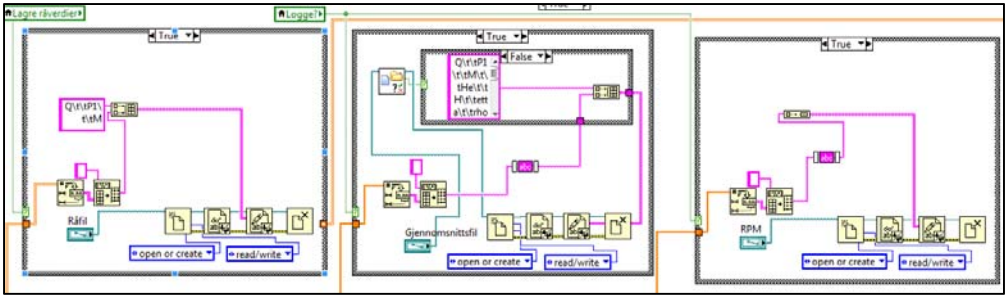


Figure 13-7 Storage

Remi Andre Stople implemented a function seen in the Figure below that plotted the efficiency vs. effective head in the user interphase. This was done in order to detect any spurious errors in the tests.

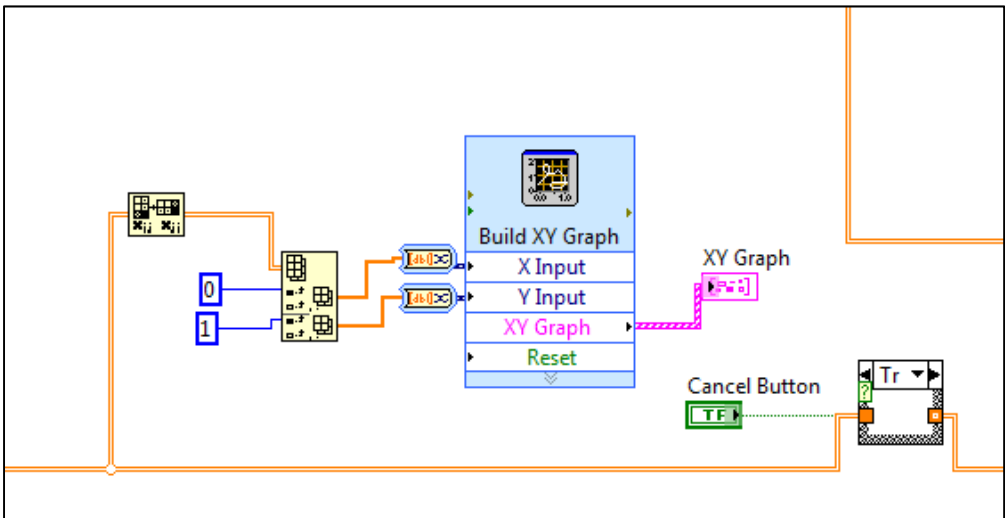
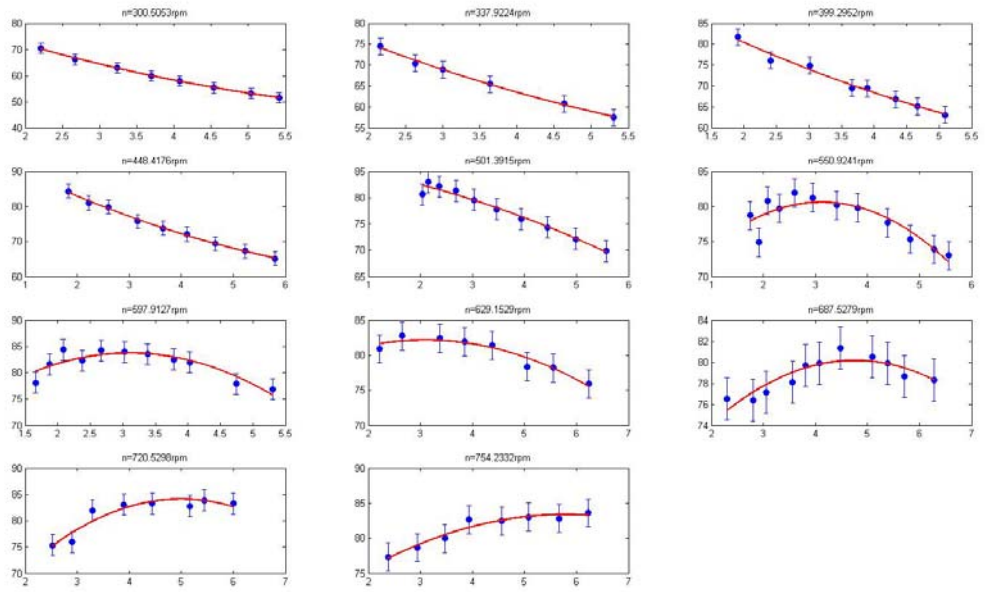


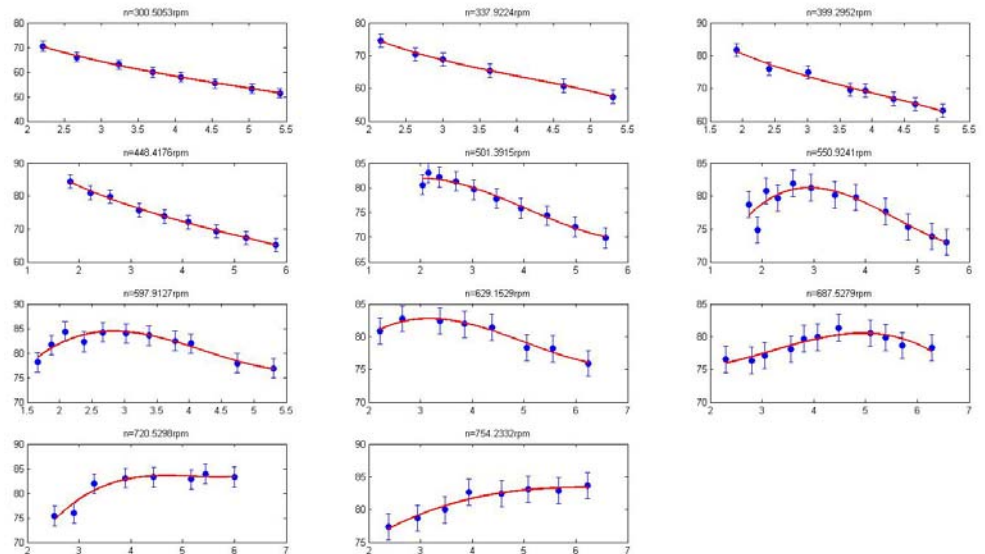
Figure 13-8 Plotting of efficiency-head graph

Appendix H

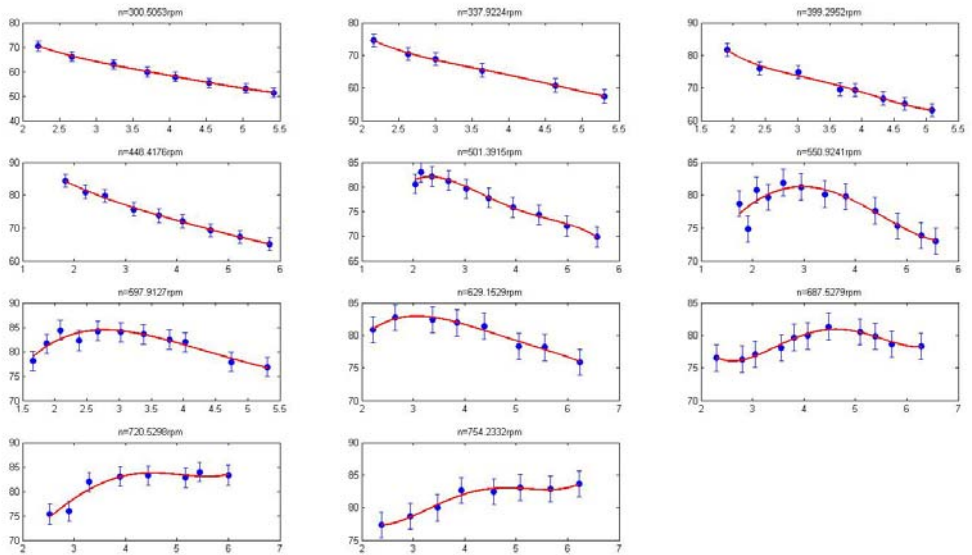
H.1 2nd order poly fit



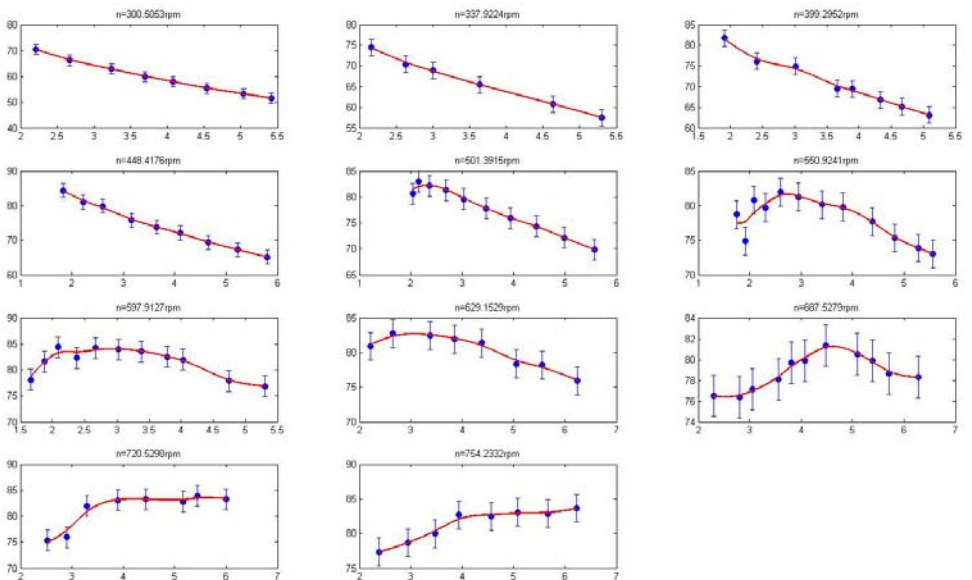
H.2 3rd order poly fit



H.3 4th order poly fit



H.4 Smoothing spline



Appendix I,

Calibration certificate Druck DPI

CALIBRATION CERTIFICATE
(POSITIVE PRESSURE)

UNIT UNDER TEST (UUT)

CALIBRATOR INFORMATION

Manufacturer : Druck
Type Number : DPI601
Serial Number : 14206/96-1
Sales Order Number : M11798-1
Parameter Range : 0 to 10 bar g
Calibration Date : 24 January 1996
Calibrated By : S.Pattison
External Sensor Serial No. :

1. Manufacturer : Budenburg
Calibration Instrument : Type 246
Serial Number : 10442
Calibrated Against (*1) : Druck Stds. Lab.
Pressure Medium : Dry Nitrogen

AMBIENT CONDITIONS

Ambient Temperature (°C) : 19.0
Local Gravity (ms⁻²) : 9.81291

PERFORMANCE DATA

| Nominal Applied Value bar | Actual Applied Value bar (*2) | Unit Under Test Reading bar (*3) | Unit Under Test Deviation (*4) | Permissible Deviation | Pass/ Fail |
|------------------------------|----------------------------------|-------------------------------------|-----------------------------------|-----------------------|---------------|
| 0.000 | 0.000 | 0.000 | 0.000 %fs | ± 0.050%fs ± 1 digit | Pass |
| 2.000 | 2.000 | 2.000 | 0.000 %fs | ± 0.050%fs ± 1 digit | Pass |
| 4.000 | 4.000 | 4.000 | 0.000 %fs | ± 0.050%fs ± 1 digit | Pass |
| 6.000 | 6.000 | 6.000 | 0.000 %fs | ± 0.050%fs ± 1 digit | Pass |
| 8.002 | 8.002 | 8.001 | - 0.010 %fs | ± 0.050%fs ± 1 digit | Pass |
| 10.002 | 10.002 | 10.003 | 0.010 %fs | ± 0.050%fs ± 1 digit | Pass |

COMMENTS

I hereby certify that the details above are correct.

Certified by: S.PATTISON

Signed: S.Pattison

Date: 24 January 1996

NOTES

- (*1) Traceable to relevant International Standards.
- (*2) Actual Applied Value corrected for gravity and temperature as appropriate. Where applicable, other scales to BS350 calculated equivalent engineering units are used.
- (*3) Actual recorded values. For specification, see Permissible Deviation column.
- (*4) Deviation calculated from U.U.T. Reading minus Actual Applied Value.

CAL1 6/92



Kværner Energy a.s
 Trondheim

Project id: U

Kalibrering av/Object: DPI 001 / 10 bar NTNU 4539-1

Formål/Purpose:

Temperatur = 23°C

| ME1 | ME110 | | 4539-1 | | | |
|----------|--------|--|--------|--|--|--|
| kPa | kPa | | Bar | | | |
| 0 | 0 | | 0 | | | |
| 249.855 | 249.6 | | 2.498 | | | |
| 511.627 | 511.1 | | 5.114 | | | |
| 752.169 | 751.5 | | 7.520 | | | |
| 1000.422 | 999.7 | | 10.003 | | | |
| 1256.085 | 1255.0 | | | | | |
| 1550.303 | 1548.1 | | | | | |
| 1822.690 | 1820.1 | | | | | |
| 2002.045 | 2000.2 | | | | | |
| 0 | -0.8 | | | | | |
| | | | | | | |
| | | | | | | |
| | | | | | | |
| | | | | | | |
| | | | | | | |
| | | | | | | |
| | | | | | | |
| | | | | | | |
| | | | | | | |
| | | | | | | |
| | | | | | | |
| | | | | | | |
| | | | | | | |
| | | | | | | |
| | | | | | | |
| | | | | | | |
| | | | | | | |
| | | | | | | |
| | | | | | | |

Dato/Date/Sign 96-04-22 Godkjent/Approved

Appendix J

Weight calibration



NTNU Vannkraftlaboratoriet
Alfred Getz vei 4
7491 TRONDHEIM

Deres ref./Your ref.
Jørgen Ramdal

Vår ref./Our ref.
06/730 - /AGA-tkv/511

Dato/Date
29.08.06

Kalibrering av lodd

Vedlagt følger Deres kalibreringsbevis nr. CAL 016-06/730-3 til Deres kalibrerte lodd.

Resultatene skal dere ha fått tilsendt pr. mail fra Nils M. Thomassen tidligere, men ved skrivning av beviset fant vi to feil i filen. For lodd NTNU VKL 52 og NTNU VKL 103 ble det oppgitt feil k-faktor, frihetsgrader og usikkerhet i filen dere fikk tilsendt. Kalibreringsbeviset inneholder riktige tall. Vi beklager dette.

Faktura vil bli sendt separat.

Med hilsen


Turid K. Viken
konsulent

KALIBRERINGSBEVIS Certificate of calibration Nr./No: CAL 016-06/730-3



Kalibreringslaboratoriets navn:
Name of the calibration laboratory:
JUSTERVESENET
Oslo justerkammer

Laboratoriets adresse:
Laboratory address:
Fetveien 99
2007 KJELLER

Side/Page: 1 av/of: 4
Ref. til måleprotokoll/Ref to records:
06/730

| | |
|--|---|
| Tid og sted for kalibrering/ <i>Date and place of calibration:</i> | Bevisets utstedelsesdato: <i>Date of issue:</i> |
| Kjeller, 9. – 15. august 2006 | Kjeller, 28. august 2006 |
| Kalibrering utført av/ <i>Calibration performed by:</i> | Ansvarlig/ <i>responsible:</i> |
| Arne Georg Andersen, avdelingsingeniør | Nils M. Thomassen, justermester |

Kunde: NTNU Vannkraftlaboratoriet, Alfred Getz v. 4, 7491 Trondheim.
Customer

Instrument: Lodd
Item

Kapasitet: 650 g – 5,7 kg
Capacity

Produsent: Ikke kjent
Manufacturer

Typebetegnelse: Se resultater side 2.
Model

Serienummer: Ikke kjent
Serial number

Intern nummer: Se side 2.
Internal number

Tidligere kalibreringsbevis nr.: CAL 016-32/05/1. NTNU VKL 103 er ikke kalibrert tidligere.
Previous calibration no.

Delte kalibreringsbeviset er utstedt av et laboratorium som er akkreditert i Norsk Akkreditering (NA). Akkrediteringen medfører at laboratoriet oppfyller de kravene NA stiller til kompetanse og kalibreringssystem for de kalibreringene akkrediteringen omfatter. Det innebærer også at laboratoriet har et tilfredsstillende kvalitetssikringssystem og sporbarhet til akkrediterte eller nasjonale kalibreringslaboratorier. Kopiering av dette kalibreringsbeviset er kun tillatt dersom beviset kopieres i sin helhet.

This certificate of calibration is issued by a laboratory accredited by Norwegian Accreditation (NA). The accreditation states that the laboratory meets the NA requirements concerning competence and calibration system for all the calibrations contained in the accreditation. It also states that the laboratory has a satisfactory quality assurance system and traceability to accredited or national calibration laboratories. This certificate of calibration may not be reproduced other than in full.

KALIBRERINGSBEVIS

Certificate of Calibration

Justervesenet

Oslo Justerkammer

Nr./No.: CAL 016-06/730-3

Side/Page: 2 av/of: 4

Måleresultater med usikkerhet:

| Nominell verdi | Kjennetegn | Konvensjonell verdi | Usikkerhet (k = 2) | k-faktor ref EA 4/02 | V _{eff} |
|----------------|-------------|---------------------|--------------------|----------------------|------------------|
| 5 kg | NTNU VKL 1 | 5 kg + 0,32 g | ± 0,15 g | k = 2 | ∞ |
| 5 kg | NTNU VKL 2 | 5 kg + 0,42 g | ± 0,15 g | k = 2 | ∞ |
| 5 kg | NTNU VKL 3 | 5 kg + 0,24 g | ± 0,15 g | k = 2 | ∞ |
| 5 kg | NTNU VKL 4 | 5 kg - 0,22 g | ± 0,15 g | k = 2 | ∞ |
| 5 kg | NTNU VKL 5 | 5 kg + 0,63 g | ± 0,15 g | k = 2 | ∞ |
| 5 kg | NTNU VKL 6 | 5 kg + 0,61 g | ± 0,15 g | k = 2 | ∞ |
| 5 kg | NTNU VKL 7 | 5 kg + 0,96 g | ± 0,15 g | k = 2 | ∞ |
| 5 kg | NTNU VKL 8 | 5 kg + 0,42 g | ± 0,15 g | k = 2 | ∞ |
| 5 kg | NTNU VKL 9 | 5 kg + 0,93 g | ± 0,15 g | k = 2 | ∞ |
| 5 kg | NTNU VKL 10 | 5 kg + 0,72 g | ± 0,15 g | k = 2 | ∞ |
| 5 kg | NTNU VKL 11 | 5 kg + 0,39 g | ± 0,15 g | k = 2 | ∞ |
| 5 kg | NTNU VKL 12 | 5 kg + 0,10 g | ± 0,15 g | k = 2 | ∞ |
| 5 kg | NTNU VKL 13 | 5 kg + 0,07 g | ± 0,15 g | k = 2 | ∞ |
| 5 kg | NTNU VKL 14 | 5 kg + 0,15 g | ± 0,15 g | k = 2 | ∞ |
| 5 kg | NTNU VKL 15 | 5 kg + 0,20 g | ± 0,15 g | k = 2 | ∞ |
| 5 kg | NTNU VKL 16 | 5 kg + 0,29 g | ± 0,15 g | k = 2 | ∞ |
| | | | | | |
| 2 kg | NTNU VKL 21 | 2 kg - 0,858 g | ± 0,070 g | k = 2 | ∞ |
| 2 kg | NTNU VKL 22 | 2 kg - 0,246 g | ± 0,068 g | k = 2 | ∞ |
| 2 kg | NTNU VKL 23 | 2 kg - 0,241 g | ± 0,060 g | k = 2 | ∞ |
| 2 kg | NTNU VKL 24 | 2 kg - 2,487 g | ± 0,062 g | k = 2 | ∞ |
| | | | | | |
| 5 kg | NTNU VKL 28 | 5 kg - 2,03 g | ± 0,15 g | k = 2 | ∞ |
| 5 kg | NTNU VKL 29 | 5 kg - 1,38 g | ± 0,15 g | k = 2 | ∞ |
| 5 kg | NTNU VKL 30 | 5 kg - 0,98 g | ± 0,15 g | k = 2 | ∞ |
| 5 kg | NTNU VKL 31 | 5 kg - 0,36 g | ± 0,15 g | k = 2 | ∞ |
| 5 kg | NTNU VKL 32 | 5 kg - 1,63 g | ± 0,15 g | k = 2 | ∞ |
| 5 kg | NTNU VKL 33 | 5 kg - 1,13 g | ± 0,15 g | k = 2 | ∞ |
| 5 kg | NTNU VKL 34 | 5 kg - 0,84 g | ± 0,15 g | k = 2 | ∞ |
| 5 kg | NTNU VKL 35 | 5 kg - 1,61 g | ± 0,15 g | k = 2 | ∞ |
| 5 kg | NTNU VKL 36 | 5 kg - 1,71 g | ± 0,15 g | k = 2 | ∞ |
| 5 kg | NTNU VKL 37 | 5 kg - 1,52 g | ± 0,15 g | k = 2 | ∞ |
| 5 kg | NTNU VKL 38 | 5 kg - 1,76 g | ± 0,15 g | k = 2 | ∞ |
| 5 kg | NTNU VKL 39 | 5 kg - 1,83 g | ± 0,15 g | k = 2 | ∞ |
| 5 kg | NTNU VKL 40 | 5 kg - 1,91 g | ± 0,15 g | k = 2 | ∞ |
| 5 kg | NTNU VKL 41 | 5 kg - 1,57 g | ± 0,15 g | k = 2 | ∞ |
| 5 kg | NTNU VKL 42 | 5 kg - 1,56 g | ± 0,15 g | k = 2 | ∞ |
| 5 kg | NTNU VKL 43 | 5 kg - 1,74 g | ± 0,15 g | k = 2 | ∞ |
| 5 kg | NTNU VKL 44 | 5 kg - 0,76 g | ± 0,15 g | k = 2 | ∞ |
| 5 kg | NTNU VKL 45 | 5 kg - 1,84 g | ± 0,15 g | k = 2 | ∞ |

Kopiering av dette kalibreringsbeviset er kun tillatt dersom beviset kopieres i sin helhet.
This certificate of calibration may not be reproduced other than in full.

KALIBRERINGSBEVIS

Certificate of Calibration

Justervesenet
Oslo Justerkammer

Nr./No.: CAL 016-06/730-3

Side/Page: 3 av/of: 4

| Nominell verdi | Kjennetegn | Konvensjonell verdi | Usikkerhet (k = 2) | k-faktor ref EA 4/02 | V _{eff} |
|----------------|--------------|---------------------|--------------------|----------------------|------------------|
| 5 kg | NTNU VKL 46 | 5 kg - 1,74 g | ± 0,15 g | k = 2 | ∞ |
| 5 kg | NTNU VKL 47 | 5 kg - 0,99 g | ± 0,15 g | k = 2 | ∞ |
| 5 kg | NTNU VKL 48 | 5 kg - 1,08 g | ± 0,15 g | k = 2 | ∞ |
| 5 kg | NTNU VKL 49 | 5 kg - 1,33 g | ± 0,15 g | k = 2 | ∞ |
| 5 kg | NTNU VKL 50 | 5 kg - 0,47 g | ± 0,15 g | k = 2 | ∞ |
| 2 kg | NTNU VKL 51 | 2 kg - 0,908 g | ± 0,065 g | k = 2 | ∞ |
| 2 kg | NTNU VKL 52 | 2 kg - 1,093 g | ± 0,089 g | k = 2,28 | 10,38 |
| 2 kg | NTNU VKL 53 | 2 kg - 0,576 g | ± 0,060 g | k = 2 | ∞ |
| 2 kg | NTNU VKL 54 | 2 kg - 0,258 g | ± 0,060 g | k = 2 | ∞ |
| 2 kg | NTNU VKL 55 | 2 kg - 0,113 g | ± 0,060 g | k = 2 | ∞ |
| 2 kg | NTNU VKL 56 | 2 kg - 0,776 g | ± 0,059 g | k = 2 | ∞ |
| 2 kg | NTNU VKL 57 | 2 kg - 0,449 g | ± 0,062 g | k = 2 | ∞ |
| 2 kg | NTNU VKL 58 | 2 kg - 0,248 g | ± 0,059 g | k = 2 | ∞ |
| 2 kg | NTNU VKL 59 | 2 kg - 1,136 g | ± 0,062 g | k = 2 | ∞ |
| 5,7 kg | NTNU VKL 101 | 5,7 kg + 74,96 g | ± 0,15 g | k = 2 | ∞ |
| 650 g | NTNU VKL 103 | 650 g - 0,019 g | ± 0,0039 g | k = 2,10 | 18 |

Loddene oppfyller ikke spesifikasjoner iht OIML R111 og er derfor ikke vurdert iht denne.

Målemetode:

Substitusjonsveiling, prosedyre JV-LM-MAS-004 utgave nr. 4.0

Sporbarhet:

Loddene er sammenlignet med loddnormaler som er sporbare til de nasjonale normaler for masse.

Forhold under kalibreringen:

Kalibreringen er basert på en antatt densitet 8000 kg/m³ på loddene ved 20 °C og antatt densitet på 1,2 kg/m³ på luften.

Temperatur under kalibreringen var fra 19,5 - 20,0 °C ± 0,1 °C

Fuktigheten under kalibreringen var fra 45,8 - 47,8 % RH ± 1,5 % RH

Måleusikkerhet, metode for beregning og hovedkomponenter:

Den rapporterte utvidede usikkerheten er fastslått som standard måleusikkerhet multiplisert med dekningsfaktor som angitt i tabellen over, som for en t-fordeling med effektive frihetsgrader (V_{eff}) som angitt i tabellen over, korresponderer til en deknings sannsynlighet på tilnærmet 95%. Standard måleusikkerhet har blitt bestemt i samsvar med EA publikasjonen "EA 4/02"

KALIBRERINGSBEVIS

Certificate of Calibration

Justervesenet
Oslo Justerkammer

Nr./No.: CAL 016-06/730-3

Side/Page: 4 av/of: 4

Benyttede instrumenter og normaler:

Temperatur og luftfuktighet ble bestemt ved å benytte termohygrograf, merket:T/HYG-OSL-02

Den konvensjonelle massen til loddene ble bestemt ved hjelp av følgende vekter og normaler:

| Nominell masse | Benyttet vekt | Benyttet normal |
|----------------|--------------------------------------|---------------------------|
| 650 g | Sartorius CC60000, serienr. 30903465 | OSL-E ₂ -21 |
| 2 – 5 kg | Sartorius CC60000, serienr. 30903465 | OSL-E2-01 |
| 5,7 kg | Sartorius CC60000, serienr. 30903465 | OSL-E2-01 og OSL-E2-21 |

Kommentar:

Resultatet bekrefter loddets tilstand på det tidspunkt og under de forhold kalibreringen ble utført.
Beregningsprogram Loddkal versjon 2.03

Appendix K

Risk assessment.

Risikovurderingsrapport

Kaplanrigg

| | |
|----------------------------------|------------------------------------|
| Prosjekttittel | Test av Kaplanturbin |
| Prosjektleder | Torbjørn Nielsen |
| Enhet | NTNU |
| HMS-koordinator | Bård Brandåstrø |
| Linjeleder | Ole Gunnar Dahlhaug |
| Riggnavn | Kaplanrigg |
| Plassering | Vannkraftlab |
| Romnummer | 42 |
| Riggansvarlig | Lars Fjærvold og Remi André Stople |
| Risikovurdering utført av | Lars Fjærvold og Remi André Stople |

INNHALDSFORTEGNELSE

| | | |
|-----|---|----|
| 1 | INNLEDNING | 1 |
| 2 | ORGANISERING..... | 1 |
| 3 | RISIKOSTYRING AV PROSJEKTET | 1 |
| 4 | TEGNINGER, FOTO, BESKRIVELSER AV FORSØKSOPPSETT | 1 |
| 5 | EVAKUERING FRA FORSØKSOPPSETNINGEN..... | 2 |
| 6 | VARSLING..... | 2 |
| 6.1 | Før forsøkskjøring..... | 2 |
| 6.2 | Ved uønskede hendelser..... | 2 |
| 7 | VURDERING AV TEKNISK SIKKERHET | 3 |
| 7.1 | Fareidentifikasjon, HAZOP..... | 3 |
| 7.2 | Brannfarlig, reaksjonsfarlig og trykksatt stoff og gass | 3 |
| 7.3 | Trykkpåkjent utstyr | 3 |
| 7.4 | Påvirkning av ytre miljø (utslipp til luft/vann, støy, temperatur, rystelser, lukt) | 4 |
| 7.5 | Stråling..... | 4 |
| 7.6 | Bruk og behandling av kjemikalier | 4 |
| 7.7 | El sikkerhet (behov for å avvike fra gjeldende forskrifter og normer)..... | 4 |
| 8 | VURDERING AV OPERASJONELL SIKKERHET..... | 4 |
| 8.1 | Prosedyre HAZOP | 4 |
| 8.2 | Drifts og nødstopps prosedyre..... | 5 |
| 8.3 | Opplæring av operatører | 5 |
| 8.4 | Tekniske modifikasjoner..... | 5 |
| 8.5 | Personlig verneutstyr | 5 |
| 8.6 | Generelt..... | 5 |
| 8.7 | Sikkerhetsutrustning | 5 |
| 8.8 | Spesielle tiltak..... | 5 |
| 9 | TALLFESTING AV RESTRISIKO – RISIKOMATRISSE | 5 |
| 10 | KONKLUSJON | 6 |
| 11 | LOVER FORSKRIFTER OG PÅLEGG SOM GJELDER | 7 |
| 12 | VEDLEGG..... | 8 |
| 13 | DOKUMENTASJON..... | 9 |
| 14 | VEILEDNING TIL RAPPORTMAL..... | 10 |

1 INNLEDNING

Beskrivelse av forsøksoppsetningen og formålet med eksperimentene. Hvor er riggen plassert?

2 ORGANISERING

| Rolle | NTNU | Sintef |
|---------------------------|------------------------------------|-----------------|
| Lab Ansvarlig: | Morten Grønli | Harald Mæhlum |
| Linjeleder: | Olav Bolland | Mona J. Mølnvik |
| HMS ansvarlig: | Olav Bolland | Mona J. Mølnvik |
| HMS koordinator | Erik Langørgen | Harald Mæhlum |
| HMS koordinator | Bård Brandåstrø | |
| Romansvarlig: | Bård Brandåstrø | |
| Prosjekt leder: | Torbjørn Nielsen | |
| Ansvarlig riggoperatører: | Lars Fjærvold og Remi André Stople | |

3 RISIKOSTYRING AV PROSJEKTET

| Hovedaktiviteter risikostyring | Nødvendige tiltak, dokumentasjon | DTG |
|-------------------------------------|--|-----|
| Prosjekt initiering | Prosjekt initiering mal | X |
| Veiledningsmøte | Skjema for Veiledningsmøte med pre-risikovurdering | X |
| Innledende risikovurdering | Fareidentifikasjon – HAZID Skjema grovanalyse | X |
| Vurdering av teknisk sikkerhet | Prosess-HAZOP Tekniske dokumentasjoner | X |
| Vurdering av operasjonell sikkerhet | Prosedyre-HAZOP Opplæringsplan for operatører | X |
| Sluttvurdering, kvalitetssikring | Uavhengig kontroll Utstedelse av apparaturkort Utstedelse av forsøk pågår kort | |

4 TEGNINGER, FOTO, BESKRIVELSER AV FORSØKSOPPSETT

Vedlegg:

Prosess og Instrumenterings Diagram, (PID)

Skal inneholde alle komponenter i forsøksoppsetningen

Komponentliste med spesifikasjoner

Tegninger og bilder som beskriver forsøksoppsetningen.

Hvor oppholder operatør seg, hvor er gassflasker, avstegningsventiler for vann/luft.

Annen dokumentasjon som beskriver oppsett og virkemåte.

5 EVAKUERING FRA FORSØKSOPPSETNINGEN

Se kapittel 14 "Veiledning til rapport mal."

Evakuering skjer på signal fra alarmklokker eller lokale gassalarmstasjon med egen lokal varsling med lyd og lys utenfor aktuelle rom, se 6.2

Evakuering fra riggområdet foregår igjennom merkede nødutganger til møteplass, (hjørnet Gamle Kjemi/Kjelhuset eller parkeringsplass 1a-b).

Aksjon på rigg ved evakuering: Trykke nødstop for stopp av pumper og nødstop for generator.

6 VARSLING

6.1 Før forsøkskjøring

Varsling per e-post, med opplysning om forsøkskjøringens varighet og involverte til:

- HMS koordinator NTNU/SINTEF
HaraldStein.S.Mahlum@sintef.no
Erik.langorgen@ntnu.no
Baard.brandaastro@ntnu.no
- *Prosjektledere på naborigger varsles for avklaring rundt bruk av avtrekksanlegget uten fare eller forstyrrelser av noen art, se rigg matrise.*

All forsøkskjøringen skal planlegges og legges inn i aktivitetskalender for lab. Forsøksleder må få bekreftelse på at forsøkene er klarert med øvrig labdrift før forsøk kan iverksettes.

6.2 Ved uønskede hendelser

BRANN

Ved brann en ikke selv er i stand til å slukke med rimelige lokalt tilgjengelige slukkemidler, skal nærmeste brannalarm utløses og arealet evakueres raskest mulig. En skal så være tilgjengelig for brannvesen/bygningsvaktmester for å påvise brannsted.

Om mulig varsles så:

| NTNU | SINTEF |
|--|--------|
| Labsjef Morten Grønli, tlf: 918 97 515 | |
| HMS: Erik Langørgen, tlf: 91897160 | |
| Instituttleder: Olav Bolland: 91897209 | |

GASSALARM

Ved gassalarm skal gassflasker stenges umiddelbart og området ventileres. Klarer man ikke innen rimelig tid å få ned nivået på gasskonsentrasjonen så utløses brannalarm og laben evakueres. Dedikert personell og eller brannvesen sjekker så lekkasjested for å fastslå om det er mulig å tette lekkasje og lufte ut området på en forsvarlig måte.

Varslingsrekkefølge som i overstående punkt.

PERSONSKADE

- Førstehjelpsutstyr i Brann/førstehjelpsstasjoner,
- Rop på hjelp,

- Start livreddende førstehjelp
- **Ring 113** hvis det er eller det er tvil om det er alvorlig skade.

ANDRE UØNSKEDE HENDELSER (AVVIK)

NTNU:

Rapporteringsskjema for uønskede hendelser på

http://www.ntnu.no/hms/2007_Nettsider/HMSRV0401_avvik.doc

7 VURDERING AV TEKNISK SIKKERHET

7.1 Fareidentifikasjon, HAZOP

Se kapittel 14 "Veiledning til rapport mal.

Forsøksoppsetningen deles inn i følgende noder:

| | |
|--------|---------------------|
| Node 1 | Rørsystem med pumpe |
| Node 2 | Roterende turbin |
| Node 3 | Generatoroppsett |

Vedlegg, skjema: Hazop_mal

Vurdering:

Node1:

Rørelementer er eksternt levert og godkjent for aktuelt trykk

Node 2:

Roterende deler er for det meste ikke tilgjengelig. Roterende deler i friluft er lett synlig, og utenfor normal arbeidssone.

Node 3:

Generatoroppsett er forsvarlig montert, vanskelig tilgjengelig fra gulv.

7.2 Brannfarlig, reaksjonsfarlig og trykksatt stoff og gass

Se kapittel 14 "Veiledning til rapport mal.

Inneholder forsøkene brannfarlig, reaksjonsfarlig og trykksatt stoff

| | |
|----|----------------|
| Ja | Trykksatt vann |
|----|----------------|

Vurdering: Arbeidsmedium er vann. Alle rør som er levert av eksternt leverandør er trykktestet.

7.3 Trykkpåkjent utstyr

Inneholder forsøksoppsetningen trykkpåkjent utstyr:

| | |
|----|--|
| JA | Utstyret trykktestes i henhold til norm og dokumenteres. |
|----|--|

Trykkutsatt utstyr skal trykktestes med driftstrykk gange faktor 1.4, for utstyr som har usertifiserte sveiser er faktoren 1.8. Trykktesten skal dokumenteres skriftlig hvor fremgangsmåte framgår.

Vedlegg: Sertifikat for trykkpåkjent utstyr.

Vurdering:

7.4 Påvirkning av ytre miljø (utslipp til luft/vann, støy, temperatur, rystelser, lukt)

Se kapittel 14 "Veiledning til rapport mal..

| | |
|-----|--|
| NEI | |
|-----|--|

Vurdering: Vil eksperimentene generere utslipp av røyk, gass, lukt eller unormalt avfall.? Mengder/konsistens. Er det behov for utslippstillatelse, ekstraordinære tiltak?

7.5 Stråling

Se kapittel 14 "Veiledning til rapport mal.

| | |
|-----|--|
| NEI | |
|-----|--|

Vedlegg:

Vurdering:

7.6 Bruk og behandling av kjemikalier

Se kapittel 14 "Veiledning til rapport mal.

| | |
|-----|--|
| NEI | |
|-----|--|

Vedlegg:

Vurdering: Inneholder eksperimentene bruk og behandling av kjemikalier *Hvilke og hvilke mengder? Hvordan skal dette avhendes, oppbevares?, risikovurder i henhold til sikkerhetsdatablad Er det behov for beskyttelses tiltak tillegges disse i operasjonell prosedyre.*

7.7 El sikkerhet (behov for å avvike fra gjeldende forskrifter og normer)

| | |
|-----|--|
| NEI | |
|-----|--|

Her forstås montasje og bruk i forhold til normer og forskrifter med tanke på berøringsfare

Vedlegg:

Vurdering:

8 VURDERING AV OPERASJONELL SIKKERHET

Sikrer at etablerte prosedyrer dekker alle identifiserte risikoforhold som må håndteres gjennom operasjonelle barrierer og at operatører og teknisk utførende har tilstrekkelig kompetanse.

8.1 Prosedyre HAZOP

Se kapittel 14 "Veiledning til rapport mal.

Metoden er en undersøkelse av operasjonsprosedyrer, og identifiserer årsaker og farekilder for operasjonelle problemer.

Vedlegg: HAZOP_MAL_Prosedyre

Vurdering:

8.2 Drifts og nødstopps prosedyre

Se kapittel 14 "Veiledning til rapport mal.

Driftsprosedyren er en sjekklister som skal fylles ut for hvert forsøk.

Nødstopps prosedyren skal sette forsøksoppsetningen i en harmløs tilstand ved uforutsette hendelser.

Vedlegg "Procedure for running experiments

8.3 Opplæring av operatører

Dokument som viser Opplæringsplan for operatører utarbeides for alle forsøksoppsetninger.

- *Kjøring av pumpesystem*
- *Bruk av LabVIEW-program*
- *Kjøring av generator*

Vedlegg: Opplæringsplan for operatører

8.4 Tekniske modifikasjoner

Vurdering: Modifikasjoner gjøres i samråd med Torbjørn Nielsen, Bård Brandåstrø og Anders Austegård

8.5 Personlig verneutstyr

Vurdering: Vernebriller påkrevd

8.6 Generelt

Vurdering: Alle forsøk kjøres med operatør til stede.

8.7 Sikkerhetsutrustning

Vernebriller

8.8 Spesielle tiltak

9 TALLFESTING AV RESTRISIKO – RISIKOMATRISSE

Se kapittel 14 "Veiledning til rapportmal.

Risikomatrissen vil gi en visualisering og en samlet oversikt over aktivitetens risikoforhold slik at ledelse og brukere får et mest mulig komplett bilde av risikoforhold.

| IDnr | Aktivitet-hendelse | Frekv-Sans | Kons | RV |
|------|----------------------------------|------------|------|----|
| 1 | <i>Roterende aksling</i> | 2 | B | B2 |
| 2 | <i>Fremmedelementer i vannet</i> | 1 | A | A1 |
| 3 | Rørbrudd | 1 | A | A1 |

Vurdering restrisiko: *Deltakerne foretar en helhetsvurdering for å avgjøre om gjenværende risiko ved aktiviteten/prosessen er akseptabel. Avsperring og kjøring utenom arbeidstid*

10 KONKLUSJON

Riggen er bygget til god laboratorium praksis (GLP).

Hvilke tekniske endringer eller endringer av driftsparametere vil kreve ny risikovurdering.

Annet medium, trykk, mekaniske inngrep

Apparaturkortet får en gyldighet på **XX måneder**

Forsøk pågår kort får en gyldighet på **XX måneder**

11 LOVER FORSKRIFTER OG PÅLEGG SOM GJELDER

Se <http://www.arbeidstilsynet.no/regelverk/index.html>

- Lov om tilsyn med elektriske anlegg og elektrisk utstyr (1929)
- Arbeidsmiljøloven
- Forskrift om systematisk helse-, miljø- og sikkerhetsarbeid (HMS Internkontrollforskrift)
- Forskrift om sikkerhet ved arbeid og drift av elektriske anlegg (FSE 2006)
- Forskrift om elektriske forsyningsanlegg (FEF 2006)
- Forskrift om utstyr og sikkerhetssystem til bruk i eksplosjonsfarlig område NEK 420
- Forskrift om håndtering av brannfarlig, reaksjonsfarlig og trykksatt stoff samt utstyr og anlegg som benyttes ved håndteringen
- Forskrift om Håndtering av eksplosjonsfarlig stoff
- Forskrift om bruk av arbeidsutstyr.
- Forskrift om Arbeidsplasser og arbeidslokaler
- Forskrift om Bruk av personlig verneutstyr på arbeidsplassen
- Forskrift om Helse og sikkerhet i eksplosjonsfarlige atmosfærer
- Forskrift om Høytrykksspyling
- Forskrift om Maskiner
- Forskrift om Sikkerhetsskilting og signalgivning på arbeidsplassen
- Forskrift om Stillaser, stiger og arbeid på tak m.m.
- Forskrift om Sveising, termisk skjæring, termisk sprøyting, kullbuemeisling, lodding og sliping (varmt arbeid)
- Forskrift om Tekniske innretninger
- Forskrift om Tungt og ensformig arbeid
- Forskrift om Vern mot eksponering for kjemikalier på arbeidsplassen (Kjemikalieforskriften)
- Forskrift om Vern mot kunstig optisk stråling på arbeidsplassen
- Forskrift om Vern mot mekaniske vibrasjoner
- Forskrift om Vern mot støy på arbeidsplassen

Veiledninger fra arbeidstilsynet

se: <http://www.arbeidstilsynet.no/regelverk/veiledninger.html>

12 VEDLEGG

13 DOKUMENTASJON

- Tegninger, foto, beskrivelser av forsøksoppsetningen
- Hazop_mal
- Sertifikat for trykkpåkjent utstyr
- Håndtering avfall i NTNU
- Sikker bruk av LASERE, retningslinje
- HAZOP_MAL_Prosegyre
- Forsøksprosegyre
- Opplæringsplan for operatører
- Skjema for sikker jobb analyse, (SJA)
- Apparatorkortet
- Forsøk pågår kort

14 VEILEDNING TIL RAPPORTMAL

Kap 5 Evakuering fra forsøksoppsetningen

Beskriv i hvilken tilstand riggen skal forlates ved en evakuerings situasjon.

Kap 7 Vurdering av teknisk sikkerhet

Sikre at design av apparatur er optimalisert i forhold til teknisk sikkerhet.

Identifisere risikoforhold knyttet til valgt design, og eventuelt å initiere re-design for å sikre at størst mulig andel av risiko elimineres gjennom teknisk sikkerhet.

Punktene skal beskrive hva forsøksoppsetningen faktisk er i stand til å tåle og aksept for utslipp.

7.1 Fareidentifikasjon, HAZOP

Forsøksoppsetningen deles inn i noder: (eks *Motorenhet, pumpeenhet, kjøleenhet.*)

Ved hjelp av ledeord identifiseres årsak, konsekvens og sikkerhetstiltak. Konkluderes det med at tiltak er nødvendig anbefales disse på bakgrunn av dette. Tiltakene lukkes når de er utført og Hazop sluttføres.

(eks "No flow", årsak: rør er deformert, konsekvens: pumpe går varm, sikkerhetsforanstaltning: måling av flow med kobling opp mot nødstop eller hvis konsekvensen ikke er kritisk benyttes manuell overvåking og punktet legges inn i den operasjonelle prosedyren.)

7.2 Brannfarlig, reaksjonsfarlig og trykksatt stoff.

I henhold til Forskrift om håndtering av brannfarlig, reaksjonsfarlig og trykksatt stoff samt utstyr og anlegg som benyttes ved håndteringen

Brannfarlig stoff: Fast, flytende eller gassformig stoff, stoffblanding, samt stoff som forekommer i kombinasjoner av slike tilstander, som i kraft av sitt flammepunkt, kontakt med andre stoffer, trykk, temperatur eller andre kjemiske egenskaper representerer en fare for brann.

Reaksjonsfarlig stoff: Fast, flytende, eller gassformig stoff, stoffblanding, samt stoff som forekommer i kombinasjoner av slike tilstander, som ved kontakt med vann, ved sitt trykk, temperatur eller andre kjemiske forhold, representerer en fare for farlig reaksjon, eksplosjon eller utslipp av farlig gass, damp, støv eller tåke.

Trykksatt stoff: Annet fast, flytende eller gassformig stoff eller stoffblanding enn brann- eller reaksjonsfarlig stoff, som er under trykk, og som derved kan representere en fare ved ukontrollert utslipp.

Nærmere kriterier for klassifisering av brannfarlig, reaksjonsfarlig og trykksatt stoff er fastsatt i vedlegg 1 i veiledningen til forskriften "Brannfarlig, reaksjonsfarlig og trykksatt stoff"

<http://www.dsb.no/Global/Publikasjoner/2009/Veiledning/Generell%20veiledning.pdf>

http://www.dsb.no/Global/Publikasjoner/2010/Tema/Temaveiledning_bruk_av_farlig_stoff_Del_1.pdf

Rigg og areal skal gjennomgås med hensyn på vurdering av Ex sone

- Sone 0: Alltid eksplosiv atmosfære, for eksempel inne i tanker med gass, brennbar væske.
- Sone 1: Primær sone, tidvis eksplosiv atmosfære for eksempel et fylle tappe punkt
- Sone 2: Sekundært utslippssted, kan få eksplosiv atmosfære ved uhell, for eksempel ved flenser, ventiler og koblingspunkt

7.4 Påvirkning av ytre miljø

Med forurensning forstås: tilførsel av fast stoff, væske eller gass til luft, vann eller i grunnen støy og rystelser påvirkning av temperaturen som er eller kan være til skade eller ulempe for miljøet.

Regelverk: <http://www.lovdatab.no/all/hl-19810313-006.html#6>

NTNU retningslinjer for avfall se: <http://www.ntnu.no/hms/retningslinjer/HMSR18B.pdf>

7.5 Stråling

Stråling defineres som

| |
|---|
| Ioniserende stråling: Elektromagnetisk stråling (i strålevernssammenheng med bølgelengde <100 nm) eller hurtige atomære partikler (f.eks alfa- og beta-partikler) som har evne til å ionisere atomer eller molekyler |
| Ikke-ioniserende stråling: Elektromagnetisk stråling (bølgelengde >100 nm), og ultralyd ¹ , som har liten eller ingen evne til å ionisere. |
| Strålekilder: Alle ioniserende og sterke ikke-ioniserende strålekilder. |
| Ioniserende strålekilder: Kilder som avgir ioniserende stråling, f.eks alle typer radioaktive kilder, røntgenapparater, elektronmikroskop |
| Sterke ikke-ioniserende strålekilder: Kilder som avgir sterk ikke-ioniserende stråling som kan skade helse og/eller ytre miljø, f.eks laser klasse 3B og 4, MR2-systemer, UVC3-kilder, kraftige IR-kilder ⁴ |
| <small>¹ Ultralyd er akustisk stråling ("lyd") over det hørbare frekvensområdet (>20 kHz). I strålevernforskriften er ultralyd omtalt sammen med elektromagnetisk ikke-ioniserende stråling. ² MR (eg. NMR) - kjernemagnetisk resonans, metode som nyttes til å «avbilde» indre strukturer i ulike materialer. ³ UVC er elektromagnetisk stråling i bølgelengdeområdet 100-280 nm. ⁴ IR er elektromagnetisk stråling i bølgelengdeområdet 700 nm – 1 mm.</small> |

For hver laser skal det finnes en informasjonssperm(HMSRV3404B) som skal inneholde:

- Generell informasjon
- Navn på instrumentansvarlig og stedfortreder, og lokal strålevernsskordinator
- Sentrale data om apparaturen
- Instrumentspesifikk dokumentasjon
- Referanser til (evt kopier av) datablader, strålevernbestemmelser, o.l.
- Vurderinger av risikomomenter
- Instruks for brukere
- Instruks for praktisk bruk; oppstart, drift, avstenging, sikkerhetsforholdsregler, loggføring, avlåsning, evt. bruk av strålingsmåler, osv.
- Nødprosedyrer

Se ellers retningslinjen til NTNU for laser: <http://www.ntnu.no/hms/retningslinjer/HMSR34B.pdf>

7.6 Bruk og behandling av kjemikalier.

Her forstås kjemikalier som grunnstoff som kan utgjøre en fare for arbeidstakers sikkerhet og helse.

Se ellers: <http://www.lovdatabasen.no/cgi-wift/ldles?doc=/sf/sf/sf-20010430-0443.html>

Sikkerhetsdatablar skal være i forøkenes HMS perm og kjemikaliene registrert i Stoffkartoteket.

Kap 8 Vurdering av operasjonell sikkerhet

Sikrer at etablerte prosedyrer dekker alle identifiserte risikoforhold som må håndteres gjennom operasjonelle barrierer og at operatører og teknisk utførende har tilstrekkelig kompetanse.

8.1 Prosedyre Hazop

Prosedyre-HAZOP gjennomføres som en systematisk gjennomgang av den aktuelle prosedyren ved hjelp av fastlagt HAZOP-metodikk og definerte ledeord. Prosedyren brytes ned i enkeltstående arbeidsoperasjoner (noder) og analyseres ved hjelp av ledeordene for å avdekke mulige avvik, uklarheter eller kilder til mangelfull gjennomføring og feil.

8.2 Drifts og nødstop prosedyrer

Utarbeides for alle forsøksoppsetninger.

Driftsprosedyren skal stegvis beskrive gjennomføringen av et forsøk, inndelt i oppstart, under drift og avslutning. Prosedyren skal beskrive forutsetninger og tilstand for start, driftsparametere med hvor store avvik som tillates før forsøket avbrytes og hvilken tilstand riggen skal forlates.

Nødstop-prosedyre beskriver hvordan en nødstop skal skje, (utført av uinnvidde), hva som skjer, (strøm/gass tilførsel) og hvilke hendelser som skal aktivere nødstop, (brannalarm, lekkasje).

Kap 9 Risikomatrixe

9 Tallfesting av restrisiko, Risikomatriksen

For å synliggjøre samlet risiko, jevnfør skjema for risikovurdering, plottes hver enkelt aktivitets verdi for sannsynlighet og konsekvens inn i risikomatriksen. Bruk aktivitetens IDnr.

Eksempel: Hvis aktivitet med IDnr. 1 har fått en risikoverdi D3 (sannsynlighet 3 x konsekvens D) settes aktivitetens IDnr i risikomatriksens felt for 3D. Slik settes alle aktivitetenes risikoverdier (IDnr) inn i risikomatriksen.

I risikomatriksen er ulike grader av risiko merket med rødt, gul eller grønt. Når en aktivitets risiko havner på rødt (= uakseptabel risiko), skal risikoreduserende tiltak gjennomføres. Ny vurdering gjennomføres etter at tiltak er iverksatt for å se om risikoverdien er kommet ned på akseptabelt nivå.

| | | | | | | |
|--------------------|-----------------------|---------------------|--------------|----------------|-------------|-------------------|
| KONSEKVENNS | Svært alvorlig | E1 | E2 | E3 | E4 | E5 |
| | Alvorlig | D1 | D2 | D3 | D4 | D5 |
| | Moderat | C1 | C2 | C3 | C4 | C5 |
| | Liten | B1 | B2 | B3 | B4 | B5 |
| | Svært liten | A1 | A2 | A3 | A4 | A5 |
| | | Svært liten | Liten | Middels | Stor | Svært Stor |
| | | SANSYNLIGHET | | | | |

Prinsipp over akseptkriterium. Forklaring av fargene som er brukt i risikomatriksen.

| Farge | Beskrivelse |
|--------------|---|
| Rød | Uakseptabel risiko. Tiltak skal gjennomføres for å redusere risikoen. |
| Gul | Vurderingsområde. Tiltak skal vurderes. |
| Grønn | Akseptabel risiko. Tiltak kan vurderes ut fra andre hensyn. |

Vedlegg til Risikovurderingsrapport

Kaplanrigg

| | |
|------------------------|------------------------------------|
| Prosjekttittel | Test av Kaplan turbin |
| Prosjektleder | Torbjørn Nielsen |
| Enhet | NTNU |
| HMS-koordinator | Bård Brandåstrø |
| Linjeleder | Ole Gunnar Dahlhaug |
| Riggnavn | Kaplanrigg |
| Plassering | Vannkraftlab |
| Romnummer | 42 |
| Riggansvarlig | Lars Fjærvold og Remi André Stople |

INNHALDSFORTEGNELSE

- VEDLEGG A HAZOP MAL..... 1
- VEDLEGG B PRØVESERTIFIKAT FOR LOKAL TRYKKTESTING..... 1
- VEDLEGG F HAZOP MAL PROSEDYRE 1
- VEDLEGG G FORSØKSPROSEDYRE 1
- VEDLEGG H OPPLÆRINGSPLAN FOR OPERATØRER 3
- VEDLEGG I SKJEMA FOR SIKKER JOBB ANALYSE..... 4
- VEDLEGG J APPARATURKORT UNITCARD..... 6
- VEDLEGG K FORSØK PÅGÅR KORT 7

• VEDLEGG A HAZOP MAL

| Project: Node: 1 | | | | | | | | Page |
|---------------------|---------------|---------------------|--|---------------------|-----------------|---------------------|-----------|------|
| Ref # | Guideword | Causes | Consequences | Safeguards | Recommendations | Action | Date Sign | |
| | No flow | | None | | | | | |
| | Reverse flow | | None | | | | | |
| | More flow | Too high pump speed | None | | | Reduce pump speed | | |
| | Less flow | Too low pump speed | None | | | Increase pump speed | | |
| | More level | | | | | | | |
| | Less level | | | | | | | |
| | More pressure | Too high pump speed | -Turbine can be overloaded - Safety valve can be opened | Emergency shut down | | Reduce pump speed | | |

| Project: Node: 1 | | Page | | | | | |
|---------------------|--------------------|-----------------|--------------|------------|-----------------|--------------|-----------|
| Ref # | Guideword | Causes | Consequences | Safeguards | Recommendations | Action | Date Sign |
| | Less pressure | Fault in system | None | | | Check system | |
| | Abnormal operation | Fault in system | None | | | Check system | |

| Project: Node: 2 | | Page | | | | | |
|---------------------|--------------|---------------------|--|------------|-----------------|-------------------|-----------|
| Ref # | Guideword | Causes | Consequences | Safeguards | Recommendations | Action | Date Sign |
| | No flow | | None | | | | |
| | Reverse flow | | None | | | | |
| | More flow | Too high pump speed | -Load may be too high -Cavitation may occur | | | Reduce pump speed | |

| Project: Node: 2 | | Page | | | | | |
|---------------------|--------------------|---------------------|----------------------------|----------------------------|-----------------|---------------------|-----------|
| Ref # | Guideword | Causes | Consequences | Safeguards | Recommendations | Action | Date Sign |
| | Less flow | Too low pump speed | None | | | Increase pump speed | |
| | More level | | | | | | |
| | Less level | | | | | | |
| | More pressure | Too high pump speed | -Turbine can be overloaded | Emergency shut down button | | Reduce pump speed | |
| | Less pressure | Fault in system | None | | | Check system | |
| | Abnormal operation | Fault in system | None | | | Check system | |

| Project: Node: 3 | | Page | | | | | |
|---------------------|--|------|--|--|--|--|--|
|---------------------|--|------|--|--|--|--|--|

| Ref # | Guideword | Causes | Consequences | Safeguards | Recommendations | Action | Date Sign |
|-------|---|-------------------------------|---------------------------|----------------------------|-----------------|--------------|-----------|
| | Abnormal operation | Fault in system | None | | | Check system | |
| | Loss of connection to the electrical grid | Turbine goes to runaway speed | Turbine can be overloaded | Emergency shut down switch | | Check system | |

- **VEDLEGG B PRØVESERTIFIKAT FOR LOKAL TRYKKTESTING**

Trykktesten skal utføres i følge NS-EN 13445 del 5 (Inspeksjon og prøving).
Se også prosedyre for trykktesting gjeldende for VATL lab

Trykkpåkjent utstyr:

Benyttes i rigg:

Design trykk for utstyr:bara

Maksimum tillatt trykk:bara
(i.e. burst pressure om kjent)

Maksimum driftstrykk i denne rigg:bara

Prøvetrykket skal fastlegges i følge standarden og med hensyn til maksimum tillatt trykk.

Prøvetrykk:bara (..... x maksimum driftstrykk)
I følge standard

Test medium: _____

Temperatur: _____°C

Start: Tid: _____

Trykk: _____bara

Slutt: Tid: _____

Trykk: _____bara

Eventuelle repetisjoner fra atm. trykk til maksimum prøvetrykk:.....

Test trykket, dato for testing og maksimum tillatt driftstrykk skal markers på
(skilt eller innslått)

Sted og dato

Signatur

- **VEDLEGG F HAZOP MAL PROSEDYRE**

| Project: | | Page | | | | | |
|----------|----------------------------------|--|--------------|------------|------|-----------------|--------|
| Node: 1 | | | | | | | |
| Ref # | Guideword | Causes | Consequences | Safeguards | Rec# | Recommendations | Action |
| | Uklar | Prosedyre er laget for ambisjøs eller preget av forvirring | | | | | |
| | Trinn på feil plass | Prosedyren vil lede til at handlinger blir gjennomført i feil mønster/rekkefølge | | | | | |
| | Feil handling | Prosedyrens handling er feil spesifisert | | | | | |
| | Uriktig informasjon | Informasjon som er gitt i forkant av handling er feil spesifisert | | | | | |
| | Trinn utelatt | Manglende trinn, eller trinn krever for mye av operatør | | | | | |
| | Trinn mislykket | Trinn har stor sannsynlighet for å mislykkes | | | | | |
| | Påvirkning og effekter fra andre | Prosedyrens prestasjoner vil trolig bli påvirket av andre kilder | | | | | |

Project:
Node: 1

Page

| Ref # | Guideword | Causes | Consequences | Safeguards | Rec# | Recommendations | Action |
|-------|-----------|--------|--------------|------------|------|-----------------|--------|
| | | | | | | | |
| | | | | | | | |
| | | | | | | | |
| | | | | | | | |
| | | | | | | | |
| | | | | | | | |
| | | | | | | | |
| | | | | | | | |
| | | | | | | | |
| | | | | | | | |
| | | | | | | | |
| | | | | | | | |
| | | | | | | | |
| | | | | | | | |
| | | | | | | | |
| | | | | | | | |
| | | | | | | | |
| | | | | | | | |
| | | | | | | | |
| | | | | | | | |
| | | | | | | | |
| | | | | | | | |
| | | | | | | | |

• **VEDLEGG G FORSØKSPROSEDYRE**

| | |
|--|-----------------------|
| Experiment, name, number: Test av Kaplanturbin | Date/ Sign |
| Project Leader: Torbjørn Nielsen | |
| Experiment Leader: Lars Fjærvold and Remi André Stople | |
| Operator, Duties: Lars Fjærvold: Operation of the rig Remi André Stople: Operation of the rig | |

| Conditions for the experiment: | Completed |
|--|--------------------|
| Experiments should be run in normal working hours, 08:00-16:00 during winter time and 08.00-15.00 during summer time. Experiments outside normal working hours shall be approved. | |
| One person must always be present while running experiments, and should be approved as an experimental leader. | |
| An early warning is given according to the lab rules, and accepted by authorized personnel. | |
| Be sure that everyone taking part of the experiment is wearing the necessary protecting equipment and is aware of the shut down procedure and escape routes. | |
| Preparations | Carried out |
| Post the "Experiment in progress" sign. | |
| <i>Start LabVIEW-program and generator</i> | |
| <i>Run the generator to 100rpm</i> | |
| <i>Start up pump</i> | |
| <i>Adjust pump and generator to wanted operation point</i> | |
| During the experiment | |
| <i>Log data with designated LabVIEW program</i> | |
| | |
| | |
| End of experiment | |
| <i>Decrease generator and pump speed stepwise to 100 rpm</i> | |
| <i>Shut down pump, then the generator</i> | |
| | |
| Remove all obstructions/barriers/signs around the experiment. | |
| Tidy up and return all tools and equipment. | |
| Tidy and cleanup work areas. | |
| Return equipment and systems back to their normal operation settings (fire alarm) | |
| To reflect on before the next experiment and experience useful for others | |
| Was the experiment completed as planned and on scheduled in professional terms? | |
| Was the competence which was needed for security and completion of the | |

| | | |
|--|---|--|
| | experiment available to you? | |
| | Do you have any information/ knowledge from the experiment that you should document and share with fellow colleagues? | |

• **VEDLEGG H OPPLÆRINGSPLAN FOR OPERATØRER**

| | |
|---|-----------------------|
| Experiment, name, number: Test av Kaplan turbin | Date/ Sign |
| Project Leader: Torbjørn Nielsen | |
| Experiment Leader: Lars Fjærvold og Remi André Stople | |
| Operator Lars Fjærvold Remi André Stople | |

| | | |
|--|---|---|
| | Kjennskap til EPT LAB generelt | |
| | Lab - adgang - rutiner/regler - arbeidstid | X |
| | Kjenner til evakueringsprosedyrer | X |
| | Aktivitetskalender | X |
| | | |
| | | |
| | Kjennskap til forsøkene | |
| | Prosedyrer for forsøkene | X |
| | Nødstopp | X |
| | Nærmeste brann/førstehjelpsstasjon | X |
| | | |
| | | |
| | | |
| | | |
| | | |
| | | |
| | | |
| | | |
| | | |
| | | |
| | | |
| | | |
| | | |

- **VEDLEGG I SKJEMA FOR SIKKER JOBB ANALYSE**

| | | | |
|---------------------------------|--------------------------|-------|--|
| SJA tittel: | | | |
| Dato: | | Sted: | |
| Kryss av for utfylt sjekkliste: | <input type="checkbox"/> | | |

| | | |
|-----------------------|--|--|
| Deltakere: | | |
| | | |
| SJA-ansvarlig: | | |

| |
|---|
| Arbeidsbeskrivelse: (Hva og hvordan?) |
| Risiko forbundet med arbeidet: |
| Beskyttelse/sikring: (tiltaksplan, se neste side) |
| Konklusjon/kommentar: |

| Anbefaling/godkjenning: | Dato/Signatur: | Anbefaling/godkjenning: | Dato/Signatur: |
|--------------------------------|-----------------------|--------------------------------|-----------------------|
| SJA-ansvarlig: | | Områdeansvarlig: | |
| Ansvarlig for utføring: | | Annen (stilling): | |

| HMS aspekt | Ja | Nei | Ikke aktuelt | Kommentar / tiltak | Ansv. |
|--|----|-----|--------------|--------------------|-------|
| Dokumentasjon, erfaring, kompetanse | | | | | |
| Kjent arbeidsoperasjon? | | | | | |
| Kjennskap til erfaringer/uønskede hendelser fra tilsvarende operasjoner? | | | | | |
| Nødvendig personell? | | | | | |
| Kommunikasjon og koordinering | | | | | |
| Mulig konflikt med andre operasjoner? | | | | | |
| Håndtering av en evt. hendelse (alarm, evakuering)? | | | | | |
| Behov for ekstra vakt? | | | | | |
| Arbeidsstedet | | | | | |
| Uvante arbeidsstillinger? | | | | | |
| Arbeid i tanker, kummer el.lignende? | | | | | |
| Arbeid i grøfter eller sjakter? | | | | | |
| Rent og ryddig? | | | | | |
| Verneutstyr ut over det personlige? | | | | | |
| Vær, vind, sikt, belysning, ventilasjon? | | | | | |
| Bruk av stillaser/lift/seler/stropper? | | | | | |
| Arbeid i høyden? | | | | | |
| Ioniserende stråling? | | | | | |
| Rømningsveier OK? | | | | | |
| Kjemiske farer | | | | | |
| Bruk av helseskadelige/giftige/etsende kjemikalier? | | | | | |
| Bruk av brannfarlige eller eksplosjonsfarlige kjemikalier? | | | | | |
| Må kjemikaliene godkjennes? | | | | | |
| Biologisk materiale? | | | | | |
| Støv/asbest? | | | | | |
| Mekaniske farer | | | | | |
| Stabilitet/styrke/spenning? | | | | | |
| Klem/kutt/slag? | | | | | |
| Støy/trykk/temperatur? | | | | | |
| Behandling av avfall? | | | | | |
| Behov for spesialverktøy? | | | | | |
| Elektriske farer | | | | | |
| Strøm/spenning/over 1000V? | | | | | |
| Støt/krypstrøm? | | | | | |
| Tap av strømtilførsel? | | | | | |
| Området | | | | | |
| Behov for befarings? | | | | | |
| Merking/skilting/avsperring? | | | | | |
| Miljømessige konsekvenser? | | | | | |
| Sentrale fysiske sikkerhetssystemer | | | | | |
| Arbeid på sikkerhetssystemer? | | | | | |
| Frakobling av sikkerhetssystemer? | | | | | |
| Annet | | | | | |

• VEDLEGG J **APPARATURKORT UNITCARD**

Apparatur/unit

Dette kortet SKAL henges godt synlig på apparaturen! *This card MUST be posted on a visible place on the unit!*

| | |
|--|---|
| Faglig Ansvarlig (Scientific Responsible) Torbjørn Nielsen | Telefon mobil/privat (Phone no. mobile/private) 91897572 |
| Apparaturansvarlig (Unit Responsible) Bård Brandastrø | Telefon mobil/privat (Phone no. mobile/private) 91897257 |
| Sikkerhetsrisikoer (Safety hazards) Rotating equipment (covered) | |
| Sikkerhetsregler (Safety rules) Use safety googles | |
| Nødstop prosedyre (Emergency shutdown) <i>Push emergency stop button</i> <i>Stop generator by turning the emergency switch on the panel</i> | |

Her finner du (Here you will find):

| |
|--------------------------------------|
| Prosedyrer (Procedures) |
| Bruksanvisning (Users manual) |

Nærmeste (nearest)

| | |
|--|----------------------|
| Brannslukningsapparat (fire extinguisher) | Main entrance |
| Førstehjelpsskap (first aid cabinet) | Main entrance |

NTNU
Institutt for energi og prosessteknikk

SINTEF Energi
Avdeling energiprosesser

Dato

Dato

Signert

Signert

- VEDLEGG K FORSØK PÅGÅR KORT

Forsøk pågår! Experiment in progress!

Dette kort skal settes opp før forsøk kan påbegynnes This card has to be posted before an experiment can start

| | |
|--|---|
| Ansvarlig / Responsible Lars Fjærvold/Remi André Stople | Telefon jobb/mobil/hjemme 90863846/48496748 |
| Operatører/Operators Lars Fjærvold/Remi André Stople | Forsøksperiode/Experiment time(start – slutt) 1.okt 2011 – 1.feb 2012 |
| Prosjektleder Torbjørn Nielsen | Prosjekt Test av Kaplan turbin |
| Kort beskrivelse av forsøket og relaterte farer Short description of the experiment and related hazards Test of characteristics of a Kaplan turbine, which includes efficiency, cavitation and runaway speed. Possible hazards is rotating equipment. (covered) | |

NTNU
Institutt for energi og prosesseteknikk

SINTEF Energi
Avdeling energiprosesser

Dato

Dato

Signert

Signert

Appendix L

Calibration report pressure

CALIBRATION REPORT

CALIBRATION PROPERTIES

Calibrated by: Remi André Stople
Type/Producer: Druck PTX 1400
SN: Z00227/07
Range: 0-4 bar g
Unit: bar g

CALIBRATION SOURCE PROPERTIES

Type/Producer: Druck DPI 601
SN: -
Uncertainty [%]: 0,01

POLY FIT EQUATION:

$Y = -999.01794012E-3X^0 + 500.28151634E-3X^1$

CALIBRATION SUMMARY:

Max Uncertainty : 0.837284 [%]
Max Uncertainty : 0.000189 [bar g]
RSQ : 0.999999
Calibration points : 37

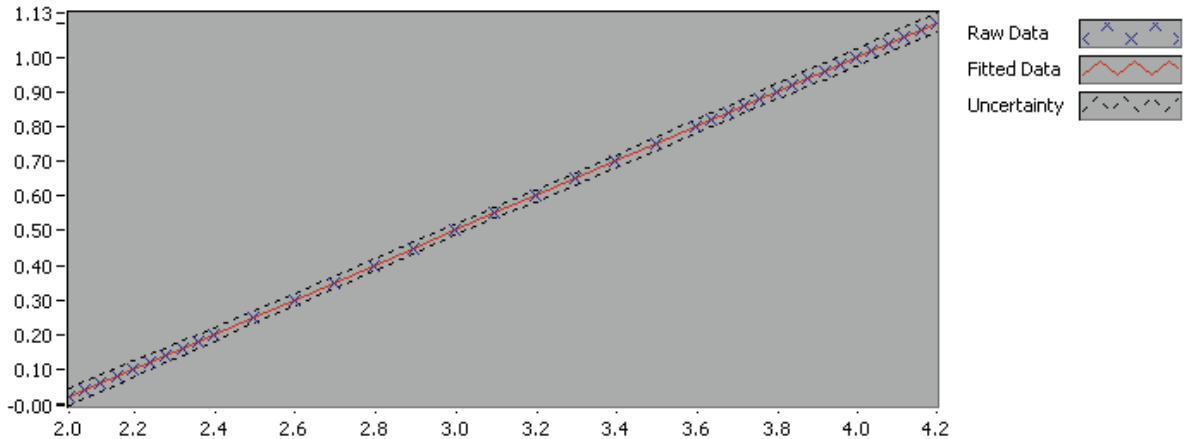


Figure 1 : Calibration chart (The uncertainty band is multiplied by 150)

Remi André Stople

CALIBRATION VALUES

| Value [bar g] | Voltage [V] | Best Poly Fit [bar g] | Deviation [bar g] | Uncertainty [%] | Uncertainty [bar g] |
|----------------------|--------------------|------------------------------|--------------------------|------------------------|----------------------------|
| 0.020000 | 2.037372 | 0.020242 | -0.000242 | 0.837284 | 0.000167 |
| 0.041000 | 2.078004 | 0.040569 | 0.000431 | 0.398230 | 0.000163 |
| 0.060000 | 2.116075 | 0.059615 | 0.000385 | 0.265707 | 0.000159 |
| 0.080000 | 2.155628 | 0.079403 | 0.000597 | 0.194368 | 0.000155 |
| 0.100000 | 2.196224 | 0.099712 | 0.000288 | 0.151557 | 0.000152 |
| 0.120000 | 2.237098 | 0.120161 | -0.000161 | 0.123050 | 0.000148 |
| 0.140000 | 2.276441 | 0.139843 | 0.000157 | 0.102859 | 0.000144 |
| 0.161000 | 2.319024 | 0.161147 | -0.000147 | 0.087052 | 0.000140 |
| 0.180000 | 2.356898 | 0.180094 | -0.000094 | 0.076068 | 0.000137 |
| 0.200000 | 2.397896 | 0.200605 | -0.000605 | 0.066751 | 0.000134 |
| 0.250000 | 2.496808 | 0.250089 | -0.000089 | 0.050335 | 0.000126 |
| 0.300000 | 2.597481 | 0.300454 | -0.000454 | 0.039451 | 0.000118 |
| 0.350000 | 2.697051 | 0.350267 | -0.000267 | 0.032351 | 0.000113 |
| 0.400000 | 2.796616 | 0.400077 | -0.000077 | 0.027185 | 0.000109 |
| 0.449000 | 2.894809 | 0.449201 | -0.000201 | 0.023731 | 0.000107 |
| 0.501000 | 2.997955 | 0.500804 | 0.000196 | 0.020863 | 0.000105 |
| 0.550000 | 3.096235 | 0.549971 | 0.000029 | 0.018401 | 0.000101 |
| 0.600000 | 3.195993 | 0.599878 | 0.000122 | 0.018059 | 0.000108 |
| 0.650000 | 3.296806 | 0.650313 | -0.000313 | 0.017224 | 0.000112 |
| 0.700000 | 3.395519 | 0.699697 | 0.000303 | 0.016760 | 0.000117 |
| 0.750000 | 3.496163 | 0.750048 | -0.000048 | 0.016477 | 0.000124 |
| 0.800000 | 3.596134 | 0.800061 | -0.000061 | 0.016396 | 0.000131 |
| 0.820000 | 3.635903 | 0.819957 | 0.000043 | 0.016386 | 0.000134 |
| 0.840000 | 3.676856 | 0.840445 | -0.000445 | 0.016414 | 0.000138 |
| 0.860000 | 3.715379 | 0.859717 | 0.000283 | 0.016433 | 0.000141 |
| 0.880000 | 3.755681 | 0.879880 | 0.000120 | 0.016459 | 0.000145 |
| 0.900000 | 3.795988 | 0.900044 | -0.000044 | 0.016503 | 0.000149 |
| 0.920000 | 3.835699 | 0.919911 | 0.000089 | 0.016562 | 0.000152 |
| 0.940000 | 3.875976 | 0.940061 | -0.000061 | 0.016011 | 0.000151 |
| 0.960000 | 3.916669 | 0.960419 | -0.000419 | 0.016706 | 0.000160 |
| 0.980000 | 3.955765 | 0.979978 | 0.000022 | 0.015872 | 0.000156 |
| 0.999000 | 3.994152 | 0.999182 | -0.000182 | 0.015458 | 0.000154 |
| 1.020000 | 4.034591 | 1.019413 | 0.000587 | 0.016178 | 0.000165 |
| 1.040000 | 4.075705 | 1.039982 | 0.000018 | 0.016971 | 0.000177 |
| 1.060000 | 4.115461 | 1.059871 | 0.000129 | 0.017056 | 0.000181 |
| 1.080000 | 4.155641 | 1.079973 | 0.000027 | 0.016984 | 0.000183 |
| 1.100000 | 4.195495 | 1.099911 | 0.000089 | 0.017197 | 0.000189 |

COMMENTS:

The uncertainty is calculated with 95% confidence. The uncertainty includes the randomness in the calibrated instrument during the calibration, systematic uncertainty in the instrument or property which the instrument under calibration is compared with (dead weight manometer, calibrated weights etc.), and due to regression analysis to fit the calibration points to a linear calibration equation. The calculated uncertainty can be used as the total systematic uncertainty of the calibrated instrument with the given calibration equation.

Appendix M

Torque gauge calibration report

CALIBRATION REPORT

CALIBRATION PROPERTIES

Calibrated by: Remi André Stople

Type/Producer: T22/200NM

SN: V4364-3

Range: 0-200 Nm

Unit: Nm

CALIBRATION SOURCE PROPERTIES

Type/Producer: Deadweights

SN: -

Uncertainty [%]: 0

POLY FIT EQUATION:

$Y = + 1.18875679E+0X^0 - 40.47256213E+0X^1$

CALIBRATION SUMMARY:

Max Uncertainty : 3.134673 [%]

Max Uncertainty : 0.925574 [Nm]

RSQ : 0.999469

Calibration points : 28

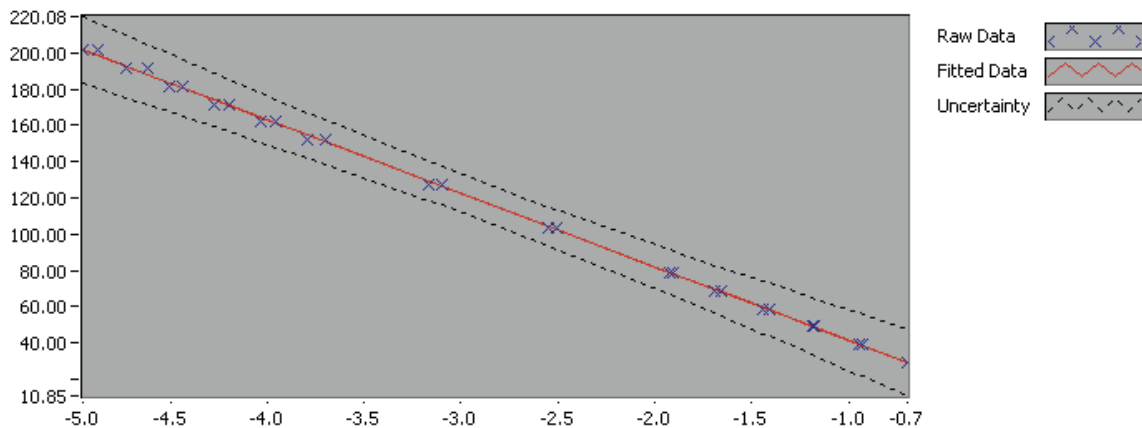


Figure 1 : Calibration chart (The uncertainty band is multiplied by 20)

Remi André Stople

CALIBRATION VALUES

| Value [Nm] | Voltage [V] | Best Poly Fit [Nm] | Deviation [Nm] | Uncertainty [%] | Uncertainty [Nm] |
|------------|-------------|--------------------|----------------|-----------------|------------------|
| 29.506137 | -0.697598 | 29.422344 | 0.083793 | 3.132472 | 0.924272 |
| 39.322023 | -0.927063 | 38.709386 | 0.612637 | 2.181250 | 0.857712 |
| 49.141284 | -1.173654 | 48.689540 | 0.451744 | 1.606597 | 0.789503 |
| 58.961531 | -1.409864 | 58.249548 | 0.711983 | 1.235138 | 0.728256 |
| 68.780167 | -1.657529 | 68.273218 | 0.506949 | 0.973467 | 0.669552 |
| 78.600366 | -1.902043 | 78.169305 | 0.431061 | 0.787094 | 0.618659 |
| 103.150300 | -2.506997 | 102.653336 | 0.496964 | 0.519086 | 0.535439 |
| 127.694920 | -3.098922 | 126.610065 | 1.084855 | 0.417186 | 0.532725 |
| 152.239210 | -3.701927 | 151.015230 | 1.223980 | 0.401435 | 0.611142 |
| 162.056210 | -3.954640 | 161.243178 | 0.813032 | 0.408801 | 0.662487 |
| 171.872310 | -4.196823 | 171.044921 | 0.827389 | 0.418339 | 0.719009 |
| 181.689970 | -4.437190 | 180.773224 | 0.916746 | 0.429651 | 0.780632 |
| 191.510880 | -4.617651 | 188.076920 | 3.433960 | 0.433284 | 0.829786 |
| 201.320130 | -4.875829 | 198.526068 | 2.794062 | 0.448794 | 0.903512 |
| 201.320130 | -4.950892 | 201.564060 | -0.243930 | 0.459752 | 0.925574 |
| 191.510880 | -4.727244 | 192.512419 | -1.001539 | 0.449321 | 0.860499 |
| 181.689970 | -4.507636 | 183.624329 | -1.934359 | 0.440058 | 0.799542 |
| 171.872310 | -4.271881 | 174.082721 | -2.210411 | 0.429225 | 0.737718 |
| 162.056210 | -4.031786 | 164.365474 | -2.309264 | 0.419470 | 0.679777 |
| 152.239210 | -3.791524 | 154.641466 | -2.402256 | 0.412721 | 0.628323 |
| 127.694920 | -3.166679 | 129.352350 | -1.657430 | 0.421142 | 0.537777 |
| 103.150300 | -2.544969 | 104.190170 | -1.039870 | 0.516460 | 0.532730 |
| 78.600366 | -1.922779 | 79.008554 | -0.408188 | 0.782114 | 0.614745 |
| 68.780167 | -1.689544 | 69.568911 | -0.788744 | 0.963144 | 0.662452 |
| 58.961531 | -1.437925 | 59.385258 | -0.423727 | 1.223328 | 0.721293 |
| 49.141284 | -1.188835 | 49.303938 | -0.162654 | 1.598337 | 0.785443 |
| 39.322023 | -0.941347 | 39.287468 | 0.034555 | 2.171092 | 0.853717 |
| 29.506137 | -0.695748 | 29.347473 | 0.158664 | 3.134673 | 0.924921 |

COMMENTS:

Weights calibrated by Justervesenet, Norway

The uncertainty is calculated with 95% confidence. The uncertainty includes the randomness in the calibrated instrument during the calibration, systematic uncertainty in the instrument or property which the instrument under calibration is compared with (dead weight manometer, calibrated weights etc.), and due to regression analysis to fit the calibration points to a linear calibration equation. The calculated uncertainty can be used as the total systematic uncertainty of the calibrated instrument with the given calibration equation.

Appendix N

Austegård calculations.

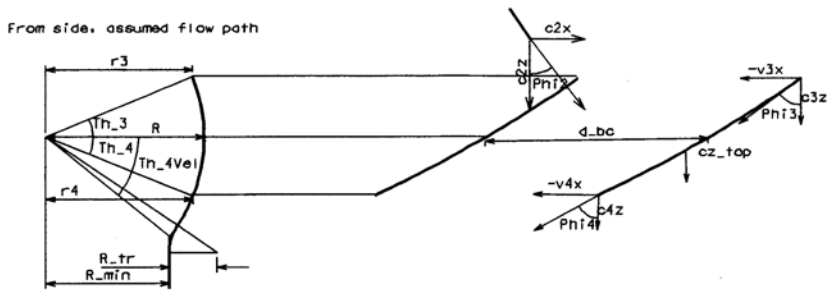


Figure 1 (KaplanSkovler.dgn)

Formulas:

Chooses: θ_3, θ_{4Tr}
 General variable:

- A_c : Cross section area (m²)
- q : Flow (m³/s)
- ω : Angular speed (rad/s)
- η_h : Hydraulic efficiency
- h : Head
- n_b : Number of blades

Speeds:

- u : Blade speed
- v : Relative speed
- c : Absolute speed
- $\phi_v(\Phi)$ Angle for v
- ϕ_b : Angle of blade

$c = u + v$

Calculation of velocities at inlet of blades:

$$c_{zTop} = \frac{q}{A_c}$$

$$r_3 = R \cos(\theta_3)$$

$$u_{x3} = \omega r_3$$

$$gh\eta_h = c_{x3}u_{x3} - c_{x4}u_{x4}$$

$$\Rightarrow c_{x3} = \frac{gh\eta_h + c_{x4}u_{x4}}{u_{x3}} \tag{1}$$

$$v_{x3} = u_{x3} - c_{x3}$$

$$c_{z3} = c_{zTop}$$

$$\phi_{v3} = \arctan(v_{x3} / c_{z3})$$

c_{z3} : Is an approximation, but little influence on result. (Have some influence on blade length)

And at outlet of blades:

$$\begin{aligned}
 r_4 &= R \cos(\max(\theta_{4c}, \theta_{4vel})) && R \cos \theta_{4c} && \text{Hvorfor? Hvorfor?} \\
 u_{x4} &= \omega r_4 \\
 c_{x4} &= 0 \\
 v_{x4} &= u_{x4} - c_{x4} && && (2) \\
 c_{z4} &= \frac{q}{A_c} \frac{R}{r_4} && ? \text{ Hvorfor dette?} \\
 \phi_{v4} &= \arctan(v_{x4} / c_{z4})
 \end{aligned}$$

Mark that this angles is flow angles, and not angles of blades.
 θ_4 is negative.

Calculation of blade profile:

Variables:

- d_{bc} : Distance between blades at center ($\theta=0$)
- l_b : Length of blades
- Δz_b : Vertical distance blades
- R_{Min} : Radius of flow when profile is cylindrical after blade
- ϕ_{b3}, ϕ_{b4} : Angle of outlet and inlet of centerline blades
- $n_r = \text{Number of blades} = 4$

Input:

$$\begin{aligned}
 l_b / d_{bc} \\
 \theta_{4vel}
 \end{aligned}$$

Uses and approximation with straight line with angle $\frac{\phi_3 + \phi_4}{2}$

wich gives:

$$\begin{aligned}
 d_{bc} &= \frac{2\pi R}{n_b} \\
 l_b &= d_{bc} (l_b / d_{bc}) \\
 \Delta z_b &= l_b \cos\left(\frac{\phi_3 + \phi_4}{2}\right) && \text{for side approximation} \\
 \theta_{4c} &= \theta_3 - \frac{\Delta z_b}{R} && \text{for side approximation} \\
 R_{Min} &= R \cos(\theta_{4vel}) && \text{Hvorfor?} && (3)
 \end{aligned}$$

This is an approximation. θ_4 can only be found whens simulating data.

Simulation:

Now we have enough data for simulation of flow around the blade.
with routine sp_ExcelSphere.sci

Uses input data:

| Variable name | | | |
|-------------------|-------------|-----------------|--|
| Excel | Scilab | Here | Description |
| R(mm) | RSph | R | Radius sphere |
| R tr | Rts | R_r | Radius for transition |
| Th4_vel | Th4 | θ_{4vel} | See Figure 1. |
| vx3 | v3x | v_{x3} | |
| vx4 | v4x | v_{x4} | |
| p | p | | Point of max deflection $0 < p < 1$ |
| tmax | tMax*L | | Max wing thickness (mm) |
| L_wing | L | L_b | Length of straight line from start of blade to end of blade |
| Inlet Th | Th_fr | θ_3 | |
| x_Turnpoint | x_TurnPoint | | Not used for calculating flow. Gives sideways position of blade |
| Change stag point | d_ifr | | Position of stagnation point at front. d_ifr=0 gives stagnation point at front of wing. d_ifr=1: At first point in simulation. |
| n Fins | n Fins | n_b | Number of blades |
| RotAxis | RotAxis | ω | Rotation speed (rad/s) |
| cz_top | czCent | $c_{z,top}$ | Downward speed: Assume it increase when radius reduces |
| Plot | doPlot | | If on should plot vector plot of velocities |
| Extra | | | Not used |

R: Radius

R_r : Radius transition from sphere profile to cylindrical profile after wing: PS: Does not calculate correct after the sphere profile.

x_TurnPoint / y_x0

Does not influence simulation, but influences geometry of blade.

Is replaced with y_{x0} : Is the y position of tangent line at $x=0$.

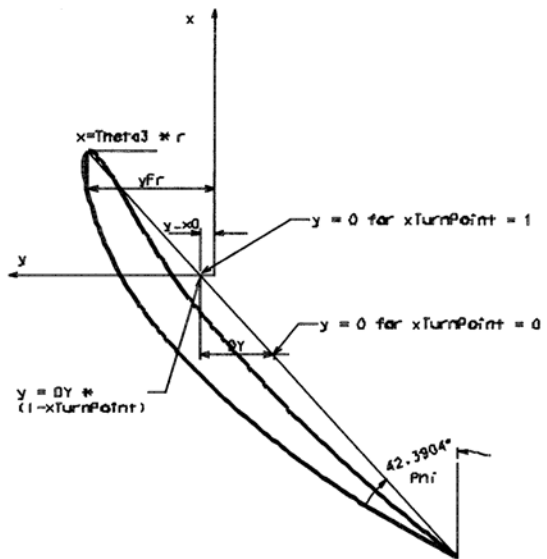


Fig 2 (WingGeom.dgn): Variables defining wing geom

Calculation of cavitation

Assumes that all hydraulic loss occur before guide vane, and the resto of turbine have no hydraulic loss. And that guide vanes and rotor is at zero head.
 Pressure on upperside of blade with relative velocity v:

In the stator windings with potential flow one have:

$$p_0 = p + \rho c^2 / 2 \tag{4}$$

Where p_0 is static pressure wich is constant and c is absolute velocity.

In the blade one get along a flow line:

$$p_0 = p + \rho c^2 / 2 - \rho u_x c_x + \rho u_{x3} c_{x3} \tag{5}$$

Where p_0 is constant. The term $\rho u_x c_x$ is the work on the blade done of the flow as in Eq.(1)
 The term $\rho u_{x3} c_{x3}$ comes from the inlet of the blade where c_{x3} is average velocity in x direction at the inlet of the blade.

By using $c = u + v$, and that $u_y=0$ one get:

$$\begin{aligned}
 c^2/2 - u_x^2 c_x &= 1/2(c_x^2 + c_y^2 - 2u_x c_x + u_x^2 - u_x^2) = 1/2((c_x - u_x)^2 + c_y^2 - u_x^2) \\
 &= 1/2(v_x^2 + v_y^2 - u_x^2) = 1/2(v^2 - u_x^2) \\
 \Rightarrow p_0 &= p + \rho(v^2 - u_x^2)/2 + \rho u_{x3} c_{x3} = \rho g(h \eta_{h,a} - h_b) + p_{Air}
 \end{aligned}$$

Then one have an expression for pressure p .

Here h_b : Is head of the blades, p_{Air} is air pressure., $\eta_{h,a}$: Is hydraulic loss above and on the blades.

With $h_b=0$, $p_{Air}=0$, $\eta_{h,a} = \eta_h$, $p_{Air} = 0$, one get Critical coefficient for cavitation:

$$\sigma_{Crit} = -\frac{p_{Min}}{\rho g h} = \frac{\max(v^2 - u_x^2)}{2gh}$$

The last term appear since $c_{x4}=0$ wich gives $p_0 = \rho u_{x3} c_{x3}$

Then one can calcualte miniumu pressure:

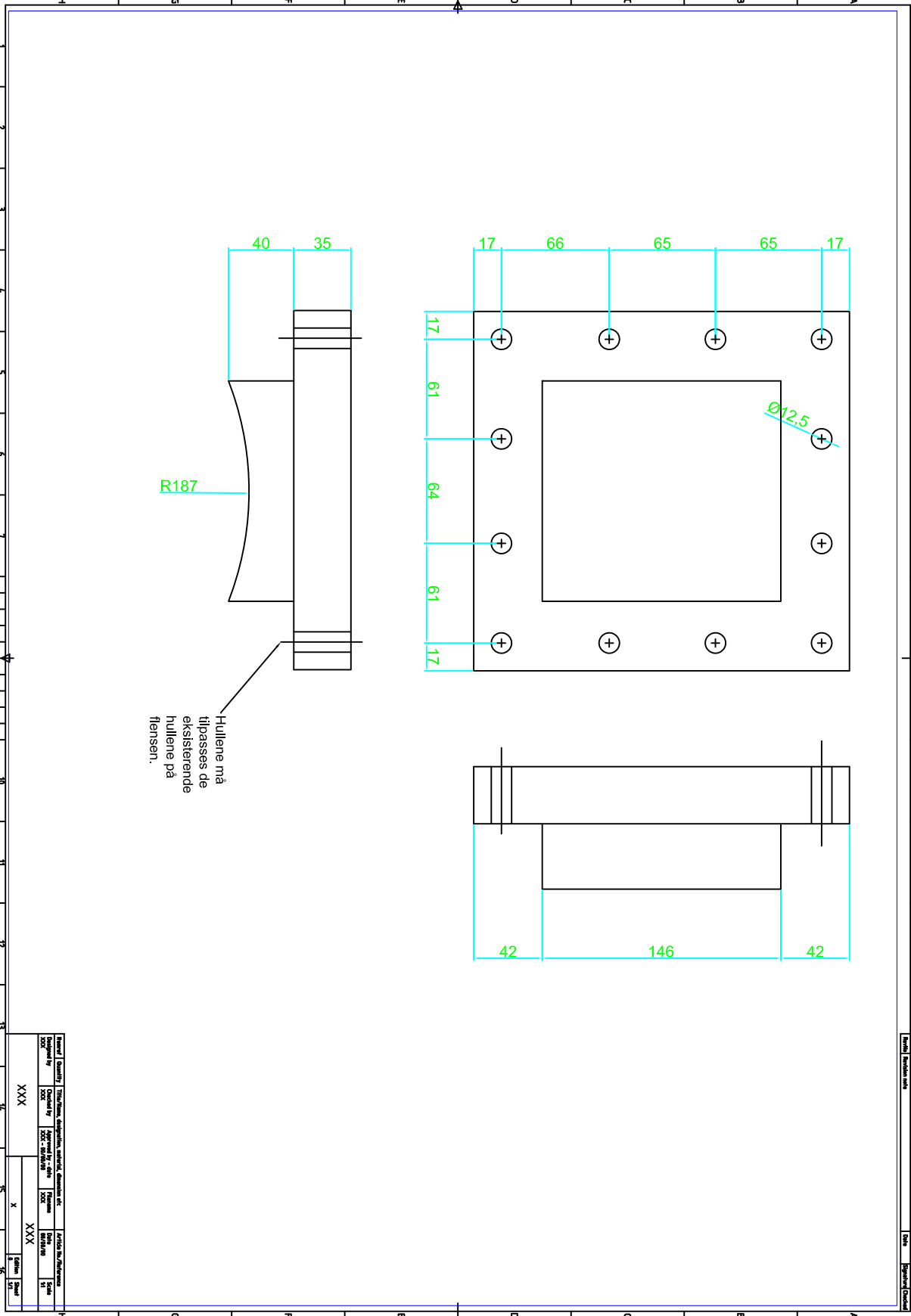
$$p_{Min} = p_{Air} - \rho g h \sigma_{Crit} - \rho g h_b$$

Wich must be above evaporating pressure with some margine.

One requires that pressure is higher than evaporating pressure.

Appendix O

Plexiglas

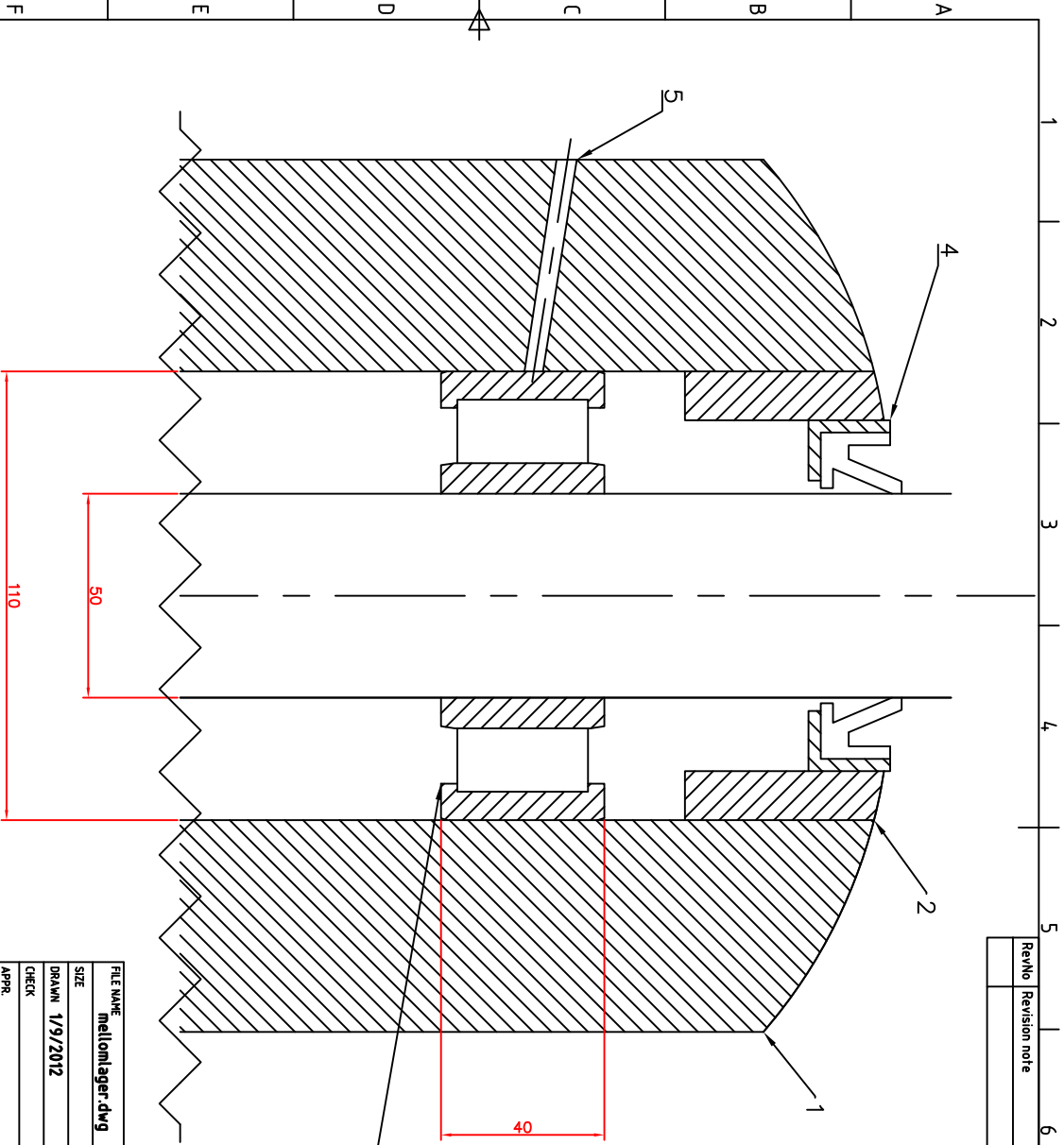


Hullene må
tilpasses de
eksisterende
hullene på
flensen.

| | | | |
|----------|----------|---|-----------------------|
| Material | Quantity | Material description, unit of measure, etc. | Article No./Reference |
| XXX | XXX | XXX | XXX |

Appendix P

Bearing drawing



| | | | | |
|-------|---------------|------|-----------|---------|
| RevNo | Revision note | Date | Signature | Checked |
| | | | | |

| | | | |
|-------------|------------------|-------------|----------|
| FILE NAME | meillonlager.dwg | FSCHEID | |
| SIZE | | SHEET | ### |
| DRAWN | 1/9/2012 | SCALE | 1:1,7507 |
| CHECK | | #### | |
| APPR | | #### | |
| ISSUED | | #### | |
| REV | | #### - #### | |
| CONTRACT NO | | | |

| NR | Description |
|----|---------------|
| 5 | Grease intake |
| 4 | Seal housing |
| 3 | Bearing |
| 2 | Spacer |
| 1 | Housing |

Appendix Q

Torque gauge calibration report



NTNU Vannkraftlaboratoriet
Alfred Getz vei 4
7491 TRONDHEIM

Deres ref./Your ref.
Jørgen Ramdal

Vår ref./Our ref.
06/730 - /AGA-tkv/511

Dato/Date
29.08.06

Kalibrering av lodd

Vedlagt følger Deres kalibreringsbevis nr. CAL 016-06/730-3 til Deres kalibrerte lodd.

Resultatene skal dere ha fått tilsendt pr. mail fra Nils M. Thomassen tidligere, men ved skrivning av beviset fant vi to feil i filen. For lodd NTNU VKL 52 og NTNU VKL 103 ble det oppgitt feil k-faktor, frihetsgrader og usikkerhet i filen dere fikk tilsendt. Kalibreringsbeviset inneholder riktige tall. Vi beklager dette.

Faktura vil bli sendt separat.

Med hilsen

Turid K. Viken
konsulent

KALIBRERINGSBEVIS Certificate of calibration Nr./No: CAL 016-06/730-3



Kalibreringslaboratoriets navn:
Name of the calibration laboratory:
JUSTERVESENET
Oslo justerkammer

Laboratoriets adresse:
Laboratory address:
Fetveien 99
2007 KJELLER

Side/Page: 1 av/of: 4
Ref. til måleprotokoll/Ref to records:
06/730

| | |
|--|---|
| Tid og sted for kalibrering/ <i>Date and place of calibration:</i> | Bevisets utstedelsesdato: <i>Date of issue:</i> |
| Kjeller, 9. – 15. august 2006 | Kjeller, 28. august 2006 |
| Kalibrering utført av/ <i>Calibration performed by:</i> | Ansvarlig/ <i>responsible:</i> |
| Arne Georg Andersen, avdelingsingeniør | Nils M. Thomassen, justermester |

Kunde: NTNU Vannkraftlaboratoriet, Alfred Getz v. 4, 7491 Trondheim.
Customer

Instrument: Lodd
Item

Kapasitet: 650 g – 5,7 kg
Capacity

Produsent: Ikke kjent
Manufacturer

Typebetegnelse: Se resultater side 2.
Model

Serienummer: Ikke kjent
Serial number

Intern nummer: Se side 2.
Internal number

Tidligere kalibreringsbevis nr.: CAL 016-32/05/1. NTNU VKL 103 er ikke kalibrert tidligere.
Previous calibration no.

Delte kalibreringsbeviset er utstedt av et laboratorium som er akkreditert i Norsk Akkreditering (NA). Akkrediteringen medfører at laboratoriet oppfyller de kravene NA stiller til kompetanse og kalibreringssystem for de kalibreringene akkrediteringen omfatter. Det innebærer også at laboratoriet har et tilfredsstillende kvalitetssikringssystem og sporbarhet til akkrediterte eller nasjonale kalibreringslaboratorier. Kopiering av dette kalibreringsbeviset er kun tillatt dersom beviset kopieres i sin helhet.

This certificate of calibration is issued by a laboratory accredited by Norwegian Accreditation (NA). The accreditation states that the laboratory meets the NA requirements concerning competence and calibration system for all the calibrations contained in the accreditation. It also states that the laboratory has a satisfactory quality assurance system and traceability to accredited or national calibration laboratories. This certificate of calibration may not be reproduced other than in full.

KALIBRERINGSBEVIS

Certificate of Calibration

Justervesenet

Oslo Justerkammer

Nr./No.: CAL 016-06/730-3

Side/Page: 2 av/of: 4

Måleresultater med usikkerhet:

| Nominell verdi | Kjennetegn | Konvensjonell verdi | Usikkerhet (k = 2) | k-faktor ref EA 4/02 | V _{eff} |
|----------------|-------------|---------------------|--------------------|----------------------|------------------|
| 5 kg | NTNU VKL 1 | 5 kg + 0,32 g | ± 0,15 g | k = 2 | ∞ |
| 5 kg | NTNU VKL 2 | 5 kg + 0,42 g | ± 0,15 g | k = 2 | ∞ |
| 5 kg | NTNU VKL 3 | 5 kg + 0,24 g | ± 0,15 g | k = 2 | ∞ |
| 5 kg | NTNU VKL 4 | 5 kg - 0,22 g | ± 0,15 g | k = 2 | ∞ |
| 5 kg | NTNU VKL 5 | 5 kg + 0,63 g | ± 0,15 g | k = 2 | ∞ |
| 5 kg | NTNU VKL 6 | 5 kg + 0,61 g | ± 0,15 g | k = 2 | ∞ |
| 5 kg | NTNU VKL 7 | 5 kg + 0,96 g | ± 0,15 g | k = 2 | ∞ |
| 5 kg | NTNU VKL 8 | 5 kg + 0,42 g | ± 0,15 g | k = 2 | ∞ |
| 5 kg | NTNU VKL 9 | 5 kg + 0,93 g | ± 0,15 g | k = 2 | ∞ |
| 5 kg | NTNU VKL 10 | 5 kg + 0,72 g | ± 0,15 g | k = 2 | ∞ |
| 5 kg | NTNU VKL 11 | 5 kg + 0,39 g | ± 0,15 g | k = 2 | ∞ |
| 5 kg | NTNU VKL 12 | 5 kg + 0,10 g | ± 0,15 g | k = 2 | ∞ |
| 5 kg | NTNU VKL 13 | 5 kg + 0,07 g | ± 0,15 g | k = 2 | ∞ |
| 5 kg | NTNU VKL 14 | 5 kg + 0,15 g | ± 0,15 g | k = 2 | ∞ |
| 5 kg | NTNU VKL 15 | 5 kg + 0,20 g | ± 0,15 g | k = 2 | ∞ |
| 5 kg | NTNU VKL 16 | 5 kg + 0,29 g | ± 0,15 g | k = 2 | ∞ |
| | | | | | |
| 2 kg | NTNU VKL 21 | 2 kg - 0,858 g | ± 0,070 g | k = 2 | ∞ |
| 2 kg | NTNU VKL 22 | 2 kg - 0,246 g | ± 0,068 g | k = 2 | ∞ |
| 2 kg | NTNU VKL 23 | 2 kg - 0,241 g | ± 0,060 g | k = 2 | ∞ |
| 2 kg | NTNU VKL 24 | 2 kg - 2,487 g | ± 0,062 g | k = 2 | ∞ |
| | | | | | |
| 5 kg | NTNU VKL 28 | 5 kg - 2,03 g | ± 0,15 g | k = 2 | ∞ |
| 5 kg | NTNU VKL 29 | 5 kg - 1,38 g | ± 0,15 g | k = 2 | ∞ |
| 5 kg | NTNU VKL 30 | 5 kg - 0,98 g | ± 0,15 g | k = 2 | ∞ |
| 5 kg | NTNU VKL 31 | 5 kg - 0,36 g | ± 0,15 g | k = 2 | ∞ |
| 5 kg | NTNU VKL 32 | 5 kg - 1,63 g | ± 0,15 g | k = 2 | ∞ |
| 5 kg | NTNU VKL 33 | 5 kg - 1,13 g | ± 0,15 g | k = 2 | ∞ |
| 5 kg | NTNU VKL 34 | 5 kg - 0,84 g | ± 0,15 g | k = 2 | ∞ |
| 5 kg | NTNU VKL 35 | 5 kg - 1,61 g | ± 0,15 g | k = 2 | ∞ |
| 5 kg | NTNU VKL 36 | 5 kg - 1,71 g | ± 0,15 g | k = 2 | ∞ |
| 5 kg | NTNU VKL 37 | 5 kg - 1,52 g | ± 0,15 g | k = 2 | ∞ |
| 5 kg | NTNU VKL 38 | 5 kg - 1,76 g | ± 0,15 g | k = 2 | ∞ |
| 5 kg | NTNU VKL 39 | 5 kg - 1,83 g | ± 0,15 g | k = 2 | ∞ |
| 5 kg | NTNU VKL 40 | 5 kg - 1,91 g | ± 0,15 g | k = 2 | ∞ |
| 5 kg | NTNU VKL 41 | 5 kg - 1,57 g | ± 0,15 g | k = 2 | ∞ |
| 5 kg | NTNU VKL 42 | 5 kg - 1,56 g | ± 0,15 g | k = 2 | ∞ |
| 5 kg | NTNU VKL 43 | 5 kg - 1,74 g | ± 0,15 g | k = 2 | ∞ |
| 5 kg | NTNU VKL 44 | 5 kg - 0,76 g | ± 0,15 g | k = 2 | ∞ |
| 5 kg | NTNU VKL 45 | 5 kg - 1,84 g | ± 0,15 g | k = 2 | ∞ |

Kopiering av dette kalibreringsbeviset er kun tillatt dersom beviset kopieres i sin helhet.
This certificate of calibration may not be reproduced other than in full.

KALIBRERINGSBEVIS

Certificate of Calibration

Justervesenet
Oslo Justerkammer

Nr./No.: CAL 016-06/730-3

Side/Page: 3 av/of: 4

| Nominell verdi | Kjennetegn | Konvensjonell verdi | Usikkerhet (k = 2) | k-faktor ref EA 4/02 | V _{eff} |
|----------------|--------------|---------------------|--------------------|----------------------|------------------|
| 5 kg | NTNU VKL 46 | 5 kg - 1,74 g | ± 0,15 g | k = 2 | ∞ |
| 5 kg | NTNU VKL 47 | 5 kg - 0,99 g | ± 0,15 g | k = 2 | ∞ |
| 5 kg | NTNU VKL 48 | 5 kg - 1,08 g | ± 0,15 g | k = 2 | ∞ |
| 5 kg | NTNU VKL 49 | 5 kg - 1,33 g | ± 0,15 g | k = 2 | ∞ |
| 5 kg | NTNU VKL 50 | 5 kg - 0,47 g | ± 0,15 g | k = 2 | ∞ |
| 2 kg | NTNU VKL 51 | 2 kg - 0,908 g | ± 0,065 g | k = 2 | ∞ |
| 2 kg | NTNU VKL 52 | 2 kg - 1,093 g | ± 0,089 g | k = 2,28 | 10,38 |
| 2 kg | NTNU VKL 53 | 2 kg - 0,576 g | ± 0,060 g | k = 2 | ∞ |
| 2 kg | NTNU VKL 54 | 2 kg - 0,258 g | ± 0,060 g | k = 2 | ∞ |
| 2 kg | NTNU VKL 55 | 2 kg - 0,113 g | ± 0,060 g | k = 2 | ∞ |
| 2 kg | NTNU VKL 56 | 2 kg - 0,776 g | ± 0,059 g | k = 2 | ∞ |
| 2 kg | NTNU VKL 57 | 2 kg - 0,449 g | ± 0,062 g | k = 2 | ∞ |
| 2 kg | NTNU VKL 58 | 2 kg - 0,248 g | ± 0,059 g | k = 2 | ∞ |
| 2 kg | NTNU VKL 59 | 2 kg - 1,136 g | ± 0,062 g | k = 2 | ∞ |
| 5,7 kg | NTNU VKL 101 | 5,7 kg + 74,96 g | ± 0,15 g | k = 2 | ∞ |
| 650 g | NTNU VKL 103 | 650 g - 0,019 g | ± 0,0039 g | k = 2,10 | 18 |

Loddene oppfyller ikke spesifikasjoner iht OIML R111 og er derfor ikke vurdert iht denne.

Målemetode:

Substitusjonsveiling, prosedyre JV-LM-MAS-004 utgave nr. 4.0

Sporbarhet:

Loddene er sammenlignet med loddnormaler som er sporbare til de nasjonale normaler for masse.

Forhold under kalibreringen:

Kalibreringen er basert på en antatt densitet 8000 kg/m³ på loddene ved 20 °C og antatt densitet på 1,2 kg/m³ på luften.

Temperatur under kalibreringen var fra 19,5 - 20,0 °C ± 0,1 °C

Fuktigheten under kalibreringen var fra 45,8 - 47,8 % RH ± 1,5 % RH

Måleusikkerhet, metode for beregning og hovedkomponenter:

Den rapporterte utvidede usikkerheten er fastslått som standard måleusikkerhet multiplisert med dekningsfaktor som angitt i tabellen over, som for en t-fordeling med effektive frihetsgrader (V_{eff}) som angitt i tabellen over, korresponderer til en deknings sannsynlighet på tilnærmet 95%. Standard måleusikkerhet har blitt bestemt i samsvar med EA publikasjonen "EA 4/02"

KALIBRERINGSBEVIS

Certificate of Calibration

Justervesenet
Oslo Justerkammer

Nr./No.: CAL 016-06/730-3

Side/Page: 4 av/of: 4

Benyttede instrumenter og normaler:

Temperatur og luftfuktighet ble bestemt ved å benytte termohygrograf, merket:T/HYG-OSL-02

Den konvensjonelle massen til loddene ble bestemt ved hjelp av følgende vekter og normaler:

| Nominell masse | Benyttet vekt | Benyttet normal |
|----------------|--------------------------------------|---------------------------|
| 650 g | Sartorius CC60000, serienr. 30903465 | OSL-E ₂ -21 |
| 2 – 5 kg | Sartorius CC60000, serienr. 30903465 | OSL-E2-01 |
| 5,7 kg | Sartorius CC60000, serienr. 30903465 | OSL-E2-01 og OSL-E2-21 |

Kommentar:

Resultatet bekrefter loddets tilstand på det tidspunkt og under de forhold kalibreringen ble utført.
Beregningsprogram Loddkal versjon 2.03

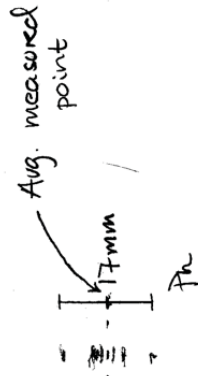
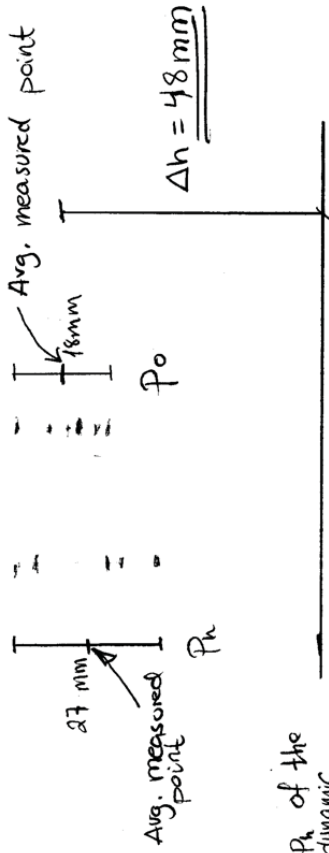
Fluctuations in the velocity in the water caused the readings to vary. An average value is therefore used in the calculation of the velocity.

$$\frac{27}{2} = 13.5$$

$$\frac{18}{2} = 9$$

$$\frac{17}{2} = 8.5$$

Avg. P_h of the two dynamic pressures.



Between centre of pitot measurements and the line there is a distance of 1970 mm

$$Q = 0,124215652 \text{ m}^3/\text{s}$$

$$A_{\text{inn}} = 0,125663 \text{ m}^2$$

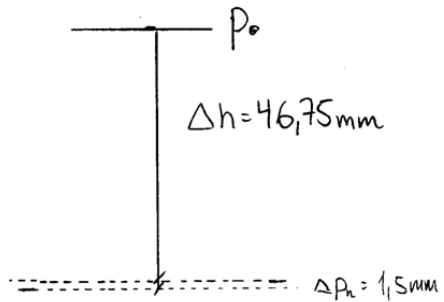
$$A_{\text{out}} = 0,11027 \text{ m}^2$$

\Rightarrow

$$V_{\text{inn}} = \underline{0,98848 \text{ m/s}}$$

$$V_{\text{out,ag}} = \underline{1,12647 \text{ m/s}}$$

$$c = \sqrt{\frac{2g \cdot \Delta h}{\varphi}}$$



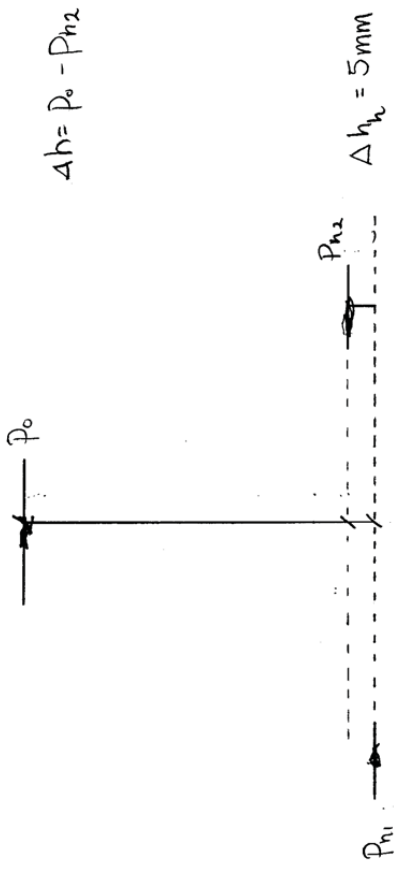
$$c = \sqrt{\frac{2 \cdot 9,82146 \cdot 0,04675}{0,99}} = \underline{\underline{0,96311 \text{ m/s}}}$$

$$V_{\text{out,ag}} - c = \underline{0,16336 \text{ m/s}}$$

$$c' = 1,092064$$

$$Q \approx 123 \text{ l/s}$$

$$\Delta h = P_0 - P_{h2} + \frac{1}{2} \Delta h_n = \underline{\underline{62,5 \text{ mm}}}$$



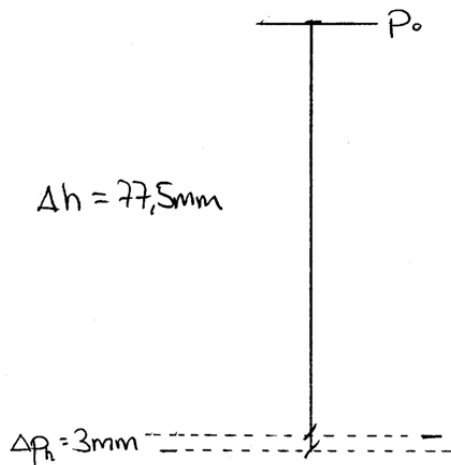
From hydraulic measurement:

$$\varphi^2 c^2 = \Delta h \cdot g \cdot d \Rightarrow c = \sqrt{\frac{\Delta h \cdot g \cdot d}{\varphi}} = \sqrt{\frac{0,0625 \cdot 9,8214652}{0,99}} = \underline{\underline{1,1136 \text{ m/s}}}$$

$$Q = 135,893 \text{ l/s} = 0,135893 \text{ m}^3/\text{s}$$

Cross section area in measured point is $\pi \cdot \frac{(d_{\text{outer}}^2 - d_{\text{inner}}^2)}{4} = \pi \cdot \frac{(0,1^2 - 0,14^2)}{4}$
 $\Rightarrow A_c = 0,11027 \text{ m}^2$ this should result in an average speed in the measured point of $\varphi/A_c = 1,2327 \text{ m/s} = V_{\text{outlet,avg}}$
 At inlet the speed is $V_{\text{inlet}} = 1,0814 \text{ m/s}$

$$V_{\text{out,avg}} - c = \underline{\underline{0,1191 \text{ m/s}}}$$



$$Q = 0,158623812 \text{ m}^3/\text{s}$$

$$A_{\text{inn}} = 0,125663 \text{ m}^2$$

$$A_{\text{out}} = 0,11027 \text{ m}^2$$

$$\Rightarrow V_{\text{inn}} = \underline{1,2623 \text{ m/s}}$$

$$V_{\text{out,avg}} = \underline{1,4385 \text{ m/s}}$$

$$\varphi C^2 = \Delta h \cdot 2g \Rightarrow c = \sqrt{\frac{2g \cdot \Delta h}{\varphi}}$$

$$c = \sqrt{\frac{2 \cdot 9,82146 \cdot 0,0775}{0,99}} = \underline{\underline{1,24 \text{ m/s}}}$$

$$V_{\text{out,avg}} - c = \underline{0,1985 \text{ m/s}}$$

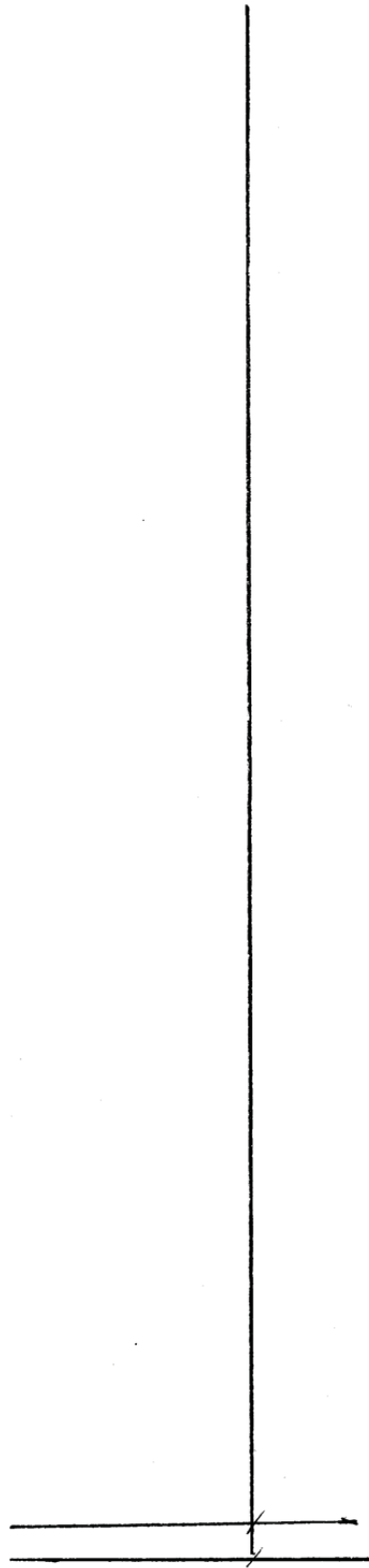
$$c' = 1,80446505$$

$Q \approx 160 \text{ l/s}$

Måling 1

1,2 cm
above
paper

$$Q = 0,41 \text{ m}^3/\text{s}$$

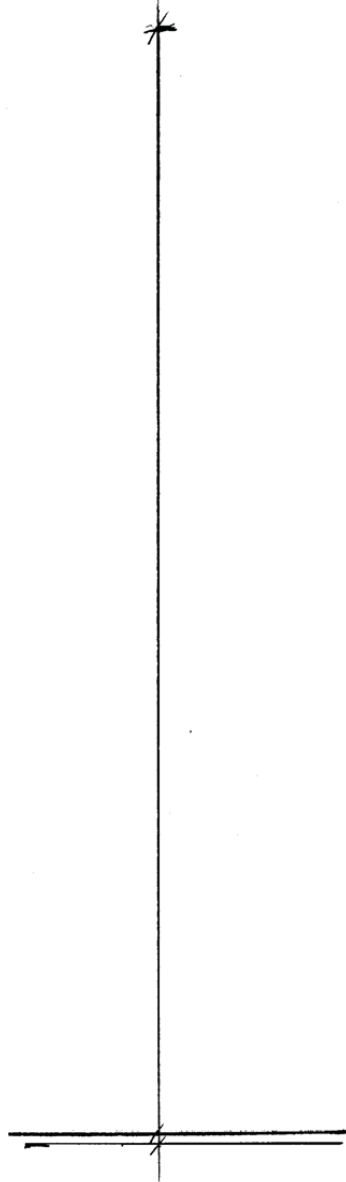


Mäxy 4

$$Q = 0,119 \text{ m}^3/\text{s}$$

$$A_{in} = 0,125663 \text{ m}^2$$

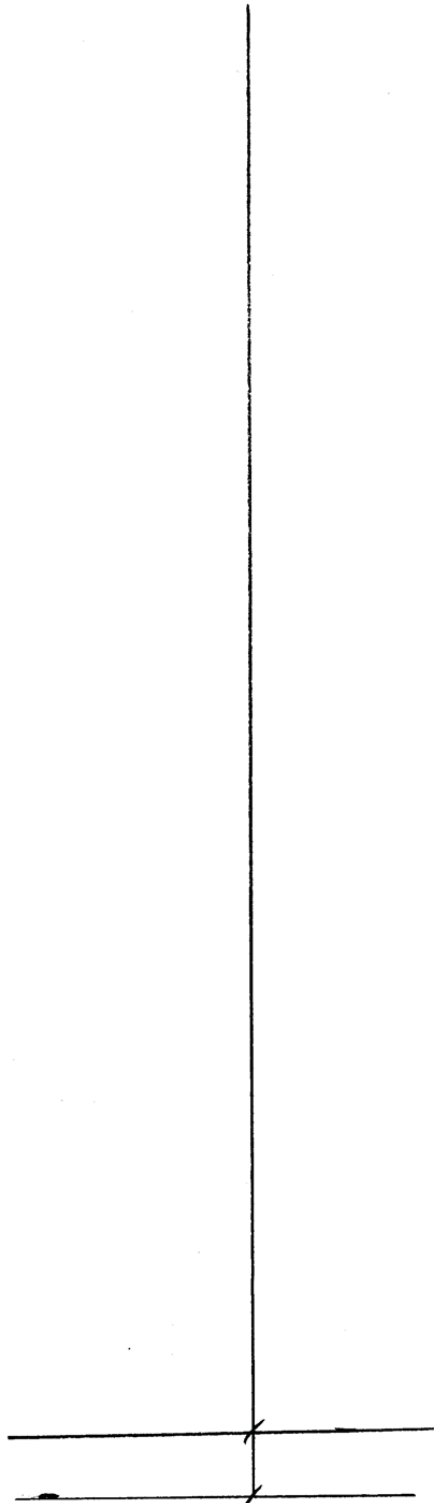
$$A_{out} = 0,11027 \text{ m}^2$$



Måling 2

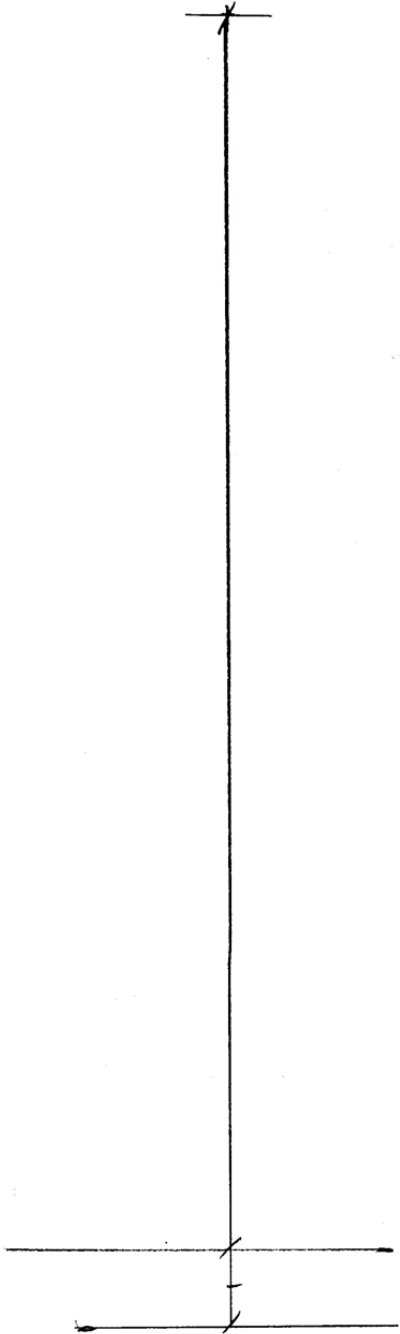
7,7
cm
above
paper

$$Q = 0,153 \text{ m}^2/\text{s}$$



Matins 3

$$Q = 0,128 \text{ m}^3/\text{s}$$



| | | | | | | | | | |
|----|-------|---------|---------|--------|-------|---------|--------|---------|-------|
| | 500.8 | 27528 | 42623.4 | 30.103 | 17.05 | 15095.4 | 500.46 | 502.613 | 30103 |
| 18 | 8.285 | | | | | | | | |
| | 509.7 | 42623.4 | 55457.4 | 25.106 | 17.08 | 12834 | 510.17 | 512.37 | 25106 |

19 8.418
521

| | | | | | | | | | |
|----|-------|---------|---------|--------|-------|---------|--------|---------|--|
| 19 | 8.530 | | | | | | | | |
| | 530 | 31086.6 | 47066.9 | 30.104 | 17.27 | 15980.3 | 529.77 | 532.357 | |

V Qvir

- 2.6 52.314
- 2.7 59.478
- 2.8 65.581
- 2.9 76.962
- 3.1 94.631
- 3.3 102.358
- 3.8 144.721
- 4.3 183.53
- 5.1 251.652
- 5.9 317.797
- 7.2 424.327
- 7.6 452.281
- 8.3 515.771
- 8.5 528.668
- 8.1 495.774
- 8.2 502.613
- 8.3 512.37
- 8.5 532.357

